

REVIEWS OF TOPICAL PROBLEMS PACS numbers: 34.80.Lx, **34.90.+q**

Electron attachment to free and bound molecules

E Illenberger, B M Smirnov

Contents

Abstract. Electron attachment to diatomic and polyatomic molecules, as well as to complexes, clusters, bulk particles, and surfaces is considered. The relevant theoretical concepts involving the formation of autodetachment states in negative ions are presented. Experimental data on electron attachment processes are analysed from a general theoretical viewpoint.

1. Introduction

The process of electron attachment to atomic systems — molecules, clusters and surfaces has a resonant character and proceeds through the formation of autodetachment states of the total system. Because of the resonant character, this process is characterized by large cross sections or rate constants. Hence, the electron attachment process is of importance for various plasma systems. It is used for the protection of electrical systems, so that small admixtures of electronegative molecules prevent these systems from electrical breakdown. Electron attachment is used in excimer lasers for prompt creation of fluorine and chlorine atoms from various halogen-containing molecules. Due to electron attachment, special forms and regimes of gas discharges may be created. Electron attachment may be responsible for the desorption of molecules from a surface on the plasma – wall boundary.

A general concept of electron attachment connects it with the formation of autodetachment states of electrons resulting from electron capture by a molecule. The subsequent development of intermediate an autodetachment state may lead to various processes including the dissociation of the system with the formation of a negative ion or the decay of the autodetachment state by electron release and excitation of the atomic system. Hence, electron attachment is connected with other resonant processes of elastic and inelastic scattering of an electron by a molecule which proceed via the formation of an autodetachment state — a bound electron-molecule state if an electron term is found in the continuous spectrum.

The classical concept of electron capture by a molecule in an autodetachment state was developed for free molecules, but works in principle for bound molecules when they form complexes, clusters, or films. Hence, the theoretical concept of electron attachment processes under consideration retains its form as when it was worked out in fifties. But the experimental data for electron attachment have varied with time due to new experimental methods and facilities. Therefore, owing to new experimental data we have obtained a

E Illenberger Institut für Physikalische und Theoretische Chemie, Freie Universität Berlin, Takustrasse 3, D-14195 Berlin, Germany
E-mail: iln@chemie.fu-berlin.de
B M Smirnov Institute for High Temperatures, Russian Academy of Sciences
Izhorskaya 13/19, Moscow 127412, Russia
E-mail: smirnov@termo.msk.su
Uspekhi Fizicheskikh Nauk **168** (7) 731 – 766 (1998)
Translated by B M Smirnov; edited by A Radzig

deeper understanding of some aspects of the processes under consideration. The goal of this review is to analyze the peculiarities of electron attachment processes to various atomic systems on the basis of experimental data and to consider the properties of autodetachment states of atomic systems which follow from the experimental study of the corresponding processes.

Electron attachment to atomic systems is considered in books [1–3] and reviews [4–10]. Recent experimental methods of studying electron attachment to gaseous molecules [9, 10] and, to clusters and films [9] have been reviewed. In [9], on the basis of results of measurements, the character of processes of formation of negative ions in electron collisions with atomic systems is analyzed. At the heart of this review are general concepts of the theory of atomic collisions and simple models of these processes allowing the connection of results of experiments with general concepts of the processes under consideration.

2. Properties of autodetachment states

2.1 Times of attachment processes

The process of electron attachment to a molecule proceeds via electron capture in an autodetachment term of the negative ion. Then the electron terms of the molecule and negative ion must intersect near the equilibrium configuration of nuclei in the molecule. Versions of this situation are given in Fig. 1, where R is the nuclear coordinate responsible for this process. Below we consider the process which proceeds through the formation of autodetachment states from the general position of quantum mechanics [1, 2, 11]. We are working within the framework of the Born–Oppenheimer approximation, i.e. the total system is divided into the fast electron subsystem and the slow nuclear subsystem. Then the wave function of this atomic system is represented in the form

$$\Psi(r, R) = \psi(r, R)\Phi(R)\,, \tag{2.1}$$

where r is the sum of coordinates of electrons, R is the sum of nuclear coordinates, $\psi(r, R)$ is the electron wave function in which coordinates of nuclei R are included as a parameter, and $\Phi(R)$ is the nuclear wave function. If we consider the Schrödinger equation only for the electron subsystem, we obtain the energy $\varepsilon(R)$ of the electron subsystem in the form

$$\varepsilon(R) = E(R) + \mathrm{i}\Gamma(R)\,, \tag{2.2}$$

where the real part of the electron energy $E(R)$ and its width $\Gamma(R)$ depend on the nuclear coordinates as on a parameter.

Thus, within the framework of the Born–Oppenheimer approximation we use the language of electron terms for description of the atomic systems under consideration. In this approximation the process of electron capture in the autodetachment state

$$\mathrm{e} + \mathrm{A} \rightarrow (\mathrm{A}^-)^{**} \tag{2.3}$$

is instant. Here e labels an electron, A is an atomic system, and $(\mathrm{A}^-)^{**}$ is the autodetachment state of the negative ion. Hence, considering the hierarchy of times for the process proceeding through the formation of an autodetachment state $(\mathrm{A}^-)^{**}$, we have within the framework of the Born–Oppenheimer approximation

$$\tau_\mathrm{e} \ll \frac{\hbar}{\Gamma}\,, \qquad \tau_\mathrm{e} \ll \frac{1}{\omega}\,. \tag{2.4}$$

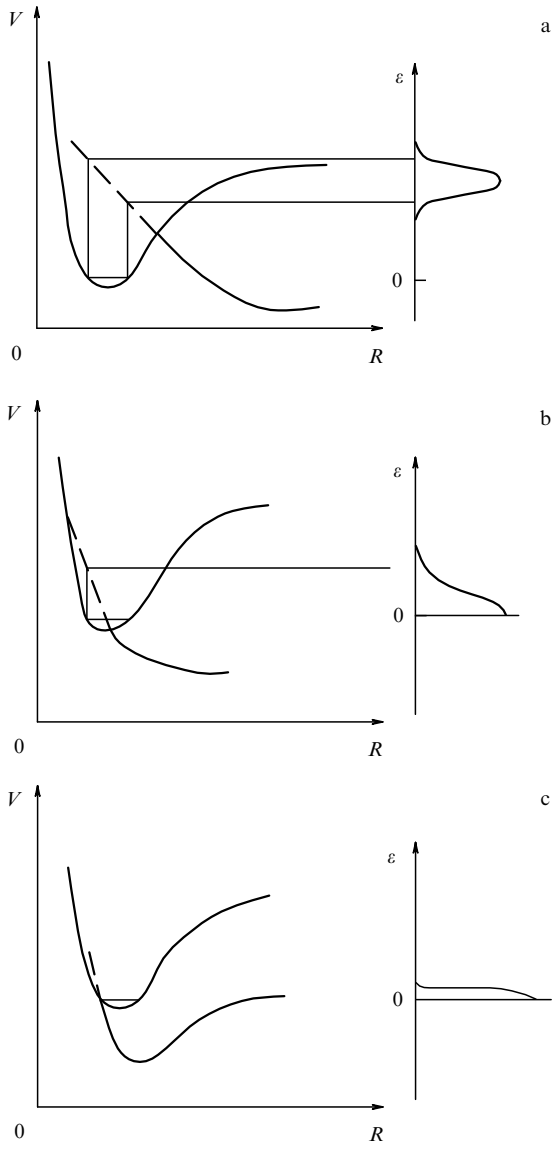

Figure 1. Possible positions of electron terms of the autodetachment state of the negative ion and the molecular ground state which are responsible for electron capture in the electron attachment process. The cross sections of the electron attachment processes as a function of the electron energy are drawn to the right of the electron terms for a given position of terms.

Here τ_e is a typical time of electron capture, $\hbar\omega$ is the difference of energies of closest states for final channels resulting from the decay of the autodetachment state $(A^-)^{**}$. For example, if the final state is a vibrationally excited state of the molecule, $\hbar\omega$ is the difference between the energies of neighboring vibrationally excited states. Note that typical times $\hbar/\Gamma$ and $1/\omega$ may be in arbitrary relation. If $\Gamma \sim \hbar\omega$, the interference of nuclear states is essential for the final state of the system. This requires a careful analysis of the transition process in this case.

2.2 Decay of autodetachment states

The autodetachment state, formed as a result of electron capture, decays over time, and the character of its decay determines the channels of the total process. Table 1 contains the list of processes which proceed from the formation of an autodetachment state. The first channel of this list corre-

Table 1. Processes proceeding via electron capture by a molecule on formation of an autodetachment state.

No.	Process	Scheme
1	Elastic electron – molecule scattering	$e + AB \rightarrow (AB^-)^{**} \rightarrow e + AB$
2	Excitation of vibrational levels by electron impact	$e + AB(v) \rightarrow (AB^-)^{**} \rightarrow e + AB(v')$
3	Dissociative attachment of electron to molecule	$e + AB \rightarrow (AB^-)^{**} \rightarrow A^- + B$
4	Associative detachment of negative ion	$A^- + B \rightarrow (AB^-)^{**} \rightarrow e + AB$
5	Three-body electron attachment to molecule	$e + AB \rightarrow (AB^-)^{**}$; $(AB^-)^{**} + C \rightarrow AB^- + C$

sponds to returning to the initial state of the electron and atomic system:

$$e + A \rightarrow (A^-)^{**} \rightarrow e + A\,. \tag{2.5}$$

In this case the intermediate state is observed in the form of resonances in the total or differential cross sections of electron scattering and this process is of importance for the simplest atomic systems — atoms and diatomic molecules.

The other channels correspond to excitation of the atomic system. The main process of this kind leads to vibrationally excited diatomic molecules:

$$e + AB(v = 0) \rightarrow (AB^-)^{**} \rightarrow e + AB(v)\,, \tag{2.6}$$

where v is the vibrational quantum number. This mechanism of excitation of diatomics leads to large cross sections of excitation of vibrational states compared to that resulting from direct excitation, and the difference between these cross sections is several orders of magnitude. Hence, the possibility of formation of an autodetachment state according to process (2.3) is principle for vibrational excitation of molecules.

For example, the excitation energy of autodetachment states of the negative ion N_2^- corresponds to typical electron energies of gas discharges, so that the electric energy of gas discharge is transformed effectively to the energy of vibrational excitations of nitrogen molecules by way of autodetachment states. It provides a high efficiency for gas discharge lasers based on this process. For oxygen molecules there is no such possibility.

The process which leads to formation of negative ions as a result of electron attachment to a molecule is known as the dissociative attachment process and proceeds according to the scheme

$$e + XY \rightarrow (XY^-)^{**} \rightarrow X + Y^-\,. \tag{2.7}$$

In this case the energy excess due to the capture of a free electron is consumed by breaking a chemical bond. The principal difference of this process for diatomic and polyatomic molecules consists in the values of the lifetime and the character of decay of the autodetachment state $(XY^-)^{**}$. In the case of a diatomic, the lifetime is determined by the time of nuclear motion along a repulsive term of the autodetachment state from a capture distance R_0 up to the distance R_c of intersection of the electron terms. At $R > R_c$ this state becomes stable. This time is of the order of

$$\tau \sim \frac{R_c - R_0}{v_a} \sim 10^{-14} - 10^{-13}\ \text{s}\,, \tag{2.8}$$

because $R_c - R_0 \sim 1$ A, and a typical nuclear velocity is $v_a \sim 10^5 - 10^6$ cm s^{-1}. In the case of a diatomic molecule, when the electron term of the autodetachment state has the form of a well, the decay of the negative ion formed proceeds over one or several oscillations of the nuclei in the negative ion depending on the width of the autodetachment level. Hence, the lifetime of this state ranges $10^{-14} - 10^{-12}$ s. Note that this lifetime corresponds to intermediate autodetachment states formed in the course of three-body collisions (see Table 2)

$$A^- + B \rightarrow (AB^-)^{**}; \quad (AB^-)^{**} + C \rightarrow AB^- + C\,. \tag{2.9}$$

Table 2. The lifetimes of autodetachment states of negative ions produced in three-body collisions of negative ions and molecules [2]. Lifetimes are expressed in 10^{-11} s and are determined on the basis of the rate constants of three-body collisions.

Ion	Lifetime, 10^{-11} s	Third particle	N_0, 10^{19} cm^{-3}
O_4^-	0.3	O_2	60
	0.3*	He	70
CO_3^-	30	CO_2	0.4
	80	He	0.2
	100*	He	0.1
CO_4^-	0.4	CO_2	3
	1	O_2	1
	3*	He	0.6
$NO^- \cdot CO_2$	3	Ar	0.5
$O_2^- \cdot H_2O$	9	O_2	0.2
$O_2^- \cdot (H_2O)_2$	30	O_2	0.05
$NO_2^- \cdot H_2O$	9	NO	0.2
$Cl^- \cdot H_2O$	7	NO	0.2
Br_3^-	3	Br_2	0.7

* $T = 200$ K.

This process leads to the formation of the bound state AB^- in three-body collisions through an autodetachment state $(AB^-)^{**}$ which is quenched by a gaseous atomic particle C. Hence the lifetime of an intermediate autodetachment state determines the rate constant of the three-body process. These lifetimes obtained from the rate constants of the process are given in Table 2, where N_0 is the number density of the third particles at which the rate of the three-body process is equal to the rate of polarization capture in pair collisions.

In the case of complex molecules the energy surplus is distributed over various oscillations of a complex negative ion, so that its lifetime significantly exceeds that for diatomic ions. Let us demonstrate this tendency with the example

$$e + SF_6 \rightarrow (SF_6^-)^{**} \rightarrow e + SF_6\,, \tag{2.10}$$

taking the electron affinity of SF_6 to be 1.0 ± 0.2 eV as follows from measurements [12–22]. Note that the formation of the autodetachment state $(SF_6^-)^{**}$ leads to a redistribution of this energy between 15 vibrational degrees of freedom and causes an increase of the vibrational temperature of the molecule by 700–800 K. The decay of the autodetachment state proceeds if an energy of more 1.0 eV collects on the degree of freedom which is responsible for this process. Because of the small probability of such an event, the lifetime of an autodetachment state of a polyatomic negative ion exceeds that of a diatomic negative ion by several orders of magnitude. In Table 3 we give the measured lifetimes of autodetachment

Table 3. The lifetimes τ (in 10^{-5} s) for autodetachment states of polyatomic negative ions formed by electron attachment to the corresponding molecules. N is the number of vibrational degrees of freedom for these molecules.

Molecule	N	τ	Molecule	N	τ
SF_4	9	1.7 [23]; 1.6 [24]	$C_6D_5NO_2$	36	2.2 [31]
SF_6	15	2.5 [14, 25]; 6.8 [24]; 1.0 [26]	m-$C_6H_4ClNO_2$	36	4.7 [31]
CH_3CO_2	15	1.2 [14]	$C_6H_3F_2NO_2$	36	4.7 [29]
C_4F_6	24	6.9 [27]; 1.6 [28]	C_7F_8	39	1.2 [27]; 3.8 [29]
c-C_4F_6	24	1.1 [28]	C_6F_{10}	42	11 [27]
C_6F_6	30	1.2 [27]; 1.3 [29]	C_5F_{12}	45	1.3 [28]
C_4F_8	30	1.2 [27]; 3.0 [28]	n-C_5F_{12}	45	3.4 [28]
c-C_4F_8	30	1.5 [28, 30]	$C_6H_4CH_3NO$	45	3.0 [29]
C_6F_5Cl	30	1.8 [31]	C_6F_{12}	48	40 [27]
C_6F_5Br	30	2.1 [31]	n-C_6F_{12}	48	24 [28]
C_5F_8	33	5 [27]	$C_{10}F_8$	48	12 [31]
c-C_5F_8	33	2.7 [28]	$C_{10}H_8$	48	0.8 [32]; 0.7 [33]
C_6H_5CN	33	0.5 [31]	$C_{10}D_8$	48	0.8 [32]
C_6F_5CN	33	1.7 [31]	$C_{10}H_6O_2$	48	35 [34]
C_6F_5CHO	36	3.6 [31]	$C_6H_3(CH_3)_2NO_2$	54	2.0 [29]
$C_6H_5NO_2$	36	4 [25]; 4.7 [21]; 4.9 [28]; 1.8 [30]	C_7F_{14}	57	79 [26]

states of polyatomic negative ions. Note that due to the nature of the decay of these states, the probability of survival for these autodetachment states does not have an exponential dependence on time [1]. Hence, these data can be considered as estimates.

2.3 Lifetime of the autodetachment state

The lifetime of long living autodetachment states of negative ions of complex molecules is determined as the lifetime of these negative ions in a mass spectrometer, i.e. it reflects a certain stage of development of this state. Table 3 contains the results of such measurements. Below we use a simple model to determine the lifetime of an unstable negative ion formed as a result of electron capture in an autodetachment term. Let us denote the nuclear configuration which is responsible for electron capture by R_m and the nuclear configuration which corresponds to maximum electron binding energy EA by R_-. Evidently, the configuration R_m corresponds to an optimal nuclear configuration in the molecule at which the excitation energy of the autodetachment state of the negative ion coincides with the energy ε of the captured electron. Hence, an energy $EA+\varepsilon$ is transformed into vibrational energy if the nuclear configuration varies from R_m up to R_-.

For determination of the lifetime of the negative complex ion in an autodetachment state we use the statistical theory of its decay in the RRKM form [35]. Assuming the surplus electron energy to be transformed into vibrational energy, we have for the lifetime τ of the formed instable state of the negative ion

$$\tau=\tau_0\frac{\int_{EA(R)>0}n(R)\,\mathrm{d}R}{\int_{EA(R)<0}n(R)\,\mathrm{d}R}\,,$$

where $n(R)$ is the number of vibrational states, τ_0 is the typical time of variation of the distribution function over vibrational states in the system. Evidently, this value is of the order of the time of nuclear vibration in the molecule, i.e. $\tau_0\sim10^{-14}-10^{-13}$ s. Because in reality $\tau/\tau_0\sim10^8-10^9$, instead of the above formula the following estimate may be used:

$$\tau=\tau_0\frac{n(R_m)}{n(R_-)}\,.$$

Using the Born–Oppenheimer approximation for the system under consideration, we assume that each nuclear configuration leads to a certain electron energy which determines the nuclear energy, i.e. the energy of vibrations. We consider the statistics of vibrations of nuclei in the simplest form, on the basis of the Kompaneets model [36], according to which all vibrational frequencies ω of the complex ion are identical. Though it is a rough approximation, the result does not depend on vibrational frequencies, which justifies this model. In this case, the total number of excitations is $p=E/(\hbar\omega)$, where E is the total excitation energy. The total number of possibilities of distributions of vibrational states is

$$n=\frac{(p+s-1)!}{p!(s-1)!}\,,$$

where s is the number of vibrational degrees of freedom. The vibrational temperature T is connected with the above numbers by the Planck formula

$$\frac{s}{p}=\exp\frac{\hbar\omega}{T}-1\,.$$

Introducing the numbers of vibrations for the initial p_i and final p_f states, we have from the law of energy conservation

$$p_i\hbar\omega+EA+\varepsilon=p_f\hbar\omega\,.$$

We take here that an electron of energy ε is captured, and EA is the electron affinity of the molecule, i.e. the electron binding energy. From this one can find the connection between the lifetime of the autodetachment state and other parameters of the system. In order to demonstrate this, let us consider the case $p_i\gg s$, $p_f\gg s$. This corresponds to a high temperature when the vibrations become classical. In this case we have $p_i\hbar\omega=sT$, and

$$\ln\frac{\tau}{\tau_0}-1=\frac{EA+sT}{s\hbar\omega}\,,\quad p_f=s\left(\ln\frac{\tau}{\tau_0}-1\right)+p_i\,.$$

In particular, in the case of the molecule C_7F_8 we have $EA=1.7\pm0.3$ eV [37], and the lifetime $\tau=12$ μs (see Table 3). Then we get $\hbar\omega\approx30$ cm^{-1}. In the case of the molecule C_6F_{10} we obtain $EA=1.4\pm0.3$ eV [37], and the lifetime $\tau=110$ μs (see Table 3), so that we have

$\hbar\omega \approx 20\,\mathrm{cm}^{-1}$. We take the initial temperature to be $T = 300$ K and the electron energy $\varepsilon = 0$ in both cases. From this, on the basis of the above formulae, one can find the lifetime of the autodetachment states for other temperatures.

From the above formula it follows that the temperature dependence for the lifetime of the autodetachment state is

$$\tau = C \exp \frac{T}{\hbar\omega} .$$

Because, in considering examples of C_7F_8 and C_6F_{10}, we have $\hbar\omega \ll T$ at room temperature, this dependence changes abruptly. In particular, variation of the temperature from 300 K up to 350 K leads to a decrease of the lifetime by a factor of 3 in the case of C_7F_8 and by a factor of 5 for the molecule C_6F_{10} if we use the above formulae and parameters.

Note that the above consideration of a long-living state of complex molecules is based on the assumption of thermodynamic equilibrium of the autodetachment electronic state and nuclear motion. The negative ion is stable in this system, but the excitation energy for nuclear motion exceeds the electron binding energy. Then the release proceeds when a large energy is concentrated on the degrees of freedom which are responsible both for formation of the autodetachment state and its decay. A certain time is required for establishment of thermodynamic equilibrium. This time is determined by nuclear motion and can be estimated from analysis of the decay of the autodetachment ion forming a stable negative ion and a radical. In particular, such a time for the process was found in [38] for the processes:

$$\mathrm{K(55p) + CF_3Cl \rightarrow K^+ + CF_3 + Cl^-} ;$$
$$\mathrm{K(55p) + CF_2Cl_2 \rightarrow K^+ + CF_2Cl + Cl^-} .$$

When an electron is captured by the molecule, the negative ion obtains a momentum as a result of the Coulomb interaction with the potassium positive ion. Hence, the final momentum of Cl^- depends on the time when this ion is formed, and measurement of the angular distribution of motion of the negative chlorine ions allows one to determine the time of formation of Cl^-. This time is equal to 3.5 ps for the first process, and 4.5 ps for the second process. In the same manner the lifetime of CCl_4^- was determined as 10 – 30 ps [39] with respect to the decay of its autodetachment state formed in chemionization collisions of a sodium Rydberg atom with the molecule CCl_4. The lifetime of the autodetachment state of CF_3I^- is less than 2 ps [40]. This decay character of the negative ion differs from that above, so that the presence of both mechanisms makes the probability of survival of the negative ion not exponential with time.

2.4 Rate constant of electron capture in the autodetachment state

The process of formation of an autodetachment state as a result of electron capture is the first stage of the process of formation of negative ions in electron-molecule collisions (see Table 1). Let us evaluate the order of the rate constant of this process under favourable conditions. In the classical limit for nuclei we have for the capture cross section, according to the Breit – Wigner formula,

$$\sigma_{\mathrm{cap}}(R) = \frac{\pi\hbar^2}{2m_e\varepsilon} \frac{\Gamma^2(R)}{\left[\varepsilon - E(R)\right]^2 + \Gamma^2(R)/4} . \qquad (2.11)$$

Here R denotes the nuclear configuration, ε is the electron energy, E is the difference of energies for electron terms of the autodetachment state of the negative ion and the initial molecular state, and Γ is the width of the autodetachment level. From this it follows for the rate constant of electron capture in the autodetachment level in the case of the Maxwell distribution function of free electrons by energies:

$$k_{\mathrm{cap}} = \langle v\sigma_{\mathrm{cap}} \rangle = \frac{2\sqrt{2\pi}\hbar^2}{m_e^{3/2}T_e^{3/2}} \times \left\langle \Gamma^2(R) \int_0^\infty \exp\left(-\frac{\varepsilon}{T}\right) \mathrm{d}\varepsilon \left\{ \left[\varepsilon - E(R)\right]^2 + \frac{\Gamma^2(R)}{4} \right\}^{-1} \right\rangle , \qquad (2.12)$$

where the angular brackets indicate averaging over the nuclear configurations at which the electron capture proceeds.

Evidently, favourable conditions for electron capture correspond to the case when the electron terms of the initial molecule state and the formed autodetachment state are close, as in Fig. 1b. Then $E \ll T$, and we have for the rate constant of electron capture

$$k_{\mathrm{cap}} = \frac{2\sqrt{2\pi}\hbar^2}{m_e^{3/2}T_e^{3/2}} \left\langle \int_0^\infty \frac{\Gamma^2}{\varepsilon^2 + \Gamma^2/4} \exp\left(-\frac{\varepsilon}{T}\right) \mathrm{d}\varepsilon \right\rangle .$$

This gives in the limiting cases:

$$k_{\mathrm{cap}} = \left(\frac{2\pi}{m_e T_e}\right)^{3/2} \hbar^2 \langle \Gamma(R) \rangle , \quad \Gamma \ll T , \qquad (2.13a)$$

$$k_{\mathrm{cap}} = \frac{4\sqrt{2\pi}\hbar^2}{m_e^{3/2}T_e^{1/2}} , \quad \Gamma \gg T . \qquad (2.13b)$$

Formula (2.13b) gives the maximum possible rate constant for electron capture in an autodetachment level of a negative ion. At room temperature, i.e. for thermal electron collisions, this formula yields $k_{\mathrm{cap}} = 2 \times 10^{-6}$ cm^3 s^{-1}. It is clear that any real rate constant of electron capture in thermal collisions is lower than this. Note that under favourable conditions of electron capture, this process gives a significant contribution to the cross section of elastic electron-molecule scattering.

Let us analyze the process of electron capture by a molecule from another standpoint. At small electron energies only s-scattering is essential for electron capture. Assuming the effective molecular field to be spherically symmetric, one can express the cross section of electron capture through the s-phase of electron scattering:

$$\sigma_{\mathrm{cap}} = \frac{2\pi\hbar^2}{m_e\varepsilon} \sin^2 \delta_c ,$$

where δ_c is the phase of s-scattering which is responsible for electron capture. One can see that the cross section of electron capture is restricted by the value

$$\sigma_{\mathrm{cap}} \leqslant \frac{2\pi\hbar^2}{m_e\varepsilon}$$

and the upper limit for the rate constant of electron capture is

$$k_{\mathrm{cap}} \leqslant \frac{4\sqrt{2\pi}\hbar^2}{m_e^{3/2}T_e^{1/2}} ,$$

that corresponds to formula (2.13b), though other assumptions were used here.

Thus, formula (2.13b) may be used as the upper limit for the rate constant of electron attachment to a molecule via formation of an autodetachment state. Comparing a measured rate constant of electron capture by a certain molecule with this one, one can determine whether the parameters of the system are optimal for this process or not.

2.5 Autodetachment states in the chemionization of Rydberg atoms

Chemionization proceeds according to the scheme

$$A^* + B \rightarrow A^+ + B^- . \tag{2.14}$$

If an atom A is found in a highly excited (Rydberg) state, process (2.14) is like electron attachment to a molecule B. Then the rate constant of process (2.14) is close to the rate constant of process (2.5). The criterion of this situation is that the Massey criterion for transition between neighboring excited states of an atom A is small. The Massey criterion is

$$\xi = \frac{a\Delta E}{\hbar v} \gg 1 , \tag{2.15}$$

where ΔE is the energy difference for neighboring excited states of identical angular quantum numbers, a is the typical distance over which parameters of the quasimolecule vary significantly, and v is a collision velocity. In this case $\Delta E = 2\mathrm{Ry}/n^3$, where n is the principal quantum number of the excited atom, $\mathrm{Ry} = 13.6$ eV is the ionization potential of the hydrogen atom in the ground state, $a \sim n^2 a_0$ is of the order of the atomic radius (considering the case $l \ll n$, where l is the quantum number of the orbital momentum). Thus in the case

$$v \gg \frac{e^2}{\hbar n} \tag{2.16}$$

one can consider the electron spectrum in the excited atom to be continuous. In reality, this criterion is established more accurately on the basis of measurements. Indeed, in the region of collision velocities or principal quantum numbers where the adiabatic criterion is fulfilled, the cross section or rate constant of process (2.14) depends sharply on the principal quantum number n of excited states. We are working in the other limiting case, as in (2.16), where the n-dependence for the rate constant is weak or absent. Then the rate constant of process (2.14) must coincide with the rate constant of electron capture by a molecule B if each electron capture leads to strong electron scattering accompanied by ionization of the Rydberg atom. Table 4 contains the measured rate constants [41 – 47] for process (2.14) involving Rydberg states of excited atoms and the electronegative molecules SF_6 and CCl_4. The statistical treatment of these data yields for a rate constant of the process: $k_{\mathrm{chem}}(SF_6) = (4.2 \pm 0.3) \times 10^{-7}$ cm^3 s^{-1}, $k_{\mathrm{chem}}(CCl_4) = (6 \pm 2) \times 10^{-7}$ cm^3 s^{-1}.

Because of the difference between processes (2.5) and (2.14) which have an identical basis for an electronegative complex molecule, we consider the character of the chemionization process in more detail. As a result of a prompt electron capture at $t = 0$, according to (2.1) the nuclear wave function takes the form

$$\Psi(R, t) = \sum_j f_{0j} \Phi_j(R) \exp\left(-\frac{\mathrm{i}E_j t}{\hbar} \right) , \tag{2.17}$$

where $\Phi_j(R)$ is the nuclear wave function which corresponds to the jth state of the nuclei, E_j is the energy of this state, R is a sum of nuclear coordinates, and f_{0j} is the amplitude of the electron capture with the nuclear transition from the initial state 0 to the final state j. In the case of resonant electron capture, the capture amplitude is given by the Breit – Wigner formula [11]

$$f_{0j} = \frac{\hbar}{\sqrt{2m_e\varepsilon}} \frac{S_{0j}\Gamma/2}{\varepsilon - E_j + \mathrm{i}\Gamma/2} . \tag{2.18}$$

Here ε is the electron energy, m_e is the electron mass, we take $E_0 = 0$, Γ is the total width of the autodetachment level, and S_{0j} is the overlapping integral for the nuclear wave functions of the initial and final configurations of nuclei. Note that this wave function may be normalized in any way, and we will use the normalization per unit flux, so that $4\pi|f_{0j}|^2$ is the cross section of the electron capture for a given nuclear state. This is the general expression for the wave function where the prompt and resonant character of electron capture is used. In the classical limit, formula (2.18) gives

$$f = \frac{\hbar}{\sqrt{2m_e\varepsilon}} \frac{\Gamma/2}{\varepsilon - E + \mathrm{i}\Gamma/2} , \tag{2.19}$$

where E is the difference energy between electron states of the transition (or between electron terms of the initial and final states). From this we have for the cross section of electron capture

$$\sigma_{\mathrm{cap}} = \frac{\pi}{k^2} \frac{\Gamma^2}{(\varepsilon - E)^2 + \Gamma^2/4} , \tag{2.20}$$

where $k = \sqrt{2m_e\varepsilon}/\hbar$ is the electron wave number.

There are two possibilities of decay of the autodetachment state formed. The first channel returns the system to the initial state, the second channel corresponds to the scheme (2.5) and leads to formation of a stable negative ion. Then one can divide the width of the autodetachment level into two parts $\Gamma = \Gamma_e + \Gamma_{\mathrm{neg}}$, so that Γ_e corresponds to elastic and vibrational excitation in electron-molecule scattering, and Γ_{neg} respects to formation of the negative ion. The cross section of electron attachment to a molecule in this case is

$$\sigma_{\mathrm{at}} = \frac{\pi}{k^2} \frac{\Gamma_{\mathrm{neg}}^2}{(\varepsilon - E)^2 + \Gamma^2/4} . \tag{2.21}$$

Table 4. Rate constants (in units 10^{-7} cm^3 s^{-1}) of the process (2.11): $A^* + SF_6 \rightarrow A^+ + SF_6^-$ or $A^* + CCl_4 \rightarrow A^+ + CCl_4^-$ in thermal collisions. Alongside with the sort of atom, the quantum number l of its angular momentum is indicated.

Atom A*	Xe(f)	Rb(s)	Rb(d)	K(d)	Na(p)	K(d)	K(p)	Ne(s)
$k_{\mathrm{chem}}(SF_6)$	4.0 ± 0.3	4.3 ± 0.7	4.2 ± 0.4	4.0 ± 0.6	4.4 ± 0.4	4.5 ± 0.5	4.0 ± 0.5	4 ± 1
$k_{\mathrm{chem}}(CCl_4)$	3.5 ± 0.5	—	—	4.0 ± 0.5	—	7 ± 1	10 ± 2	5 ± 1
Ref.	[41]	[42]	[42]	[43]	[44]	[45]	[46]	[47]

Now let us return to the problem under consideration. Considering the chemionization process (2.19), we construct the electron wave function as a combination of two states, so that in the first case its centre is the positive ion, and in the second case it is the molecule. Then the amplitude of the location of the electron near the molecule is determined by the amplitude (2.21) with the total width of the autodetachment level. This means that the cross section of the chemionization process (2.19) is given by formula (2.16). From this follows the ratio of the rate constant of electron attachment to a molecule $k_{\rm at}$ and the rate constant of the chemionization $k_{\rm chem}$ involving a Rydberg atom and this molecule:

$$\frac{k_{\rm at}}{k_{\rm chem}} = \frac{\Gamma_{\rm neg}^2}{\Gamma^2} \,. \tag{2.22}$$

Note that the cross section of the chemionization process is the total cross section of electron scattering by the molecule, and this cross section coincides with the cross section of the capture of a slow electron by the molecule only if the electron capture determines electron scattering. We compare only the limiting cross sections in the region of small electron energies when the rate constant of the process does not depend on the electron energy. In another region of electron energies this correspondence disappears because of the different character of scattering for free and bound electrons. In addition, the range of quantum numbers of Rydberg atoms, from which the asymptotic character of the process starts, is $n^* = 30-50$. For larger values of the principal quantum number, the Massey parameter (2.15) is small and criterion (2.16) is fulfilled. This means classical behaviour for the bound electron. Hence, at these values of the principal quantum number the rate constant of chemionization does not depend on n^*, so that it coincides with the rate constant of scattering of a very slow free electron by the molecule.

Table 4 contains values of the rate constants for chemionization of Rydberg atoms in thermal collisions with molecules SF_6 and CCl_4. The statistical error of results is given in Table 4, so that the systematic error of each measurement is not taken into account. Note that the rate constant of electron attachment to the SF_6 molecule tends to its asymptotic limit at electron energies $\varepsilon < 2$ meV, corresponding to $n^* \sim 100$. In reality, a weak dependence of the rate constant of the chemionization process is observed at smaller values of the principal quantum numbers n^*, and the rate constant in this range is taken as the asymptotic one. A subsequent comparison with the asymptotic rate constant of the capture of slow free electrons shows the coincidence of these values within the limits of the accuracy of the data, though this accuracy is not high.

2.6 Excitation of the vibrational levels of molecules via the autodetachment state

Formation of an autodetachment state in electron-molecule collisions may be an intermediate stage in the excitation of a molecule by electron impact. Due to the resonant character of this process, such a mechanism for excitation of vibrational molecular levels is more effective than direct excitation of molecular vibrations. For this reason, the cross sections of vibrational excitation of molecules by electron impact in a given energy range may differ by orders of magnitude for some molecules, depending on the existence of an autodetachment electron term through which this process can proceed. In particular, for nitrogen molecules and electron energies of the order of electronvolts, the vibrational excitation proceeds effectively because of the existence of an autodetachment state for the nitrogen diatomic negative ion with profitable parameters for this process. For this reason, in nitrogen gas discharges, the energy of an external field is transmitted to vibrational excitation of molecules at the first stage of energy transformation. This leads to a high efficiency in CO_2-gas lasers where this way of transforming electrical energy is used.

Now our goal is the deduction of formulae for the cross section of vibrational excitation of molecules via an autodetachment state in electron-molecule collisions [48]. We consider this process under condition (2.4), so that instant electron capture in an autodetachment state takes place. Subsequent development of this system and its decay is accompanied by the interference of intermediate states in the general case. If we neglect this interference (see, for example, [49]), the result will be not correct for any relation between a typical decay time $\hbar/\Gamma$ and a typical vibrational time $1/\omega$, where $\hbar\omega$ is the difference of energies of neighboring vibrational levels of a molecule which we model by a harmonic oscillator.

Let us construct the wave function of the electron-molecule system. Take the wave function of an autodetachment state in form (2.17). This wave function is normalized per unit electron flux, so that the cross section of electron capture is

$$\sigma_{\rm cap} = 4\pi \sum_j \left| \langle \Phi_j(R) | \Psi(R,t) \rangle \right|^2 = 4\pi \sum_j |f_{0j}|^2 \,, \tag{2.23}$$

where $\Phi_j(R)$ is the nuclear wave function of the autodetachment state, and R is the sum of nuclear coordinates. Labelling the molecular nuclear wave function $\varphi_k(R)$, the initial molecular state we denote by the subscript 0. Then after decay of the autodetachment state the nuclear wave function takes the form

$$\Psi_{\rm mol}(R,t) = \sum_{j,k} f_{0j} S_{jk} \varphi_k(R) \exp\left(-\frac{{\rm i}E_k t}{\hbar} \right), \tag{2.24}$$

where the overlapping integral is $S_{jk} = \langle \Phi_j(R) | \varphi_k(R) \rangle$. From this we obtain the cross section of excitation of the molecule to k-th level, if decay of the autodetachment state proceeds at time t after its formation:

$$\begin{aligned} \sigma_{0{\rm k}}(t) &= 4\pi |\langle \varphi_k(R) | \Psi_{\rm mol}(R,t) \rangle|^2 \\ &= 4\pi \sum_{j,j'} f_{0j} f_{0j'}^* S_{jk} S_{j'k}^* \varphi_k(R) \exp\left[-\frac{{\rm i}(E_j - E_{j'})t}{\hbar} \right]. \end{aligned} \tag{2.25}$$

Now let us average formula (2.25) over a decay time. We use the probability of decay of the autodetachment state during a time interval from t up to $t + {\rm d}t$:

$$\frac{\Gamma\,{\rm d}t}{\hbar} \exp\left(-\frac{\Gamma t}{\hbar} \right).$$

Note that here we assume the level width Γ to be independent of the nuclear configuration. Using this in formula (2.25), as a result of averaging we get

$$\sigma_{0{\rm k}} = \int_0^\infty \sigma_{0{\rm k}}(t) \frac{\Gamma\,{\rm d}t}{\hbar} \exp\left(-\frac{\Gamma t}{\hbar} \right) = 4\pi \sum_{j,j'} f_{0j} f_{0j'}^* S_{jk} S_{j'k}^* \times \frac{\Gamma}{\Gamma + {\rm i}(E_j - E_{j'})} \,. \tag{2.26}$$

We use the Breit–Wigner formula (2.18) for the capture amplitude taking into account the variation of the nuclear wave function resulting from electron capture. It gives the cross section of a vibrational excitation of a molecule by electron impact if this process proceeds via formation of the autodetachment state of the negative molecular ion [48]:

$$\sigma_{0k} = \frac{\pi\hbar^2}{2m_e\varepsilon}\sum_{j,j'}\frac{\Gamma S_{0j}S_{jk}}{\varepsilon - E_j + i\Gamma/2}\,\frac{\Gamma S_{0j'}S^*_{j'k}}{\varepsilon - E_{j'} - i\Gamma/2} \times \frac{\Gamma}{\Gamma + i(E_j - E_{j'})}\,. \tag{2.27}$$

In accordance with the deduction, this formula accounts for the interference of nuclear states in the course of the electron transition. Below we consider the limiting cases of this formula.

In the case when the lifetime of the autodetachment state is relatively small, we use the relation

$$\sum_j S_{mj}\,S_{jk} = \sum_j \langle\varphi_m(R)|\Phi_j(R)\rangle\langle\Phi_j(R)|\varphi_k(R)\rangle = \langle\varphi_m(R)|\varphi_k(R)\rangle = \delta_{mk}$$

that gives for the cross section of electron capture

$$\sigma_{\rm cap} = \sum_k \sigma_{0k} = \frac{\pi\hbar^2}{2m_e\varepsilon}\sum_{j,j'}\frac{|\Gamma S_{0j}|^2}{(\varepsilon - E_j)^2 + \Gamma^2/4}\,, \quad \Gamma \gg \Delta E\,,$$

in accordance with formula (2.23). Here ΔE is a typical separation between neighboring nuclear levels.

In the limit of small width Γ of the autodetachment level, the interference disappears, and exchanging the value $\Gamma\,[\Gamma + i(E_j - E_{j'})]$ in formula (2.27) in this limit for $\delta_{jj'}$, we transform this formula to the form

$$\sigma_{0k} = \frac{\pi\hbar^2}{2m_e\varepsilon}\sum_j\frac{\Gamma^2|S_{0j}|^2|S_{jk}|^2}{(\varepsilon - E_j)^2 + \Gamma^2/4} = \sum_j \sigma^{(j)}_{\rm cap}|S_{jk}|^2\,, \quad \Gamma \ll \Delta E\,, \tag{2.28}$$

where $\sigma^{(j)}_{\rm cap}$ is the cross section of electron capture in the autodetachment state with the nuclear jth state.

We denote a vibrational level of the autodetachment state by the subscript j, i.e. we consider the electron term of the autodetachment state to be attractive. But the formal apparatus of quantum mechanics allows one to consider this electron term as both attractive and repulsive. In order to transit to a repulsive electron term of the autodetachment state, we will consider the nuclear spectrum of the autodetachment state to be continuous. Then the nuclear wave function is concentrated near the turning point of the nuclei. We denote by R the nuclear coordinate which is responsible for the transitions under consideration. R_j is the turning point of jth nuclear state, and it satisfies the relation $E(R_j) = \varepsilon$, where $E(R)$ is the difference of the energies of electron terms for the autodetachment state and the initial molecular state. Then the nuclear wave function of the nuclear state is [50]

$$\Phi_j(R) = \sqrt{\frac{\hbar\omega}{E'(R_j)}}\,\delta(R - R_j)\,, \tag{2.29}$$

where $E'(R_j)$ is the derivative of the difference of the potential curves at the turning point, and $\hbar\omega$ is the energy difference between neighboring levels. From this we have

$$S_{0j} = \sqrt{\frac{\hbar\omega}{E'(R_j)}}\,\varphi_0(R_j)\,.$$

Accounting for $\mathrm{d}j = \mathrm{d}E_j/(\hbar\omega) = E'(R_j)\,\mathrm{d}R_j/(\hbar\omega)$, we obtain for the cross section of vibrational excitation on the basis of formula (2.27) [48]:

$$\sigma_{0k} = \frac{\pi\hbar^2}{2m_e\varepsilon} \times \int\frac{\mathrm{d}R\,\mathrm{d}R'\Gamma^3(R)\varphi_0(R)\varphi^*_0(R')\varphi_k(R)\varphi^*_k(R')}{[\varepsilon - E(R) + i\Gamma(R)/2]\,[\varepsilon - E(R') - i\Gamma(R')/2]} \times \frac{1}{[\Gamma(R) + iE(R) - iE(R')]}\,. \tag{2.30}$$

We introduce the dependence of the level width on the nuclear coordinate into the formula. This formula is valid for a repulsive autodetachment electron term. In particular, it follows that for the total cross section of electron capture

$$\sigma_{\rm cap} = \frac{\pi\hbar^2}{2m_e\varepsilon}\int\frac{\mathrm{d}R\Gamma^2(R)|\varphi_0(R)|^2}{[\varepsilon - E(R)]^2 + \Gamma^2(R)/4} \tag{2.31}$$

in accordance with the Breit–Wigner formula and Born–Oppenheimer approximation. Above we have used the relation

$$\sum_k \varphi_k(R)\varphi^*_k(R') = \delta(R - R')\,,$$

which accounts for the completeness of the system of the wave functions $\{\varphi_k\}$.

Thus, this analysis allows us to deduce expressions for the cross sections of electron-molecule collisions which proceed through electron capture in an autodetachment level. We make use of the fact that the electron subsystem is faster than the nuclear one (the Born–Oppenheimer approach) and the electron capture has a resonant character. The interference of intermediate states influences the development of the electron-molecule system. The formulae obtained can be used for any channels of decay of the autodetachment state.

3. Attachment of electrons to diatomic molecules

3.1 Peculiarities of electron attachment to molecules

The process of attachment of electrons to molecules proceeds through the formation of an autodetachment state:

$$e + AB \to (AB^-)^{**} \to A^- + B\,. \tag{3.1}$$

The cross section of the first stage of the process — electron capture is given by formulae (2.11), (2.31):

$$\sigma_{\rm cap} = \frac{\pi\hbar^2}{2m_e\varepsilon}\int\frac{\mathrm{d}R\Gamma^2(R)|\varphi_0(R)|^2}{[\varepsilon - E(R)]^2 + \Gamma^2(R)/4}\,, \tag{3.2}$$

where R is the nuclear coordinate responsible for the process under consideration, and for a diatomic molecule R is the distance between molecular nuclei; the averaging is over the positions of nuclei where the electron capture process proceeds. We account for the nuclear spectrum for the

autodetachment electron term being continuous. The character of formation of the stable negative ion is as follows. When an electron is captured into a repulsive autodetachment term, the nuclei move until they reach a distance R_c starting from which the negative ion state becomes stable. Therefore, one can divide the width of the autodetachment state into two parts $\Gamma(R) = \Gamma_e(R) + \Gamma_{neg}(R)$, so that

$$\Gamma_e(R) = \Gamma(R)\left[1 - \exp\left(-\frac{1}{2}\int_R^{R_c}\frac{\Gamma(R')\,dR'}{\hbar v_R}\right)\right],$$

$$\Gamma_{neg}(R) = \Gamma(R)\exp\left(-\frac{1}{2}\int_R^{R_c}\frac{\Gamma(R')\,dR'}{\hbar v_R}\right). \tag{3.3}$$

Here Γ_e corresponds to elastic scattering and excitation of vibrational states, $\Gamma_{neg}(R)$ is the part of the level width which corresponds to formation of a stable negative ion, and $v_R = dR/dt$ is the velocity of nuclear motion along the electron term of the autodetachment state. Then $\exp(-\int \Gamma\,dt/\hbar)$ is the probability of survival of the autodetachment state. In principle, this value can be found from comparison of the rate constants of the electron attachment process and the chemionization process on the basis of formula (2.22). Unfortunately, the restricted accuracy of these values does not allow one to use this relation in reality.

Now we find the cross section of formation of a stable negative ion using the same method as for the deduction of formula (2.28), but taking into account the dependence $\Gamma(R)$. Then we obtain for the electron attachment cross section, i.e. for the cross section of the process (3.1):

$$\sigma_{at} = \frac{\pi\hbar^2}{2m_e\varepsilon}\int dR\frac{\Gamma^2(R)|\varphi_0(R)|^2}{[\varepsilon - E(R)]^2 + \Gamma^2(R)/4} \times \exp\left(-\int_R^{R_c}\frac{\Gamma(R')\,dR'}{\hbar v_R}\right), \tag{3.4}$$

where R is the capture coordinate. This formula admits the convenient integral relation

$$\int_0^\infty \sigma_{at}\varepsilon\,d\varepsilon = \frac{\pi^2\hbar^2}{m_e}\left\langle\Gamma(R)\exp\left(-\int_R^{R_c}\frac{\Gamma(R')\,dR'}{\hbar v_R}\right)\right\rangle, \tag{3.5}$$

where the averaging is over the distance R of electron capture.

Let us rewrite formula (3.4) in the limit

$$\Gamma \ll \frac{dE}{dR}\Delta R, \tag{3.6}$$

where ΔR is the amplitude of nuclear vibrations. Then one can use the change in formula (3.4):

$$\frac{1}{2\pi}\frac{\Gamma(R)}{[\varepsilon - E(R)]^2 + \Gamma^2(R)/4} = \delta[\varepsilon - E(R)],$$

and this formula gives

$$\sigma_{at}(\varepsilon) = \frac{\pi^2\hbar^2\Gamma(R_\varepsilon)}{m_e\varepsilon}\frac{|\varphi_0(R_\varepsilon)|^2}{dE/dR}\exp\left(-\int_{R_\varepsilon}^{R_c}\frac{\Gamma(R')\,dR'}{\hbar v_R}\right), \tag{3.7}$$

where the energy resonance gives $\varepsilon = E(R_\varepsilon)$.

If the initial molecular state is the vibrational ground state, the nuclear wave function has the form

$$|\varphi_0(R)|^2 = \frac{1}{\sqrt{\pi}\Delta R}\exp\left[-\frac{(R - R_0)^2}{\Delta R^2}\right], \tag{3.8}$$

where R_0 is the equilibrium distance between nuclei, and ΔR is the vibration amplitude. If criterion (3.6) is fulfilled, formula (3.7) yields

$$\sigma_{at}(\varepsilon) = \sigma_{max}\exp\left[-\frac{(\varepsilon - \varepsilon_0)^2}{(\Delta R\,dE/dR)^2}\right], \tag{3.9a}$$

where the maximum cross section corresponds to the electron energy $\varepsilon_0 = E(R_0)$, and is

$$\sigma_{max} = \frac{\pi^{3/2}\hbar^2}{m_e\varepsilon_0}\frac{\Gamma(R_0)}{\Delta R\,dE/dR}\exp(-\zeta), \tag{3.9b}$$

with

$$\zeta = \int_{R_0}^{R_c}\frac{\Gamma(R)\,dR}{\hbar v_R}. \tag{3.9c}$$

Let us consider this expression for the case when the level width Γ does not depends on R and $E(R)$ is a linear function. Then

$$E(R) = \varepsilon_0 = \frac{dE}{dR}(R_c - R_0)$$

and formula (3.9b) gives

$$\sigma_{max} = \frac{\pi^{3/2}\hbar^2}{m_e\varepsilon_0^2}\frac{\Gamma(R_c - R_0)}{\Delta R}\exp\left(-\frac{\Gamma\tau}{\hbar}\right), \tag{3.10}$$

where

$$\tau = \sqrt{\frac{2\mu(R_c - R_0)}{dE/dR}}$$

and μ is the reduced mass of the nuclei. Here at the distance R_c the excitation energy of the autodetachment term is zero, i.e. we introduce this distance taking into account the quantum character of vibrations. Note that the maximum of the cross section (3.10) with respect to Γ corresponds to $\Gamma\tau = 1$. The corresponding maximum cross section is

$$\sigma_{max} = \frac{\pi^{3/2}\hbar^2}{e\sqrt{2\mu}\,m_e\varepsilon_0^{3/2}\Delta R} = \frac{1.4\hbar^2}{\sqrt{\mu}m_e\varepsilon_0^{3/2}\Delta R}. \tag{3.11}$$

Because $\Delta R \sim \mu^{-1/4}$, formally we have $\sigma_{max} \sim \mu^{-1/4}$. But because in reality ε_0 is smaller than a typical atomic value, this cross section may be comparable with a typical atomic value. These results arise when the resonance in electron capture corresponds to a not small energy, i.e. the intersection of electron terms corresponds to Fig. 1a ($R_c > R_0$). From the above formulae it follows that the cross section of electron attachment is a monotone function of the electron energy, if the intersection of electron terms proceeds in the bottom of the molecular electron term or left of it (Fig. 1b, c).

The rate constant of the electron attachment process is determined in accordance with formula (3.5) and in the case $\Gamma \ll T_e$ has the form

$$k_{\rm at} = \frac{2}{\sqrt{\pi}T_{\rm e}^{3/2}}\int_0^\infty \sqrt{\frac{2\varepsilon}{m_{\rm e}}}\,\sigma_{\rm at}(\varepsilon)\sqrt{\varepsilon}\exp\left(-\frac{\varepsilon}{T_{\rm e}}\right)\mathrm{d}\varepsilon$$
$$= \left(\frac{2\pi}{m_{\rm e}T_{\rm e}}\right)^{3/2}\hbar^2\left\langle \Gamma(R)\exp\left[-\frac{E(R)}{T_{\rm e}}-\zeta\right]\right\rangle, \quad (3.12a)$$

where the angular brackets mean averaging over positions of nuclei and $E(R)$ is the excitation energy of the autodetachment state at a given distance between nuclei. In the case $E'_R\Delta R \gg T_{\rm e}$ the main contribution to the integral gives a small range of distances between nuclei as compared to ΔR. Then, assuming a weak dependence $\Gamma(R)$ for excitation energies $E(R) \sim T_{\rm e}$, from formula (3.12a) for the rate constant of electron attachment we obtain

$$k_{\rm at} = \hbar^2\left(\frac{2\pi}{m_{\rm e}}\right)^{3/2}\frac{\Gamma\varphi^2(R)}{\sqrt{T_{\rm e}}E'_R}\exp(-\zeta), \quad (3.12b)$$

where the excitation energy of the autodetachment state is zero at the distance R.

It is necessary to keep in mind that the above formulae correspond to certain quantum numbers of a free electron which are determined by the quantum numbers of the molecule and autodetachment state. The transition of the electron system from the molecular to autodetachment state of a given symmetry proceeds only for a certain orbital momentum or other quantum numbers of the captured electron.

3.2 Isotope effect in the dissociative attachment of electrons to diatomic molecules

The above formulae allows us to analyze the character and peculiarities of dissociative attachment of electrons to diatomic molecules. We start from the analysis of the isotope effect which was first predicted by Demkov [51] and observed by Schulz and Asundi [52]. In the case of isotope molecules, the main factor which depends on nuclear mass in formula (3.4) for the attachment cross section, is the survival factor. Let us introduce the probability of survival for the electron term of the autodetachment state:

$$P = \exp(-\zeta), \qquad \zeta = \int_{R_0}^{R_{\rm c}}\frac{\Gamma(R)\,\mathrm{d}R}{\hbar v_R}. \quad (3.13)$$

Since $\zeta \sim \mu^{-1/2}$, where μ is the reduced mass of the nuclei, we have

$$P_2 = (P_1)^{\sqrt{\mu_2/\mu_1}}. \quad (3.14)$$

Here μ_1, μ_2 are the reduced masses of the nuclei for two isotopes, and P_1, P_2 are the probabilities of survival which correspond to these reduced masses.

In the most spread case the isotope effect corresponds to diatomic molecules containing a hydrogen atom, so that changing the proton for a deuteron in this molecule leads to the isotope effect. In particular, in the case of hydrogen molecules according to experiments [53–55] we have for the maximum cross section of electron attachment $\sigma_{\rm at}({\rm H_2}) = 1.6\times10^{-21}\,{\rm cm^2}$, $\sigma_{\rm at}({\rm HD}) = 2.1\times10^{-22}\,{\rm cm^2}$ and $\sigma_{\rm at}({\rm D_2}) = 8\times10^{-24}\,{\rm cm^2}$. From this we obtain $\zeta = 13.1$ if we use formula (3.14) for the relation $\sigma_{\rm at}({\rm H_2})/\sigma_{\rm at}({\rm HD})$, we have $\zeta = 12.8$ on the basis of the relation $\sigma_{\rm at}({\rm H_2})/\sigma_{\rm at}({\rm D_2})$, and $\zeta = 12.6$ from the relation $\sigma_{\rm at}({\rm HD})/\sigma_{\rm at}({\rm D_2})$. This gives a maximum cross section of electron capture in the autodetachment term $\sigma_{\rm cap} = 6\times10^{-16}\,{\rm cm^2}$, and this cross section according to its nature does not depend on the nuclear mass. Next, the width of the autodetachment level is about 2 eV that is comparable to the calculated value of the width of the autodetachment level $H_2(^2\Sigma_u^+)$ [56–58] which has an excitation energy of about 4 eV.

In the case of HX molecules, where X is a halogen atom, this effect is weaker than in the above case. Table 5 gives some parameters of the attachment cross section. Then the maximum attachment cross section and the isotope effect allows us to find the parameter ζ which is defined according to formula (3.9c), and the maximum of the capture cross section $\sigma_{\rm cap}$. The effective width of the autodetachment level, on which the electron is captured in the process under consideration, is taken on the basis of formula $\Gamma_{\rm eff} = 2\int\sigma_{\rm at}(\varepsilon)\,\mathrm{d}\varepsilon/\sigma_{\max}$. As is seen, in these cases the parameter ζ is lower than in the case of the hydrogen molecule, so that the isotope effect is weaker. Note that in the case of the HI and DI molecules, the electron terms of the molecule and negative ion intersect near the bottom of the molecular terms. Hence, the above formulae give only a qualitative description of the process in this case. The rate constants for the electron attachment process are $(3.0\pm0.9)\times10^{-7}$ cm^3 s^{-1} and $(2.2\pm0.8)\times10^{-7}$ cm^3 s^{-1} for the HI and DI molecules, correspondingly [59]. Also, according to [25], the rate constant for electron attachment to the molecule HI at the temperature $T = 300$ K is 3.0×10^{-7} cm^3 s^{-1}, and for the molecule HBr it is 3.0×10^{-10} cm^3 s^{-1} at $T = 515$ K.

Table 5. Parameters of electron attachment to hydrogen-halogen molecules obtained on the basis of experiment [54].

Molecule	$\sigma_{\max}$, Å^2	ξ, eV Å^2	$\sigma_{\rm cap}$, Å^2	ζ	$\Gamma_{\rm eff}$, eV
HCl	0.18	0.078	0.5 ± 0.2	0.5 – 1.2	0.9
DCl	0.12	0.06	—	—	—
HBr	4.0	1.2	17	1.4	0.6
DBr	2.2	0.7	—	—	—
HI	230	3.7	760	1.2	0.03
DI	140	2.6	—	—	—

3.3 Energy and angular distribution of negative ions

Because of the energy conservation law for the processes of electron capture in the autodetachment electron term and its decay, the energy of the negative ions formed is connected with the energy of the incident electrons. Indeed, denoting the mass of a negative ion by m_-, the mass of an atom B in process (3.1) by m, the energy of incident electrons by ε and the energy of formed negative ions by ε_-, we have from the law of energy conservation

$$\varepsilon - D + EA = \frac{m}{m+m_-}\,\varepsilon_-, \quad (3.15)$$

where D is the dissociation energy of an AB molecule, and EA is the electron affinity of an A atom. This relation may be a basis for determination of the electron affinity. Such a method was used for this goal in the first stage of studying negative ions (see [1, 2]). Then the thermal motion of the molecule introduces an error into this value, and our goal is to find the distribution of negative ions by energies if these ions are formed as a result of process (3.1) and the incident electron energy ε is given.

If the initial molecular velocity is u, and the negative ion moves in the direction x in the centre-of-mass frame, the final

velocity of a negative ion formed is $[(v_- - u_x)^2 + u_\rho^2]^{1/2}$, where u_x, u_ρ are the components of the molecular velocity at the beginning, and according to formula (3.15) the velocity of the formed negative ion is

$$v_- = \sqrt{\frac{2(m+m_-)}{mm_-}(\varepsilon - D + EA)}\,.$$

Assuming $v \gg u$, one can neglect the transverse component of the initial molecular velocity. Therefore, we take the initial Maxwell distribution of molecular velocities in the form

$$f(u_x) = \sqrt{\frac{m+m_-}{2\pi T}}\,\exp\left[-\frac{(m+m_-)u_x^2}{2T}\right],$$

where T is the temperature of the molecules expressed in energy units. Since the final velocity of a negative ion is $v = v_- - u_x$, from this we have for the distribution of formed negative ions over energies $\varepsilon_- = m_- v^2/2$:

$$f(v)\,\mathrm{d}v = \sqrt{\frac{m_-}{2\pi T}}\exp\left[-\frac{(\sqrt{\varepsilon_-} - \sqrt{\varepsilon_0})^2}{T}\right]\mathrm{d}v\,, \qquad (3.16)$$

normalized per unit, and

$$\varepsilon_0 = \frac{m+m_-}{m}(\varepsilon - D + EA)$$

is the energy of a negative ion formed at zero molecular velocity.

Usually $\varepsilon_0 \gg T$ and the distribution function is narrow. But the width of the distribution function is of the order of $\sqrt{\varepsilon_0 T}$ that significantly exceeds the typical thermal energy. This fact decreases the accuracy of this method for determination of the electron affinity of atoms and molecules on the basis of the parameters of process (3.1) if we use the conservation law (3.15). In particular, the experimental results for the electron affinity obtained from the threshold of this process [60–64] are accompanied by an additional analysis. Measurement of the most probable kinetic energy of negative ions formed improves the accuracy of this method [62–64].

Because of the resonant character of the process (3.1), measurement of the energy dependence for the attachment cross section and comparison of it with the positions of the corresponding autodetachment electron terms allows one to determine the parameters of the autodetachment states responsible for the process at a given electron energy. The reliability of results is improved if the distribution of negative ions by energy is determined simultaneously. In particular, in this way one can extract the channels where the products of process (3.1) are found in an excited state. Additional information about the autodetachment state of the negative ion follows from the angular distribution of negative ions with respect to the direction of the incident electron beam. For example, in the case of the process

$$\mathrm{e} + \mathrm{O_2} \to (\mathrm{O_2^-})^{**} \to \mathrm{O^-} + \mathrm{O} \qquad (3.17)$$

at an electron energy of several electronvolts the process can proceed via the autodetachment states $^2\Pi_g$ and $^2\Pi_u$. Capture in these autodetachment states leads to a different angular dependence of the distribution of negative ions, and measurement of these dependences allows one to separate these processes. Table 6 gives the results of such a separation for channels of the process at various electron energies ε.

Table 6. Cross section of electron attachment to the oxygen molecule σ_{at} and the partial cross sections of this process σ_g and σ_u proceeding via the autodetachment states $^2\Pi_g$ and $^2\Pi_u$, correspondingly [65]. The cross sections are given in 10^{-19} cm^2.

ε, eV	σ_{at}	σ_g	σ_u
5.75	9.1	1.1	7.9
6.70	13.7	2.2	11.4
7.80	5.7	1.4	4.3
8.40	2.4	0.70	1.7

Additional information about this process follows from the mass-spectrometric analysis of the products of the electron attachment process in the pulse regime. The possibilities of this method are demonstrated by Fig. 2 which contains time-of-flight spectra for the process (3.17). In this method, the delay time of negative ions formed is connected with the kinetic energy of ions [7, 8]. Note the two-humped form of the ion spectrum in this case. This means that the negative ions are formed owing to two autodetachment terms $^2\Pi_g$ and $^2\Pi_u$. Next, the energy of the released negative ions O^- is connected with the energy of incident electrons by formula (3.15). This is demonstrated by Fig. 2c. The threshold of this process corresponds to the initial electron energy $\varepsilon = 3.56$ eV, because the dissociation energy of the oxygen molecule is $D = 5.12$ eV, and the electron affinity of the oxygen atom $EA = 1.46$ eV.

These data can be analyzed on the basis of the above formulae connecting the parameters of the attachment process with the parameters of the autodetachment state through which the process proceeds. In particular, in the case of a narrow resonance when electron attachment takes place at electron energies near ε_{max}, formula (3.5) takes the form

$$\langle \Gamma \exp(-\zeta)\rangle = \frac{m_e \varepsilon_{max}}{\pi^2\hbar^2}\int \sigma_{at}(\varepsilon)\,\mathrm{d}\varepsilon\,.$$

From this, for the oxygen resonance near 6.7 eV we get $\langle \Gamma \exp(-\zeta)\rangle = 2.9$ meV on the basis of measurements [66] and $\langle \Gamma \exp(-\zeta)\rangle = 3.2$ meV from experiment [67].

Let us analyze process (3.17) from the standpoint of electron states in the oxygen molecule. The outer electron shell of the oxygen atom is $O(2p^4)$ if we consider valent electrons to be identical and to be located in a spherically symmetric electric field. Then within the model of molecular orbits, the ground state of the oxygen molecule is characterized by the following distribution of electrons over molecular orbitals $O_2(\sigma_g^2\sigma_u^2\pi_g^2\pi_u^2)^3\Sigma_g$, so that according to the usual notation we denote the angular momentum projection onto the molecular axis by σ, π; subscripts g, u denote the symmetry of the electron wave function as a result of reflection with respect to the plane which is perpendicular to the molecular axes and bisects it, and the superscripts denote the number of electrons in a given state. The ground state of the negative molecular oxygen ion is $O_2^-(\sigma_g^2\sigma_u^2\pi_g^3\pi_u^2)^2\Pi_g$. The vibrationally excited states of this electron state of the negative molecular oxygen ion with vibrational quantum numbers $v \geqslant 4$ correspond to the autodetachment states which are formed as a result of collisions of a slow electron and oxygen molecule. But such collisions do not lead to the formation of negative atomic ions because of the small resonant electron energy compared to the dissociation

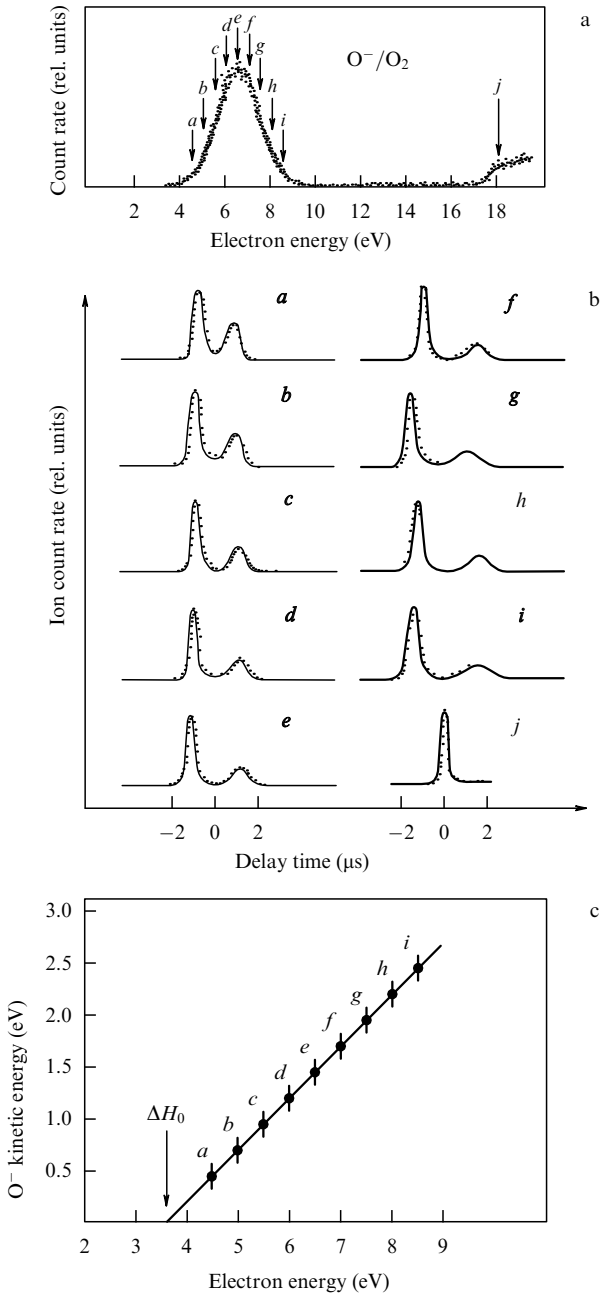

Figure 2. Electron attachment to the oxygen molecule. (a) The cross section of this process with formation of O^-. Values of the electron energy are indicated at which time-of-flight (TOF) spectrum was made. (b) TOF mass spectrum of ions O^-. (c) The kinetic energy of the negative ion O^- obtained from the above spectra as a function of the electron energy at indicated points.

energy of the oxygen molecule. The broad resonance in the cross section of electron attachment to an oxygen molecule in the range 5 – 8 eV corresponds to the following processes:

$$e + O_2(\sigma_g^2\sigma_u^2\pi_g^2\pi_u^2)^3\Sigma_g \rightarrow \left(O_2^-(\sigma_g^2\sigma_u^2\pi_g^2\pi_u^3)^2\Pi_u\right)^{**} \rightarrow \rightarrow O^-(^2P) + O(^3P)\,, \qquad (3.18a)$$

$$e + O_2(\sigma_g^2\sigma_u^2\pi_g^2\pi_u^2)^3\Sigma_g \rightarrow \left(O_2^-(\sigma_g^2\sigma_u^2\pi_g^3\pi_u^2)^2\Pi_g\right)^{**} \rightarrow \rightarrow O^-(^2P) + O(^3P)\,. \qquad (3.18b)$$

These processes do not change the internal molecular shell and hence are more intense than the processes which require reconstruction of the electron shell of the molecule. As follows from the Table 6 data, process (3.18a) is more intense than (3.18b).

A certain symmetry of the initial and intermediate electron states leads to a certain angular dependence for the amplitude of electron capture. In particular, in the case of the hydrogen molecule, when the molecular electron term has the symmetry $^1\Sigma_g^+$, the symmetry of the autodetachment state $^2\Sigma_g^+$ corresponds to a capture of s-electron, i.e. the angular distribution of captured electrons is spherically symmetric in this case. Table 7, as a demonstration of such an analysis, gives the connection of quantum numbers of the initial and intermediate electron states of molecular particles and the angular distribution of captured electrons in the case of hydrogen and oxygen molecules [68].

Table 7. Quantum numbers of transient states for electron capture in the autodetachment states of hydrogen and oxygen molecules and the angular distribution of captured electrons [68] (l is the angular momentum of the attaching electron, m is its projection onto the molecular axis, θ is the angle between the molecular axis and the incident electron).

Molecule	Autodetachment state	Electron parity	l	m	Angular distribution
$H_2(^1\Sigma_g^+)$	$H_2^-(^2\Sigma_u^+)$	−1	1	0	$\cos^2\theta$
$H_2(^1\Sigma_g^+)$	$H_2^-(^2\Sigma_g^+)$	1	0	0	const
$O_2(^3\Sigma_g^-)$	$O_2^-(^2\Pi_u)$	−1	1	1	$\sin^2\theta$
$O_2(^1\Sigma_g^+)$	$O_2^-(^2\Pi_u)$	−1	1	1	$\sin^2\theta$
$O_2(A^3\Sigma_u^+)$	$O_2^-(^2\Pi_u)$	1	2	1	$\sin^2 2\theta$

3.4 Dissociative attachment involving heated and excited molecules

The resonant character of electron capture in an autodetachment electron term in the electron attachment process involving a molecule determines the peculiarities of this process for heated molecules. One can see that the vibrational excitation of molecules widens the range of distances between nuclei for which electron capture takes place. It leads to a broadening of the resonance in the cross section of electron attachment to an excited molecule because the electron capture for vibrationally excited molecules becomes possible at lower energies than for molecules in the ground state. In addition, the cross section of electron attachment increases if the probability of survival of the autodetachment state is small, because the electron capture can proceed for larger distances between nuclei for which the probability of survival is not so small. These peculiarities of the attachment process are demonstrated in Fig. 3 where the cross section of electron attachment to the oxygen molecule as a function of the electron energy is given for different temperatures [70]. As is seen, an increase of the temperature of oxygen molecules leads to a shift of the resonance in electron attachment to low energies, to its broadening and to an increase of the maximum cross section of electron attachment [68, 70, 71]. The same character of the temperature dependence is shown for electron attachment to a molecule CO_2 [71 – 74], whereas in the case of electron attachment to the hydrogen molecule, variation of the temperature from 300 K up to 1300 K does not change the maximum cross section of this process [75].

Thus, if the probability of survival of the autodetachment state in which the electron capture takes place is small, the

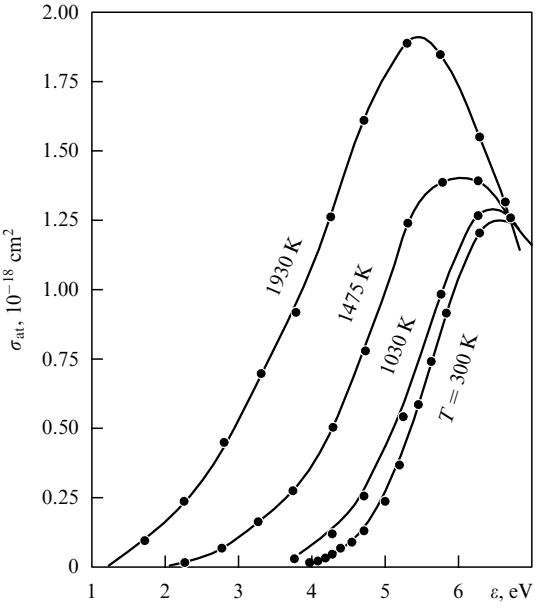

Figure 3. Cross section of dissociative attachment of an electron to an oxygen molecule as a function of the electron energy at different gas temperatures [66].

electron attachment cross section increases with the vibrational state of the molecule. In particular, in the case of the oxygen molecule, when the maximum cross section of the electron attachment process is 1.2×10^{-18} cm^2, the maximum cross section of electron attachment for the first vibrational level is estimated as 4×10^{-18} cm^2. Note that at a temperature of 1930 K only 21% of molecules are found in the first vibrational state and these maximum cross sections are small compared to the electron capture cross section.

Besides vibrational excitation, electron excitation of molecules influences the efficiency of the electron attachment process. Measurements of electron attachment to the metastable oxygen molecule $O_2(^1\Delta_g)$ show that the main resonance is like process (3.18a) and proceeds according to the scheme

$$e + O_2(\sigma_g^2\sigma_u^2\pi_g^2\pi_u^2)^1\Delta_g \rightarrow \left(O_2^-(\sigma_g^2\sigma_u^2\pi_g^2\pi_u^3)^2\Pi_u\right)^{**} \rightarrow O^-(^2P) + O(^3P)\,. \qquad (3.19a)$$

Note that the configuration of the electron shell is the same for the ground $^3\Sigma_g$ and metastable $^1\Delta_g$ states within the framework of the model of molecular orbitals. The maximum cross section for process (3.19a) is shifted with respect to the cross section maximum of process (3.18a) by about 1 eV [the excitation energy of $O_2(^1\Delta_g)$] to smaller electron energies, and the maximum cross section is several times more than in the case of process (3.18a) [76–78]. In particular, according to [78] the maximum cross section of electron attachment is 6.1×10^{-18} cm^2 at an energy of 5.7 eV, and the resonance width is 2.7 eV. From this, on the basis of formula (3.5), we have $\langle \Gamma \exp(-\zeta)\rangle = 14$ meV. This exceeds the same value for the ground state of the oxygen molecule by several times.

Evidently, by analogy with process (3.18b), the autodetachment state of this process must be formed in the case of the molecule $O_2(^1\Delta_g)$, i.e. the following channel corresponds to this case:

$$e + O_2(\sigma_g^2\sigma_u^2\pi_g^2\pi_u^2)^1\Delta_g \rightarrow \left(O_2^-(\sigma_g^2\sigma_u^2\pi_g^3\pi_u^2)^2\Pi_g\right)^{**} \rightarrow O^-(^2P) + O(^3P)\,. \qquad (3.19b)$$

This resonance is observed at higher electron energies and is characterized by smaller cross sections, as in the case of the ground oxygen molecule.

The role of excitation for the electron attachment process was analyzed in the case of the molecules HCl and DCI. The maximum cross section of electron attachment at low temperatures is 8.9×10^{-18} cm^2 and 1.8×10^{-18} cm^2 [74] for the molecules HCl and DCl, correspondingly. From this one can evaluate the survival probability for the molecule HCl as 0.018. Variation of the temperature over the range 300 – 1200 K leads to a sharp increase of the electron attachment cross sections [80]. From the temperature dependence one can evaluate the dependence of the maximum cross section of electron attachment σ_{max} on the vibrational state v of the molecule $\sigma_{max}(v)$. The ratio of these cross sections $\sigma_{max}(v=1)/\sigma_{max}(v=0)$ is 38 and 32 for the molecules HCl and DCI, correspondingly, and the ratio $\sigma_{max}(v=2)/\sigma_{max}(v=0)$ is 880 and 580 for these molecules. Note that in the case $v=2$ the optimal electron capture proceeds near the turning point and an intersection distance R_c for the electron terms. Hence in this case together with an increase of the probability of survival of the autodetachment state, the cross section of electron capture also increases with vibrational excitation.

The above conclusions on the temperature dependence of the electron attachment cross section correspond to the case of a small value of this cross section because of the small probability of survival of the autodetachment state resulting from electron capture by a molecule. This means that in these cases the potential curve of the autodetachment term is located above the molecular term at capture distances between the nuclei, so that the electron capture proceeds far from the distance of intersection of these terms. If the intersection of the molecular and autodetachment electron terms proceeds near the bottom of the molecular electron term, the electron attachment process becomes effective. Then the temperature dependence of the electron attachment cross section becomes weak. Furthermore, in this case the electron attachment cross section may drop with increase of the temperature.

3.5 Electron attachment to halogen-containing molecules

Halogen atoms are the atoms of most electronegativity, and therefore the electron attachment process to halogen-containing molecules is of importance. Because of the relatively high electron affinity of halogen atoms, this process has a low threshold and is of interest for some applications. Let us start from the process

$$e + HCl \rightarrow (HCl^-)^{**} \rightarrow H + Cl^-\,, \qquad (3.20)$$

studied in experiments [52–54, 79–87]. The statistical treatment of these data gives 0.65 ± 0.04 eV for the threshold energy of the process (3.20), and the cross section maximum is observed at the electron energy 0.78 ± 0.08 eV. Note that the electron affinity of the chlorine atom is 3.62 eV and the dissociation energy of the molecule HCl is 4.31 eV. This leads to a threshold for process (3.20) for an unexcited molecule of 0.69 eV in accordance with the above data. The excitation energy 0.69 eV corresponds to a distance 1.6 A between nuclei for the molecule HCl. This value can be used as an estimate

for the intersection distance R_c of the electron terms of process (3.18).

Figure 4 gives a schematic form of the electron terms for process (3.20). The autodetachment terms correspond to the systems $H + Cl^-$ and $H^- + Cl$ at large distances between nuclei. In the first case the electron term has symmetry $^2\Sigma$; in the second case we have two electron terms of symmetry $^2\Sigma$ and $^2\Pi$. Evidently, only the electron terms $^2\Sigma$ are of importance for this process because the molecular ground electron state is $^1\Sigma^+$ and these autodetachment states are formed as a result of capture of an s-electron. As a result of interaction of the autodetachment electron terms $^2\Sigma$, the upper term of this symmetry corresponds to a sharp repulsion and the lower term to a weak repulsion or to attraction in the range of electron capture. Next, the vibrational energy of the molecule HCl is 0.37 eV, so that only two vibrational levels are of importance for the electron attachment process (3.20), and different capture cross sections correspond to molecules in different vibrational states. This makes the dependence on the electron energy for the electron attachment cross section complex. The temperature dependence for the electron attachment cross section of the molecules HCl and DCl at high temperatures [88]

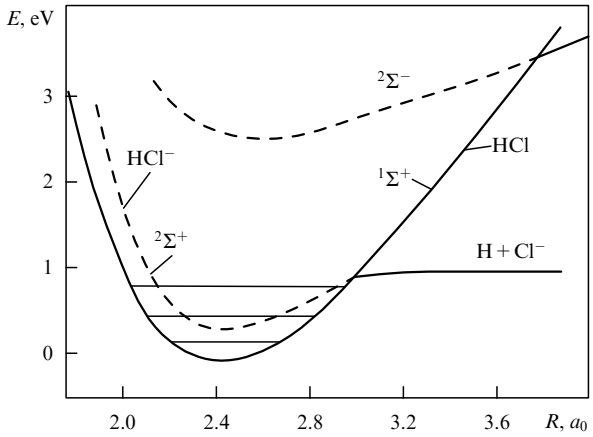

Figure 4. Positions of lower electron terms of HCl and HCl^- which are responsible for electron attachment to the HCl molecule [6].

confirms this conclusion.

Additional information about the electron terms of the autodetachment states $(HCl^-)^{**}$ follows from the analysis of vibrational excitation of the HCl molecule by electron impact [85, 89]. The cross section of this process has a sharp maximum near the threshold of process (3.20) which is of the order of 10^{-15} cm^2 and a second wide maximum of the cross section is observed at an electron energy of about 2.5 eV. This character of vibrational excitation of the molecule by electron impact confirms the existence of two autodetachment terms $(HCl^-)^{**}$ [90] which have symmetry $^2\Sigma$ (see Fig. 4). The rate constant for the detailed-inverse process with respect to (3.20),

$$H^- + Cl \rightarrow e + HCl\,,$$

is 9.6×10^{-10} cm^3 s^{-1} at room temperature [91]. It coincides in the order of magnitude with the cross section of the polarization capture of a negative hydrogen ion by a chlorine atom which is 2×10^{-9} cm^3 s^{-1}. According to measurements [92], this process leads mostly to population of the vibrational level $v = 2$ of the HCl molecule. Comparison of the intensities for radiative transitions between vibrationally excited states formed in this process gives the ratio of partial rate constants on formation of HCl molecule in vibrational states $v = 2$ and $v = 1$ as 5:3. Thus, from the total information it follows that the intersection of the electron terms of the ground state of HCl and the autodetachment state $(HCl^-)^{**}$ proceeds near the turning point of the second vibrational level of the HCl molecule. This influences process (3.20).

The process of electron attachment to halogen molecules

$$e + X_2 \rightarrow (X_2^-)^{**} \rightarrow X^- + X \qquad (3.21)$$

is energetically profitable and can proceed at zero temperature. But this possibility depends on the positions of the electron terms of the autodetachment states. In particular, Fig. 5 gives the lower electron terms of Cl_2^- together with the molecular term of the ground state of the molecule Cl_2. The ground state of the negative molecular ion Cl_2^- at large distances between atoms transits into $Cl(^2P) + Cl^-(^1S)$, so that there are four lowest electron terms of Cl_2^- of symmetry $^2\Sigma_u^+$, $^2\Pi_g$, $^2\Pi_u$, $^2\Sigma_g^+$. One can find the sequence of these terms if we take the system $Cl^- + Cl^-$ with a complete electron shell $(\sigma_g^2)(\pi_u^4)(\pi_g^4)(\sigma_u^2)$ as a basis and then take one electron from it to form the system Cl_2^-. Then we obtain the electron terms of

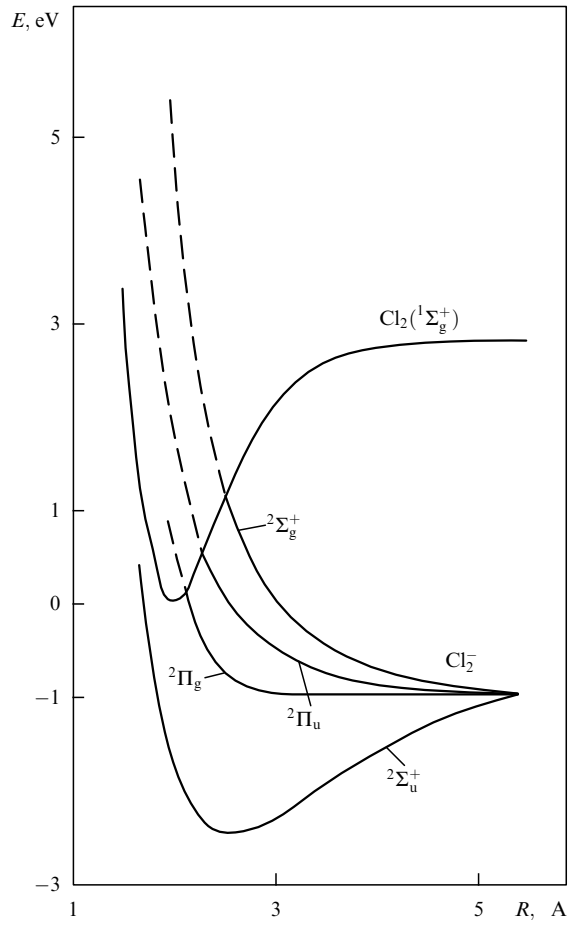

Figure 5. Positions of the lower electron terms of Cl_2 and Cl_2^- responsible for electron attachment to the chlorine molecule [6].

Cl_2^- in order of increasing energy: $^2\Sigma_u^+$, $^2\Pi_g$, $^2\Pi_u$, $^2\Sigma_g^+$, and the electron term $^2\Sigma_u^+$ corresponds to the stable negative molecular ion. One can connect the positions of these terms with the resonances in the cross sections of electron attachment to halogen molecules given in Table 8. As is seen, except for the fluorine molecule case, the ground state term of the molecular ion does not intersect with the molecular ground state term for these systems [93].

Table 8. Positions and widths (in parentheses) of resonances (in eV) for the corresponding terms of the autodetachment states due to cross sections of electron attachment to halogen molecules [93].

Term	F_2	Cl_2	Br_2	I_2
$^2\Sigma_u^+$	0.09 (sharp)	—	—	—
$^2\Pi_g$	4	0.03 (sharp)	0.07 (sharp)	0.05 (sharp)
$^2\Pi_u$	7	2.5 (1.3)	1.4 (1.2)	0.9 (1.2)
$^2\Sigma_g^+$	10	5.5 (2.0)	3.7 (1.60)	2.5 (1.7)

Note that because the electron state of a halogen molecule X_2 is $^1\Sigma_g^+$, the autodetachment states $^2\Sigma_u^+$, $^2\Sigma_g^+$ may be formed as a result of capture of an s-electron, whereas capture of a p-electron leads to formation of the autodetachment states $^2\Pi_g$, $^2\Pi_u$ at small electron energies. Hence, the cross section of electron capture by the molecules Cl_2, Br_2 and I_2 must be smaller than for an F_2 molecule. This contradicts some experiments, so this behaviour of electron terms requires an additional check.

Table 9 contains some energy parameters of process (3.21) and the rate constants of this process in thermal electron collisions. As is seen, in the bromine case this process is not effective, though according to Table 8 the electron terms of the autodetachment state $^2\Pi_g$ pass close to the bottom of the molecular potential curve. In other cases the process is more intensive. Note large dispersion of these data. The cross section of electron attachment to the chlorine molecule versus the electron energy is given in Fig. 6. The observed resonance at small electron energies corresponding to the formation of the autodetachment state $Cl_2^-(^2\Sigma_u^+)$ contradicts the data of Table 8. The temperature dependence of the rate constant of this process for the fluorine molecule is represented in Fig. 7.

Table 9. Rate constants of electron attachment k_{at} to halogen molecules in the temperature range 300 – 350 K.

Molecule	$EA(X_2)$, eV	$EA(X) - D$, eV	k_{at}, 10^{-10} cm^3 s^{-1}
F_2	3.0	2.2	70 [88]; 31 [91]
Cl_2	2.4	1.14	37 [91]; 2.9 [92, 94]; 3.1 [95]; 2.0 [96]; 3.3 [93]; 2.8 [97]; 20 [98]; 12 [99]
Br_2	2.5	1.40	0.1 [91]; 1.3 [97]; 0.008 [100]
I_2	2.5	1.53	1.4 [97]; 42 [101]; 1.8 [102]

3.6 Electron attachment to molecules in the limit of small energies

The electron attachment cross section as a function of the electron energy has a resonant form only if intersection of the molecular and negative ion terms proceeds far from the bottom of the molecular potential curve. In the opposite case the cross section of electron attachment is a monotone function of the electron energy and in the limit of small electron energies ε this dependence has the form $\sigma_{at}(\varepsilon) \sim 1/\sqrt{\varepsilon}$. This dependence is like that of the case of capture of a slow neutron by a nucleus [109] and reflects a general law for processes of releasing a slow particle [110]. In particular, for this process we have [1, 2]

$$\Gamma \sim \varepsilon^{l+1/2},$$

where l is the electron angular momentum. Indeed, let us write the general expression for the width of an autodetachment state of a negative ion:

$$\Gamma = \frac{2\pi}{\hbar}\left|\langle \Psi_- | V | \Psi_{mol}\psi_q \rangle\right|^2 \rho_\varepsilon ,$$

where Ψ_-, Ψ_{mol}, ψ_q are the corresponding wave functions of the negative ion, neutral molecule and free electron, q is the electron wave vector, V is the interaction operator producing

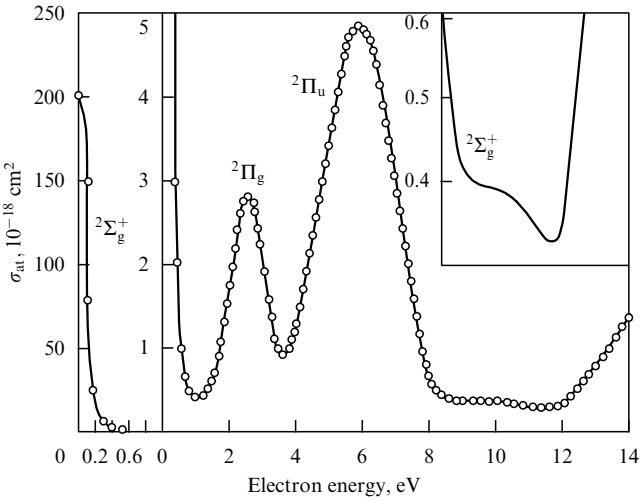

Figure 6. Cross section of the dissociative attachment of an electron to a chlorine molecule as a function of electron energy [88]. The autodetachment states of Cl_2^- through which the process proceeds are indicated.

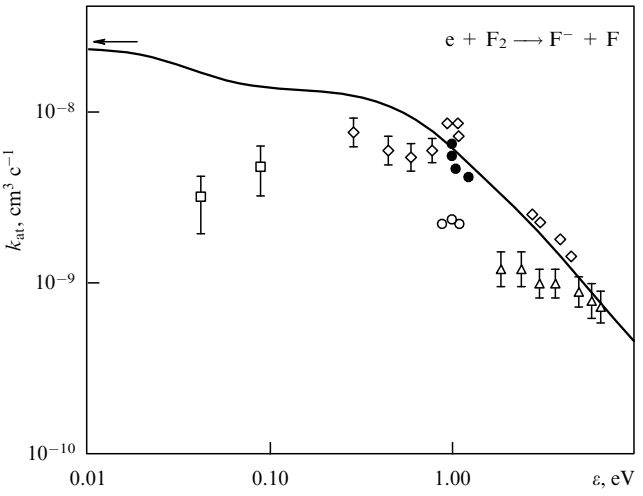

Figure 7. Rate constant of the dissociative attachment of an electron to a fluorine molecule. Solid curve [103], □ — [91], o — [104], △ — [105], ◇ — [106], • — [107]. The arrow indicates the asymptotic value [108] in the limit of small electron energies.

a correlation between the states of the negative ion and the electron system consisting of the molecule and free electron, and ρ_ε is the density of states of the free electron and molecule per unit energy interval. When the wave vector of the free electron q is small and the wave function of the free electron ψ_q is normalized to $\delta(q-q')$, we obtain $\psi_q \sim q^l$, where l is the angular momentum of the electron, and $\rho_\varepsilon \sim q$, so that [1, 2]

$$\Gamma \sim q^{2l+1} \sim \varepsilon^{l+1/2} . \tag{3.22}$$

Note that this dependence is valid if the width of the autodetachment state Γ is small in comparison with the energy ε of a released electron. Substituting the dependence (3.22) into formula (3.7), we prove that at small electron energies

$$\sigma_{\rm at}(\varepsilon) \sim \frac{1}{\sqrt{\varepsilon}} . \tag{3.23a}$$

Note some peculiarities of the electron attachment process at small electron energies. Firstly, one cannot in principle distinguish autodetachment states for which $\varepsilon \leqslant \Gamma$ because of the respectively strong interaction between these states. Hence, one can consider them as a group of states adjoining the boundary of the continuous spectrum and having identical parameters. Secondly, in spite of the small width Γ of the autodetachment states, the Born – Oppenheimer approximation is valid in this case because reconstruction inside the electron system proceeds with typical electron times, and a large decay time in this case means only the weakness of the interaction responsible for the electron transition. This means that the decay proceeds quickly but weakly.

The expression for the rate constant in the limit of small electron energies follows from formula (3.12a) if we take $\Gamma(\varepsilon) \sim \sqrt{\varepsilon}$. In this case for the electron attachment rate constant by analogy with (3.12b) we obtain

$$k_{\rm at} = \frac{\pi^2\hbar^2}{\sqrt{2}m_{\rm e}^{3/2}} \frac{\Gamma/\sqrt{\varepsilon}}{E'_R} \varphi^2(R) ,$$
$$E'_R \Delta R \gg T_{\rm e} \gg \Gamma , \quad \Gamma(\varepsilon) \sim \sqrt{\varepsilon} . \tag{3.23b}$$

In this case the excitation energy of the autodetachment state is small, so that we take $\zeta = 0$, i.e. the cross sections of electron capture and electron attachment are identical.

The dependence (3.23a) starts from relatively small electron energies. For example, according to measurements [108] for the molecule F_2, the asymptotic dependence (3.23) is valid at electron energies $\varepsilon < 5$ meV. The asymptotic rate constant of electron attachment to the fluorine molecule is $k_{\rm at}(\varepsilon) = 2.9 \times 10^{-7}$ cm^3 s^{-1}. As is seen, measurements of the asymptotic cross sections of the electron attachment process require a low width of the distribution function of electrons by energies and a high degree of resolution when the electrons are detected.

3.7 Electron attachment to molecules in three-body processes

In a dense gas, attachment of electrons to molecules can result from three-body collisions according to the scheme

$$e + AB + M \to AB^- + M . \tag{3.24}$$

The third particle M in this process takes the energy surplus that leads to the stable state of the negative ion formed. Though we consider electron attachment to diatomic molecules, this process can also lead to formation of atomic negative ions if the colliding particle AB is replaced by an atom. The rate constant $K_{\rm a}$ of this process is expressed in the units cm^6 s^{-1} and according to the definition of this rate constant, the balance equation for forming negative ions as a result of process (3.24) has the form

$$\frac{{\rm d}[AB^-]}{{\rm d}t} = K_{\rm a} N_{\rm e} [AB][M] , \tag{3.25}$$

where $N_{\rm e}$ is the electron number density, and $[Z]$ is the number density of species Z. Values of the rate constant $K_{\rm a}$ for some processes involving diatomic molecules are given in Table 10.

Table 10. Rate constants of three-body processes of electron attachment to diatomic molecules at room temperature.

Process	$K_{\rm a}$, 10^{-31} cm^6 s^{-1}
$e + O_2 + He \to O_2^- + He$	0.33 [111]; 0.3 [112]; 0.7 [113]
$e + O_2 + Ne \to O_2^- + Ne$	0.23 [111]
$e + O_2 + Ar \to O_2^- + Ar$	0.5 [111]
$e + O_2 + Kr \to O_2^- + Kr$	0.5 [111]
$e + O_2 + Xe \to O_2^- + Xe$	0.85 [111]
$e + O_2 + H_2 \to O_2^- + H_2$	4.8 [114]
$e + O_2 + D_2 \to O_2^- + D_2$	1.4 [114]
$e + O_2 + N_2 \to O_2^- + N_2$	0.85 [111]; 1.1 [113]; 1.6 [115]; 0.6 [116]; 0.78 [117]; 1.5 [118]
$e + 2NO \to NO^- + NO$	2.7 [119]; 8 [120]
$e + O_2 + H_2O \to O_2^- + H_2O$	140 [121, 122]; 150 [123]
$e + O_2 + CO_2 \to O_2^- + CO_2$	31 [121]; 32 [123]
$e + O_2 + H_2S \to O_2^- + H_2S$	100 [123]
$e + O_2 + NH_3 \to O_2^- + NH_3$	65 [123]
$e + O_2 + C_2H_4 \to O_2^- + C_2H_4$	30 [111, 122]; 17 [123]; 23 [124]

One can connect the rate constant of a three-body process with the rate constant of the detailed-inverse process — detachment of the diatomic negative ion in collisions with a particle M. In this case we presume that both processes pass through the same channels but in inverse directions. Then the rate constant of the three-body process $K_{\rm a}$ is expressed through the rate constant of detachment of the negative ion $k_{\rm det}$ by the relation

$$K_{\rm a}(T) = \frac{g_-}{2g_{\rm AB}} \left(\frac{2\pi\hbar^2}{m_{\rm e}T}\right)^{3/2} k_{\rm det}(T) \exp\left(\frac{EA}{T}\right) . \tag{3.26}$$

Here g_-, $g_{\rm AB}$ are the statistical weights of the negative ion AB^- and molecule AB with respect to their electron state, EA is the electron binding energy in the negative ion, the distribution of atomic particles (electrons, molecules and negative ions) by kinetic energies in both channels of the process is assumed to be Maxwellian with the same temperature T. Correspondingly, the mean rate constant $k_{\rm det}(T)$ in formula (3.26) is expressed through the cross section $\sigma_{\rm det}(E)$ of detachment of the negative ion AB^- in collisions with the third particle M at an energy E in the centre-of-mass frame by the formula

$$k_{\rm det}(T) = \frac{2}{\sqrt{\pi}T^3} \int_0^\infty \sqrt{\frac{2E}{\mu}} \sigma_{\rm det}(E) \sqrt{E} \exp\left(-\frac{E}{T}\right) {\rm d}E ,$$

where μ is the reduced mass of particles AB and M. This relation is useful for the analysis of process (3.24) on the basis of information from the detailed-inverse process.

A special mechanism of three-body attachment of electrons to atoms and molecules corresponds to the formation of the autodetachment state. This mechanism is often called the Bloch – Bradbury mechanism [125] of electron attachment and was first considered for electron attachment to an oxygen molecule. This process proceeds according to the scheme

$$e + AB \rightarrow (AB^-)^{**}, \quad (AB^-)^{**} + M \rightarrow AB^- + M\,. \quad (3.27)$$

In this case an electron is captured in an autodetachment state and then this state decays or is quenched in collisions with the gaseous particles M. Hence the rate constant of the process is expressed through the rate constant of quenching of the autodetachment state k_q in the second stage of the process. Then for the rate constant of this process by analogy with formula (3.26) we have

$$K_a(T) = \frac{g_-}{2g_{AB}} \left(\frac{2\pi\hbar^2}{m_e T}\right)^{3/2} k_q \exp\left(-\frac{E_a}{T}\right), \quad (3.28)$$

where E_a is the energy of excitation of the autodetachment state from the ground molecular state, and T is the temperature of electrons and atomic particles which are assumed to be identical.

This process is of interest for a gas discharge plasma where the distribution function of electrons by energy differs from Maxwellian. In this case formula (3.28) for the rate constant of three-body electron attachment via the autodetachment state can be rewritten in the form [126]

$$K_a = \frac{g_-}{2g_{AB}} \frac{2\pi^2\hbar^3}{m_e^{3/2}} k_q f(E_a)\,, \quad (3.29)$$

here the distribution function of electrons over energy $f(\varepsilon)$ is normalized by the condition

$$\int_0^\infty \sqrt{\varepsilon} f(\varepsilon)\, d\varepsilon = 1\,,$$

so that the corresponding Maxwell distribution function has the form

$$f(\varepsilon) = \frac{2}{\sqrt{\pi} T^{3/2}} \exp\left(-\frac{\varepsilon}{T}\right),$$

where T is the electron temperature.

Note the different temperature dependence for the three-body rate constants in formula (3.28) in comparison to (3.26) owing to the nature of the process. For this reason, the rate constant of a three-body electron attachment to atoms and molecules may increase with temperature for this type of the electron attachment process. In particular, it takes place in the case of oxygen (see Fig. 8b), and the resonant character of quenching in this process via the charge exchange process $(O_2^-)^{**} + O_2 \rightarrow O_2^* + O_2^-$ leads to an oscillating quenching cross section at low electron energies.

The three-body process (3.27) of electron attachment to a molecule has an analogy with the pair process (3.1) for electron attachment to a molecule through formation of an autodetachment state. It is clear that a pair process is more effective than a three-body one. Hence process (3.27) is realized if process (3.1) is forbidden for some reasons. In particular, in the case of the oxygen molecule the transition from an autodetachment to a negative ion stable state in the course of removal of nuclei is absent, so that formation of a stable molecular negative ion results in quenching of the autodetachment state through process (3.27). In this case the rate constant of process (3.27) increases with temperature if the activation energy E_a of this process exceeds the thermal energy. This takes place for oxygen (Fig. 9a), while for electron attachment to NO we have another temperature dependence (Fig. 9b). Comparing the data of Fig. 8 and 9a for the oxygen case, one can conclude that because of the resonant character of formation of the autodetachment state, the three-body rate constant depends on the distribution function of electrons by energy.

Note that processes (3.1) and (3.27) for oxygen proceed via different autodetachment states. In the case of the three-body process, this is the ground state of the negative ion

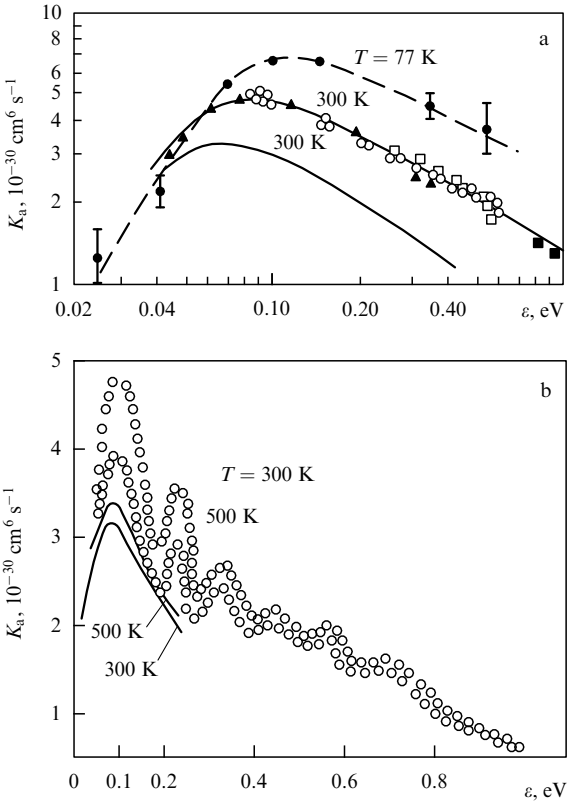

Figure 8. Rate constant of three-body electron attachment to an oxygen molecule in oxygen as a function of the electron energy: (a) a smooth electron energy distribution in a gas in an external electric field [112, 127]; (b) a monoenergetic electron beam [116]. The solid curve corresponds to calculations with a Maxwell distribution function for the electrons [2].

Table 11. Parameters of low autodetachment states of the ground electron term of the negative oxygen molecular ion $O_2^-(X^2\Pi_g)$ [4, 130 – 130]; v is the vibrational quantum number of the state, E is the excitation energy from the ground state of the oxygen molecule, and Γ is the level width.

v	4	5	6	7	8	9	10
E, meV	90	215	338	458	577	694	809
Γ, meV	0.004	0.036	0.12	0.26	0.46	0.74	1.1

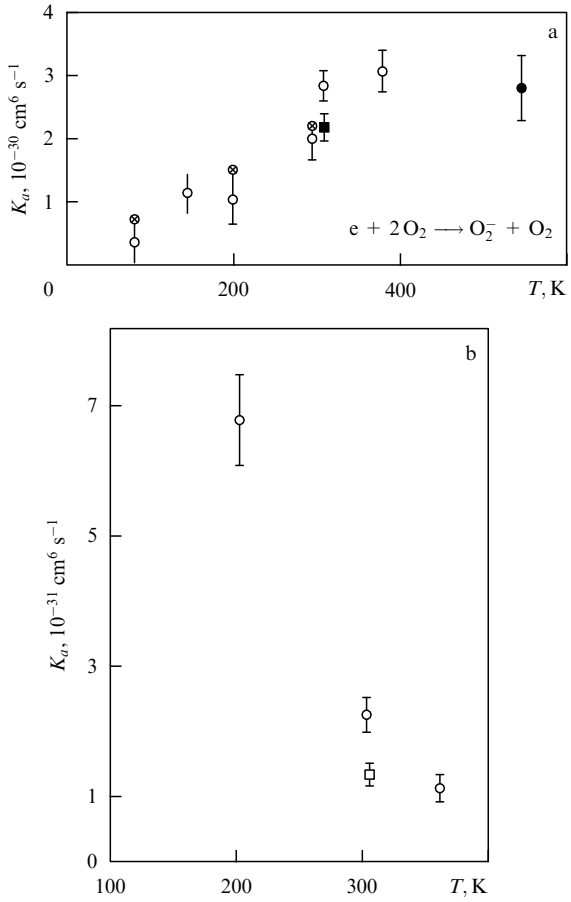

Figure 9. Temperature dependence for the three-body rate constant of electron attachment: (a) an oxygen molecule in oxygen; × — [124], ○ — [116], • — [127], □ — [115]; (b) a molecule of NO in the parent gas; ○ — [128], □ — [129].

$O_2^-(X^2\Pi_g)$ which is an autodetachment state due to vibrational excitation. Table 11 contains the parameters of low vibrational autodetachment states of this ion.

4. Electron attachment to polyatomic molecules

4.1 Autodetachment states of negative ions of complex molecules

The mechanism of electron attachment to polyatomic molecules is in principle the same as in the case of diatomic molecules. Indeed, this process proceeds via electron capture in an autodetachment term, and the Born – Oppenheimer approximation is valid for this process, allowing one to divide the system of interacting electron-molecule into a fast electron subsystem and slow nuclear subsystem. Hence, the electron capture proceeds promptly on motionless nuclei, and then this system develops as a result of motion of the nuclei. The existence of an autodetachment electron term is of principle for this process in both cases, and in order to continue this analogy, it is necessary to extract the nuclear coordinate R in the case of polyatomic molecules which is responsible for a given channel of the process.

But the complexity of polyatomic molecules leads to new features of the process under consideration. First, usually negative ions based on electronegative polyatomic molecules have several autodetachment states with a low excitation energy, and these states can be responsible for electron capture. Interaction and intersections of these autodetachment electron terms lead to a higher efficiency of the process compared to diatomic molecules. Second, polyatomic molecules have many vibrational degrees of freedom. Their excitation during the evolution of the electron-molecule system in an autodetachment state creates an irreversible character for the development of this system, in contrast to diatomic molecules. Third, electronegative polyatomic molecules show stable states of negative ions. The transition to these states from autodetachment states is possible as a result of motion of the nuclei. Then the energy surplus due to electron transitions from the autodetachment state to the stable state goes into vibrational degrees of freedom. Hence, electron capture in an autodetachment electron term leads to formation of a metastable negative ion with a large lifetime (see Table 3). This all influences the character of processes which proceed through formation of a negative ion autodetachment state.

Below we consider the electron attachment process involving halomethane molecules and the molecule SF_6. These molecules are used in gaseous discharges with electronegative additives, in electric protection systems and excimer lasers. Because of the applications, most measurements for electron attachment processes are made for these cases. The data for these molecules may be used for the analysis of concepts describing the processes under consideration and also for the demonstration of these concepts.

In order to understand the character of electron attachment to these complex molecules, let us analyze in detail the properties of the autodetachment states through which the process proceeds. Let us consider the electron states of the halomethane molecule CX_4 and its negative ion CX_4^-, where X is a hydrogen or halogen atom. Due to the high efficiency of electron attachment to such molecules, these systems are of importance for electron attachment processes. The system CX_4 is symmetric, so that the X nuclei form a tetrahedron, with a C nucleus at the centre. The wave function of this system has the form

$$\Psi = \sum_{i=1}^{4} a_i \psi_i \,, \tag{4.1}$$

where the electron wave function ψ_i describes the state when an extra electron forms a negative ion with the ith X-atom; a_i is the amplitude of this state.

As is seen, there are 4 electron states which result from joining an electron to the X atoms. Let us analyze the types of symmetry of these states. The symmetric figure, tetrahedron, contains 8 regular surface triangles if we join the nearest X nuclei. This figure has 4 symmetry axes of the third order. Each axis joins the centre with an X nucleus and rotation of this system by an angle $2\pi/3$ does not change the electron Hamiltonian. In addition, the electron Hamiltonian is conserved as a result of reflection with respect to 6 symmetric planes which pass through the symmetry axis and another atom (or through two symmetry axes). Because the Hamiltonian is conserved for the above operations, its eigenstates are characterized simultaneously by quantum numbers of the corresponding operators. One of the electron states is symmetric with respect to the above operations and is described by the symmetric wave function (4.1) with $a_1 = a_2 = a_3 = a_4$. Other electron states of CX_4^- are asym-

metric, i.e. their wave functions vary as a result of the above operations. Because the number of asymmetric transformations exceeds the number of electron states, we conclude that the energies of three asymmetric electron states are the same when the nuclei form a tetrahedron, i.e. the corresponding electron terms intersect at this nuclear configuration.

The electron system under consideration admits certain selection rules for electron capture in an autodetachment term CX_4^-. A slow s-electron can be captured only in the symmetric electron state of CX_4^-, while capture of a p-electron can lead to formation of three asymmetric autodetachment states. Next, the symmetry of nuclear vibrations is conserved during this transition. The vibration energy is established some time after the electron capture because the electron capture process is fast compared to the nuclear motion. Hence, the electron capture process may be accompanied by vibrational excitation.

Now let us change a halogen atom in the above molecule for a halogen atom of another type. For definiteness, we consider the molecule CF_3Cl, though the analysis applies to any molecule of this structure. Because the bond length C – Cl is more than that for C – F, in the case of CF_3Cl^- part of the symmetry of CX_4^- is lost. Indeed, one can divide the electron states of CF_3Cl^- into $CF_3 - Cl^-$ and $CF_3^- - Cl$ depending on the electron location. Next, F atoms of the negative ion CF_3Cl^- form a regular triangle whose plane is perpendicular to the axis C – Cl. Hence, there is the symmetry of the negative ion $CF_3^- - Cl$ with respect to rotation of the electrons around this axis by the angle $2\pi/3$. This operation leads to a transposition of fluorine atoms. Among the three electron states of $CF_3^- - Cl$, the lowest is symmetric with respect to the above rotation, i.e. its wave function is conserved as a result of these rotations. The energy of the two other electron states are the same when the three F atoms form a regular triangle. The capture of an s-electron by the molecule CF_3Cl leads to the formation of the electron state of $CF_3 - Cl^-$ or the symmetric electron state of $CF_3^- - Cl$; asymmetric electron states result from the capture of a p-electron. Note that the above electron properties of CF_3Cl^- also apply to any negative ion CX_3M^- with close electron shells of atomic negative ions X^- and M^-. This character of behaviour of electron terms of halomethanes follows from numerical calculations [22, 134–137].

Let us consider the SF_6^- system. It has 6 lower electron states which are formed as a result of joining of the 5 fluorine atoms in the ground state and the fluorine atomic negative ion with the sulfur atom which is located in the centre. In the case of a symmetrical configuration of nuclei, all the S – F bonds have identical lengths and the fluorine nuclei form a regular octahedron. Then one can extract the electron term of the symmetrical autodetachment state, so that the wave function of this state is conserved as a result of a symmetric transformation of electrons of this system. These transformations are rotations through an angle of $\pi/2$ around the three symmetry axes of the figure and reflections with respect to the three symmetry planes. The energies of the 5 other electron autodetachment states of the molecule coincide when the fluorine atoms form a regular octahedron. The motion of the fluorine atoms as a result of molecular vibrations partially removes this degeneracy of terms. One may expect that transitions between these states in the course of evolution of the system is of importance for the formation of certain products in the process.

This behaviour of the autodetachment states as well as electron terms characterizes the complexity of the electron capture process involving a polyatomic molecule. Firstly, several electron states of the negative ion partake in the electron capture process, and the contribution of these states to the total capture cross section varies significantly with increasing electron energy. Secondly, this process depends significantly on the configuration of nuclei, so that vibrational excitation can change the cross section of the process. Thirdly, the cross section of the electron capture depends on the type of vibrations. One can see that antisymmetric vibrations violate the symmetry of the electron system, so that they lead to a splitting of the electron terms of asymmetric electron states. Hence, excitation of antisymmetric vibrations can change the character of development of this electron system along the electron terms. Thus, the cross section of the electron capture by a complex molecule in an autodetachment term may depend both on the electron energy and on the molecular distribution by vibrational states (or by vibrational temperature).

4.2 Cross section of electron attachment to complex molecules and the spectra of attaching electrons

As follows from the above analysis, several autodetachment states of electronegative molecules are characterized by low excitation energies, and a slow electron may be captured in these states. But usually a certain autodetachment state corresponds to electron capture at a given electron energy, so that for the analysis of this process one can use the formulae of Section 2 which relate to one autodetachment state. Let the capture process be effective, and we use formula (3.7) for the cross section of electron capture. Choosing the optimal autodetachment state and the optimal ways for its evolution, we rewrite formula (3.7) in the form

$$\sigma_{\mathrm{at}}(\varepsilon) = \frac{\pi^2\hbar^2}{m_{\mathrm{e}}\varepsilon} f(\varepsilon)\,,$$

where

$$f(\varepsilon) = \Gamma(R_\varepsilon)\frac{\mathrm{d}W(R_\varepsilon)}{\mathrm{d}E}\,\exp(-\zeta)\,, \quad \zeta = \int_{R_\varepsilon}^{R_c} \frac{\Gamma(R')\,\mathrm{d}R'}{\hbar v_R}\,. \tag{4.2}$$

Here R_ε is the nuclear coordinate at which the electron capture takes place, i.e. $E(R_\varepsilon) = \varepsilon$, $E(R)$ is the excitation energy of the autodetachment term in which the capture takes place and $W(R_\varepsilon)$ is the probability of the R_ε configuration for nuclei. The integral ζ is taken along the trajectory of the subsequent nuclear motion. According to formula (3.5), we have

$$\int_0^\infty \sigma_{\mathrm{at}}\varepsilon\,\mathrm{d}\varepsilon = \frac{\pi^2\hbar^2}{m_{\mathrm{e}}}\left\langle \Gamma(R)\exp(-\zeta)\right\rangle, \tag{4.3}$$

where the angular brackets mean averaging over nuclear coordinates R.

The final channel of the electron attachment process depends on the autodetachment term which in turn is determined by the electron energy or the resonance energy. Hence, different channels of the process involving complex molecules are usually separated. This is demonstrated in Fig. 10 [7, 8] which gives the relative cross sections of electron attachment to some halomethane molecules containing

fluorine and chlorine atoms, identifying the products of the process. Figure 11 represents time-of-flight spectra of negative ions formed as a result of some of these processes [138]. One can see two groups of ion energies for some resonances. This means that either the resonance corre sponds to two autodetachment states, or a certain internal state is excited in fragments (CF_3, CF_3^-) of this process.

Let us consider in detail the energy dependence of the cross section for the electron attachment process

$$e + SF_6 \rightarrow (SF_6^-)^{**} \rightarrow \text{ Products.} \qquad (4.4)$$

For the analysis of this dependence, it is convenient to separate the electron energy region into three parts. In the limit of small electron energies, the cross section of electron attachment is given by the dependence (3.23)

$$\sigma_{at}(\varepsilon) \sim \frac{1}{\sqrt{\varepsilon}}\,, \qquad (4.5)$$

where ε is the electron energy. This dependence is valid at electron energies where $\Gamma \sim \sqrt{\varepsilon}$, so that the resolution of electron energies is less significantly in comparison to Γ. The rate constant of process (4.4) is given in Fig. 12a [139, 140] for small electron energies and room temperature. Note the high resolution of up to 0.1 meV in this experiment owing to the method of generation of electrons and to advanced experimental technique. The method uses laser generation of electrons as a result of atomic photoionization [141, 142]. In the scheme of [139, 140] free electrons were generated as a result of two-step photoionization of metastable argon atoms, so that in the first stage metastable atoms were excited

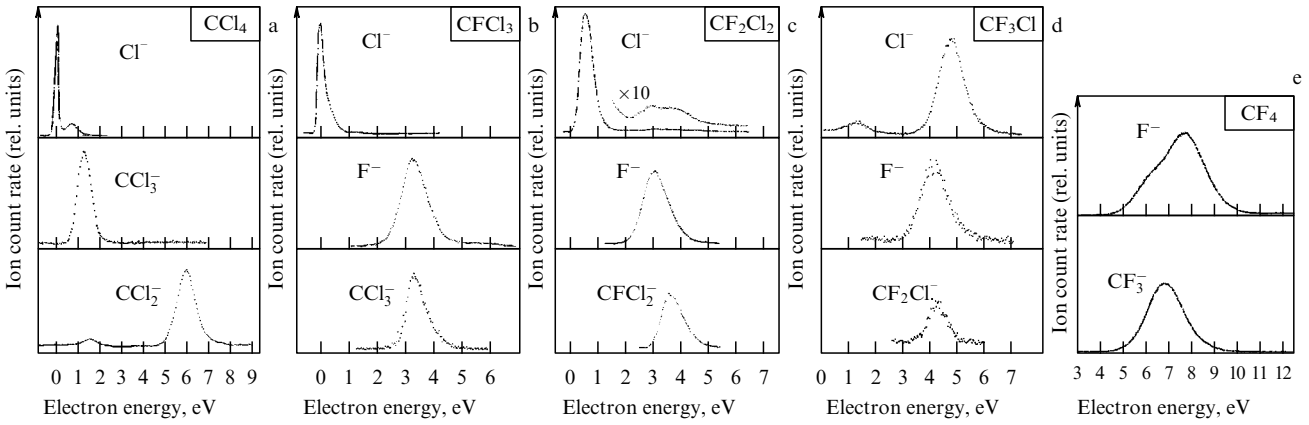

Figure 10. Cross sections (in relative units) of electron attachment to halomethane molecules as a function of electron energy for possible channels of the process [7, 8]: (a) CCl_4; (b) CCl_3F; (c) CCl_2F_2; (d) $CClF_3$; (e) CF_4.

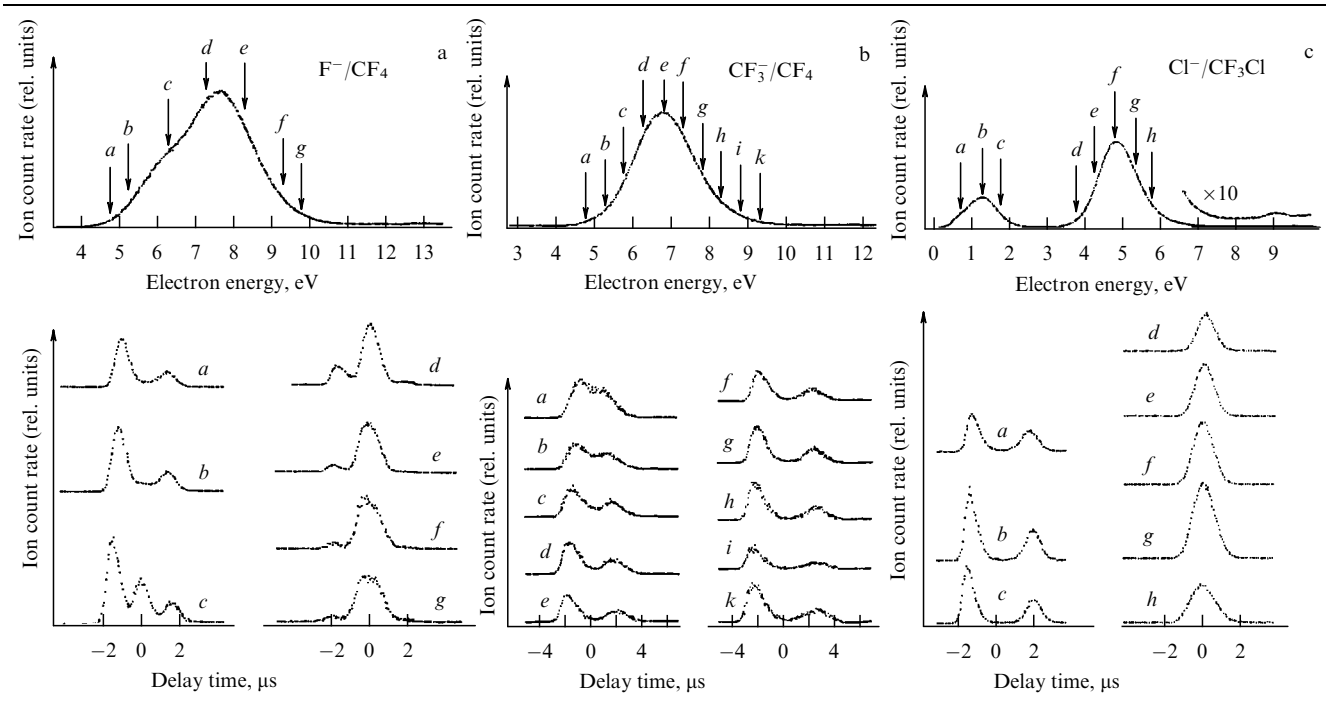

Figure 11. Time-of-flight spectra for the following electron attachment processes: (a) $e + CF_4 \rightarrow F^- + CF_3$; (b) $e + CF_4 \rightarrow F + CF_3^-$: (c) $e + CF_3Cl \rightarrow Cl^- + CF_3$ [138]. The upper part of each figure is the energy dependence of the cross section of this process and the energies at which the time-of-flight spectrum is taken are indicated.

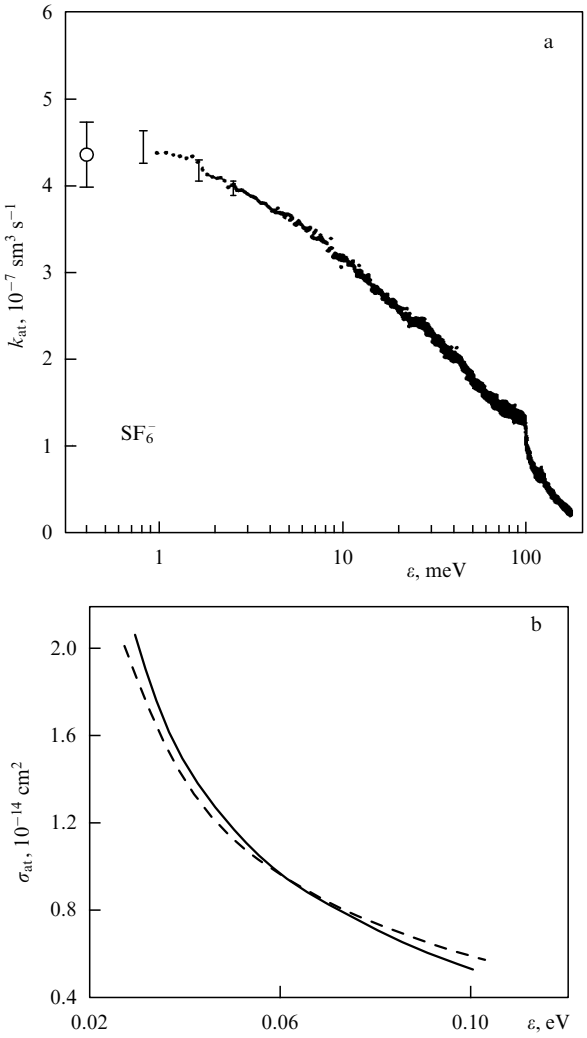

Figure 12. Dependence on the electron energy for the rate constant [139, 140] (a) and the cross section [66] (b) for electron attachment to the molecule SF_6. The measurements correspond to room temperature of nuclei.

into a more excited state, and in the second stage these excited atoms were ionized by another laser. The metastable argon atoms were formed in a gas discharge plasma, and the laser excitation was produced in a collimated beam of a plasma in a free-field region. As a result, an argon beam with monoenergetic electrons was created that allowed one to measure the electron attachment cross sections to the SF_6 molecule for electron energies of 0.1 – 170 meV.

The boundary of the range of small electron energies for which the cross section of electron attachment does not depend on the electron energy is approximately 2 meV. For $\varepsilon < 2$ meV the rate constant of electron attachment to the molecule SF_6 according to [139, 140] (see Fig. 12a) is

$$k_{at} = \sqrt{\frac{2\varepsilon}{m_e}}\sigma_{at}(\varepsilon) = (5.4 \pm 0.8) \times 10^{-7}\ \text{cm}^3\,\text{s}^{-1}\,. \qquad (4.6)$$

This value must coincide with the rate constant of chemionization of Rydberg atoms colliding with the molecule SF_6 which is, as follows from the data of Table 3,

$$k_{chem} = (4.3 \pm 0.3) \times 10^{-7}\,\text{cm}^3\,\text{s}^{-1}\,. \qquad (4.7)$$

Indeed, the process of chemionization of Rydberg atoms colliding with an electronegative molecule can be represented as collision of a weakly bound electron found in the Coulomb field of the atomic core with this molecule. The average kinetic energy of this electron is equal to its binding energy. Note that the cross section (4.6) does not connect with the polarization electron capture by the molecule in spite of the close values of these quantities [139] because of another character of the processes under consideration.

The second range of electron energies for process (4.4) is approximately 2 – 80 meV. For these electron energies the autodetachment state of the negative SF_6^- ion exists among states of continuous spectrum of this system, so that formula (4.2) is valid for these electron energies. Taking $\Gamma = \text{const}$, we obtain that the cross section of electron attachment is inversely proportional to the electron energy:

$$\sigma_{at} = \frac{A}{\varepsilon}\,, \qquad (4.8)$$

and according to formula (4.2) we have

$$A = \frac{\pi^2\hbar^2}{m_e}\frac{dW}{dE}\,\Gamma\exp(-\zeta)\,. \qquad (4.9)$$

In the case of SF_6, $A = 7.1\,\text{Å}^2$ eV according to measurements [139, 140], and $A = 5.8\,\text{Å}^2$ eV at an electron energy near 0.05 eV, as follows from Table 11 [66]. According to calculations [143], we have $\zeta \ll 1$ and $\Gamma \approx 2 \times 10^{-4}$ eV.

The second range of electron energies transits smoothly into the third one which in the SF_6-case corresponds to $\varepsilon > 0.1$ eV. In this energy range the overlap of the nuclear wave functions becomes small, and the cross section decreases with increasing electron energy more strongly. Let us approximate the cross section of electron attachment by the formula [66, 144, 145]

$$\sigma_{at} = \sigma_0\left(\frac{\varepsilon_0}{\varepsilon}\right)^{\gamma}. \qquad (4.10)$$

According to the nature of the process $\gamma > 1$. In the case of the SF_6 molecule the parameter $\gamma = 1.12$, i.e. it is close to unity, so that the cross section of electron attachment to the SF_6 molecule can be approximated by the energy dependence (4.2) with $f = 0.77$ (see Fig. 12b). Table 12 contains the parameters of formula (4.10) for the cross sections of electron attachment. The parameter $\varepsilon_0 = 0.05$ eV, so that σ_0 is the electron attachment cross section at an electron energy of 0.05 eV.

Table 12. Parameters of the cross sections of electron attachment to complex molecules for small electron energies.

Molecule	γ	σ_0, 10^{-16} cm^2	References
CCl_4	1.23	140	[144]
	1.23	120	[145]
CH_3Br	1.84	0.9	[144]
SF_6	1.12	117	[66]
$C_{10}H_{14}O_2$	1.39	25	[145]
	1.41	22	[66]
$C_{14}H_{10}$	1.15	1	[66]
$C_{18}H_{12}$	1.07	5.8	[145]
	1.03	5.2	[66]
n-$C_{10}H_{21}Br$	1.40	2.3	[144]
	1.38	2.4	[145]

Above we concentrate mainly on the case of electron attachment to the SF_6 molecule because of the careful experimental study of this process. Note that the above behaviour of the cross section of electron attachment is typical for any complex molecule if the intersection of its molecular term and electron term of the autodetachment state proceeds not far from the bottom of the electron potential surface of the molecule. Then the electron attachment process is intensive. In particular, in the limit of small electron energies the cross section of electron attachment is determined by formula (4.5), so that the rate constant of this process does not depend on the electron energy. Table 13 contains asymptotic values of the rate constants of the electron attachment process. In these cases the asymptotic expressions are valid if the electron energy is lower than 3–5 meV [146].

Table 13. Asymptotic rate constants of electron attachment to some halomethane molecules.

Molecule	k_{as}, 10^{-8} cm^3 s^{-1}
CF_3Br	0.57*
CF_2Br_2	21*
CCl_3Br	1.7*
CH_2Br_2	6.0*
CH_3I	7.0*
CCl_4	32**
$CFCl_3$	28**
CF_2Cl_2	0.36**

* On the basis of [146].
** On the basis of [147] if we accept that the asymptotic form (4.5) of the cross section is established at the electron energy $\varepsilon = 20$ meV.

Note the monotone energy dependence for the cross section of electron attachment to complex molecules. This allows one to use swarm methods for measurements of the electron attachment cross sections instead of electron beam methods with a monoenergetic electron beam. Then an electron cloud moves in a gas in an external electric field. In this case the width of the energy distribution function of the electrons is comparable with the mean electron energy whose variation is governed by the electric field strength.

Thus, we have an analogy in the character of the electron attachment process for diatomic and polyatomic molecules because in both cases the process proceeds via formation of an autodetachment state. Then in the case of a polyatomic molecule it is necessary to find the coordinate along which this process proceeds. For example, in the case of the SF_6 molecule it is the distance between sulfur and fluorine nuclei, and in the case of the electron attachment process

$$e + CF_3Cl \rightarrow (CF_3Cl^-)^{**} \rightarrow CF_3 + Cl \qquad (4.11)$$

this coordinate is the length of the C–Cl bond. Figure 13a gives the dependence of the cross section of electron attachment to the molecule CF_3Cl for different gaseous temperatures. Because the C–Cl bond is responsible for process (4.10), Figure 13b represents the electron term of the molecule CF_3Cl and the lowest terms of its negative ion. At room temperature, formation of the second autodetachment state is possible, leading to the resonance in the electron capture cross section at electron energies of about 2 eV. As a result of vibrational excitation of the molecule, which varies

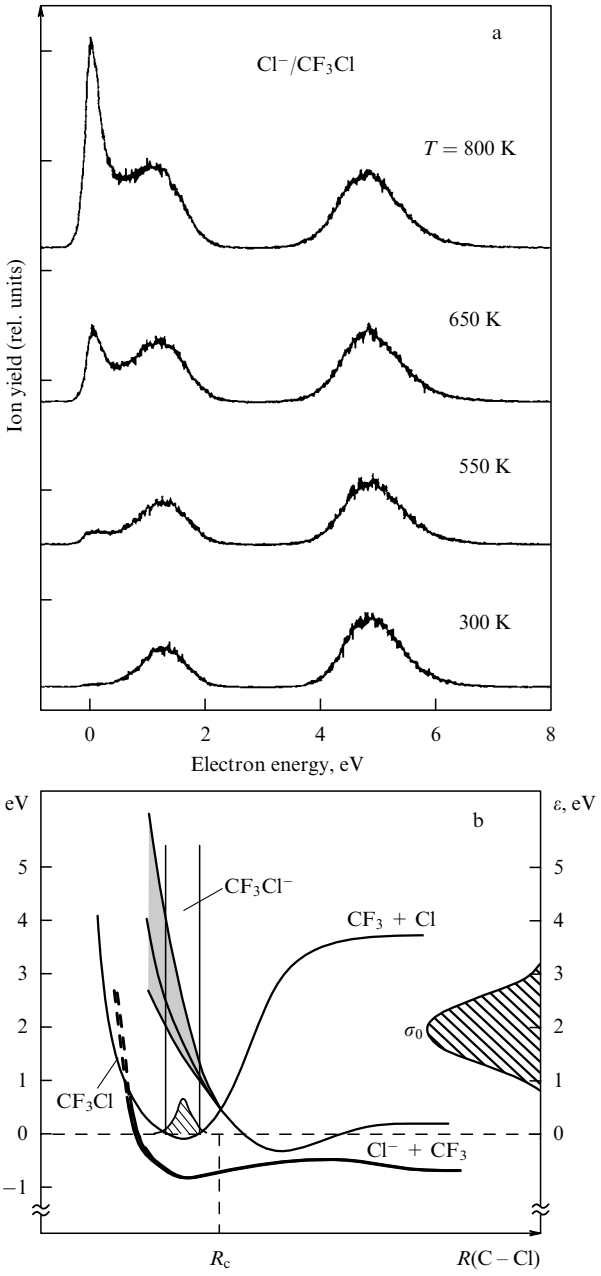

Figure 13. Dependence on the electron energy for the cross section of the process $e + CF_3Cl \rightarrow (CF_3Cl^-)^{**} \rightarrow CF_3 + Cl^-$ at different temperatures [9] (a) and positions of electron terms of the autodetachment states of the negative ion (b) which explains the form of the cross sections.

the range of lengths for the bond C–Cl , it becomes possible for the lowest autodetachment state to form. This autodetachment state is responsible for the peak at zero electron energy. Note that one can explain the data of Fig. 13a only in this way.

One more example of such a type is given in Fig. 14, where electron terms for the process of electron attachment to the molecule CF_3I are given. Note that the two lowest autodetachment terms correspond to different channels of the process. Indeed, in the case of the first lowest autodetachment state the final channel of the process is $CF_3 + I^-$, whereas the second autodetachment state decays into $CF_3^- + I$.

Table 14. Rate constants of attachment of thermal electrons to halomethane molecules.

Molecule	k_{at}, 10^{-8} cm^3 s^{-1}	Recommended
CCl_4	41 [99, 148 – 150]; 36 [151]; 33 [152]; 29 [153, 154]; 15 [155]; 40 [98, 156, 157]; 43 [97]; 44 [158]; 38 [159]; 37 [160]; 28 [144]; 25 [161]	35
$CHCl_3$	0.20 [156]; 0.49 [155]; 0.38 [97, 153, 160]; 0.44 [88]; 0.62 [152]; 0.24 [99, 149]; 0.13 [162]	0.35
CH_2Cl_2	4.8×10^{-4} [99, 161]; 1.7×10^{-4} [152]; 1.5×10^{-3} [153]	5×10^{-4}
CH_3Cl	$< 10^{-5}$ [99]; $< 2 \times 10^{-7}$ [163]; 7×10^{-8} [164]	$< 2 \times 10^{-7}$
$CFCl_3$	26 [98]; 13 [164]; 12 [153, 155]; 10 [165, 166]; 18 [156]; 24 [159, 167,168]; 31 [160]	19
CF_2Cl_2	0.32 [98]; 0.04 [155]; 0.23 [169]; 0.12 [165]; 0.07 [166]; 0.06 [170]; 0.6 [171]; 0.14 [172]; 0.17 [173]	0.1
CF_3Cl	$\sim 1.0 \times 10^{-5}$ [151, 161, 164, 166]	$\sim 1.0 \times 10^{-5}$
CH_3Br	0.07 [144]; 0.0005 [164, 174]; 0.0011 [175]; 0.0007 [163, 176]; 0.0004 [150]; 0.0006 [177]	0.0007
CH_2Br_2	9 [177, 178]; 11 [146]	10
CF_4	$< 1 \times 10^{-8}$ [130]	$< 1 \times 10^{-8}$
CH_3I	9 [158]; 12 [179, 177]; 10 [178]; 7 [180]	10
CF_3Br	1.4 [153, 155]; 0.9 [156]; 1.5 [160]; 1.6 [177]	1.4
CF_3I	20 [156]; 17 [158]; 19 [181]	19
CF_2Br_2	26 [153, 155]	26
CCl_3Br	4.9 [146]; 8.2 [179]	5

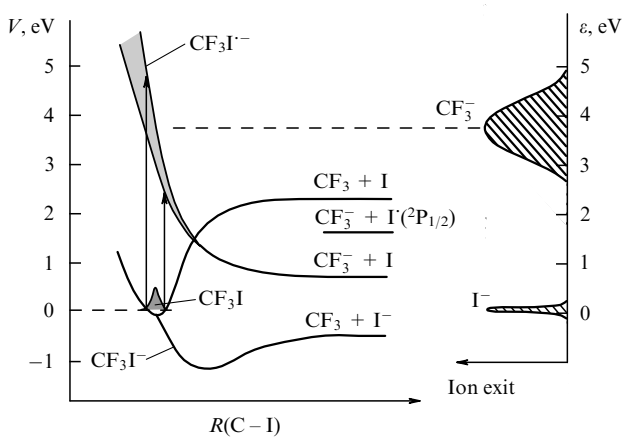

Figure 14. Positions of electron terms which are responsible for electron attachment to the molecule CF_3I [9].

4.3 Rate constant of electron attachment to electronegative molecules

The behaviour of the rate constant of electron attachment to complex molecules, like the cross section of this process, depends on the positions of electron terms corresponding to the autodetachment states of the negative ion. Table 14 gives the rate constants of this process for halomethane molecules. In spite of the close electron structure of these molecules and their negative ions, the rate constants for the electron attachment process are different because of their sensitivity to the positions of the autodetachment electron terms.

A small rate constant for some halomethane molecules is determined not only by the positions of the autodetachment electron terms, but also by the energetics of the process. Table 15 gives the energetic parameters which are responsible for electron attachment to chlorofluoromethane molecules. As follows from this data, some channels of the processes under consideration are energetically acceptable, others are forbidden at zero electron energy. In particular, formation of the fluorine negative atomic ion is impossible at zero electron energy.

Table 15. Energetic parameters of chlorofluoromethane molecules [7]: D is the molecule dissociation energy required for release of the chlorine or fluorine atom, and ε_{th} is the threshold energy consumed for release of the chlorine or fluorine negative ion. All the energies are expressed in eV.

Molecule	$D(R - Cl)$	$\varepsilon_{th}(R + Cl^-)$	$D(R - F)$	$\varepsilon_{th}(R + F^-)$
CCl_4	3.17 ± 0.1	-0.45 ± 0.1	—	—
$CFCl_3$	3.17 ± 0.1	-0.45 ± 0.1	4.42 ± 0.1	1.02 ± 0.1
CF_2Cl_2	3.30 ± 0.1	-0.32 ± 0.1	4.77 ± 0.3	1.37 ± 0.3
CF_3Cl	3.74 ± 0.2	$+0.12 \pm 0.2$	5.33 ± 0.1	1.93 ± 0.1
CF_4	—	—	5.66 ± 0.2	2.26 ± 0.2

Below we focus on the case of the SF_6 molecule. Table 16 gives the values of the rate constant for process (4.4) at room temperature of electrons and nuclei. The average value is equal to $(2.5 \pm 0.3) \times 10^{-7}$ cm^3 s^{-1}. From these data one can estimate the typical accuracy of measurements on the basis of different methods as $\sim 20\%$. Process (4.4) can be considered as an optimal electron attachment process, so that the autodetachment electron term and molecular term intersect near the bottom of the well of the molecular term. Then the probability of survival of the autodetachment state in the course of its evolution to the stable state is close to unity.

Table 16. Rate constants (in units 10^{-7} cm^3 s^{-1}) of electron attachment to molecule SF_6 ($e + SF_6 \rightarrow SF_6^-$) in thermal collisions.

k_{at}	2.0	2.1	2.2	2.3	2.4
Ref.	[181]	[182, 183]	[161, 168, 184, 185]	[156, 186, 187]	[188]
k_{at}	2.5	2.6	2.7 – 2.8	2.8	3.1
Ref.	[189]	[148, 150, 190 – 192]	[66, 193]	[97, 160, 194]	[98, 195]

For thermal electron energies one can approximate the cross section of electron attachment by formula (4.8). Then, if the electron and gaseous temperatures coincide, the rate constant of electron attachment is

$$k_{at} = \langle v\sigma_{at} \rangle = A\sqrt{\frac{8}{\pi m_e T}}\,. \qquad (4.12)$$

If we use the above values of parameter A in the case of the SF_6 molecule, for the rate constant of electron attachment at room temperature we obtain $k_{at} = 3.0 \times 10^{-7}$ cm^3 s^{-1} on the basis of the data of [139, 140] and $k_{at} = 2.4 \times 10^{-7}$ cm^3 s^{-1} on the basis of the data of [66]. This agrees with the data of Table 16.

4.4 Temperature dependence of the rate constant for complex molecules

In the limit of zero electron temperature the rate constant of electron attachment to a complex molecule tends to a constant. Evidently, one can take as this limit the value (4.6) for the SF_6 molecule and the rate constant must increase with decreasing electron energy. In reality, according to measurements [191] for the SF_6-case we have $k_{at}(300\,\mathrm{K}) = 2.9 \times 10^{-7}\,\mathrm{cm^3\ s^{-1}}$, and $k_{at}(73\,\mathrm{K}) = 1.2 \times 10^{-7}\,\mathrm{cm^3\ s^{-1}}$, where the argument indicates the temperature, and in this case there is equality of the gas and electron temperatures. The explanation of this contradiction can be connected only with the vibrational excitation. Let the cross section of electron attachment to vibrationally excited molecules be higher than that for the ground vibrational state of this molecule. Then increasing the gas temperature leads to an increase of both the electron attachment cross section and the rate constant. In the case of identical electron and gas temperatures, this effect competes with the decrease of the rate constant owing to the increasing mean electron energy. In the case of the SF_6 molecule, the vibrational excitation starts from a gas temperature of about 100 K [191], so that measurements at the temperature $T = 70$ K corresponds to the ground vibrational state, whereas at room temperature the probability of the ground vibrational state of this molecule is small. Hence, from experimental data follows a strong dependence of the rate of the electron attachment process on its vibrational state in the case of SF_6. This means that the intersection of the molecular electron term with the electron term of the autodetachment state of the negative ion SF_6^- occurs left of the well bottom of the SF_6 potential curve, as in Fig. 1c.

Let us estimate the role of vibrational excitation for the electron attachment process involving SF_6. According to measurements [98] within the framework of the flowing afterglow method, the rate constants of electron attachment to SF_6 are 3.1, 3.1, 4.5, $4.0 \times 10^{-7}\,\mathrm{cm^3\ s^{-1}}$ for the temperatures 205 K, 300 K, 455 K and 590 K, correspondingly. The maximum at the temperature 455 K may mean that vibrational excitation becomes unimportant at higher temperatures. Taking the electron energy dependence for the cross section of electron attachment to be according to formula (4.8), we obtain on the basis of this experiment that heating SF_6 molecules from 300 K to 455 K leads to an increase of parameter A in formula (4.8) by a factor 1.8 due to vibrational excitation. Using the data of [191], we obtain an increase of this parameter by a factor 4.6 due to vibrational excitation as a result of heating the molecules and electrons from 73 K to 300 K.

Note that the restricted accuracy of the data may influence some conclusions. In particular, let us give the results [194] for the temperature dependence of the rate constant under consideration. According to this measurement, the rate constant at temperatures 300 K, 411 K and 545 K is 2.3, 3.1 and 2.2 $\times 10^{-7}$ $\mathrm{cm^3\ s^{-1}}$, correspondingly. Variation of the temperature from 300 K to 411 K leads to a variation of parameter A in formula (4.8) by a factor 1.6 according to these data. Though these [194] and above [98] data lead to the same tendency, one can see a difference in the values of the rate constants. Errors of experimental data often lead to contradiction when we analyze different aspects of the electron attachment process.

From this standpoint we consider the integral cross section of electron attachment

$$I = \int \sigma_{at}\,\mathrm{d}\varepsilon\,. \tag{4.13}$$

Assuming that the main contribution to this value is given by the energy range where the cross section is governed by formula (4.8), we obtain

$$I = \int \sigma_{at}\,\mathrm{d}\varepsilon = A \ln\frac{\varepsilon_2}{\varepsilon_1}\,, \tag{4.14}$$

where ε_1, ε_2 are boundary electron energies where the dependence (4.8) is violated. Taking $\varepsilon_1 \sim 3$ meV, $\varepsilon_2 \sim 100$ meV, and the above values for the parameter A, we obtain $I = 2.2 \pm 0.2\,\text{Å}^2$ eV at room temperature in accordance with the measurements of Spence and Schulz [180]. But according to these measurements, the integral cross section I for SF_6 does not depend on the temperature in the range 300–1300 K, while from the above analysis it follows that in the temperature range 300–400 K the value A, and correspondingly I, varies by a factor 1.6–1.8. This contradiction can be explained by the restricted accuracy of measurements [180].

Let us represent formula (4.8) in a more general form

$$\sigma_{at} = \frac{A}{\varepsilon + \sqrt{\varepsilon\varepsilon_1}}\,, \tag{4.15}$$

so that formula (4.8) also describes the range of low electron energies. Then the boundary energy ε_1 is connected with the rate constant k_0 at zero energy by the relation

$$\varepsilon_1 = \frac{2A^2}{m_e k_0^2}\,. \tag{4.16}$$

Using formulae (4.6), (4.7) for k_0 and the above values of the parameter A, we obtain $\varepsilon_1 = 7 \pm 3$ meV for SF_6, while according to measurements [139, 140] it is about 2 meV. This diversity testifies to the errors in values used.

The temperature dependence of the rate constant is strong if a channel of the process is weak at small temperatures and is opened at high temperatures. It proceeds, in particular, if the positions of electron terms of the molecule and the negative ion are like that of Fig. 1c, i.e. the intersection of these terms proceeds left from the bottom of the molecular potential curve. Then the process is weak at small vibrational temperatures and is opened as a result of excitation of vibrational levels of the molecule, i.e. the process of electron capture proceeds effectively at high temperatures. Evidently, this position of electron terms is spread. It partially takes place in the case of the SF_6 molecule when vibrational excitation of the molecule increases the rate constant of the process several times. It this way one can explain the appearance of a new channel for the electron attachment process involving the molecule CF_3Cl (see Fig. 13) as a result of the temperature increase. A new resonance in electron attachment at small electron energies connects with the vibrational excitation of the molecule. This effect is very strong in the case of the CH_3Br molecule [175] when an increase of the temperature from 300 K to 700 K leads to an increase of the rate constant of the electron attachment process from 1.1×10^{-11} to 3.3×10^{-9} $\mathrm{cm^3\ s^{-1}}$ that corresponds to an activation energy of 0.26 eV. In the case of electron attachment to $CHCl_3$ the activation energy is equal to 120 ± 20 meV which is the mean statistical value from measurements [98, 99, 149, 164, 196, 197]. Actually, the existence of the activation energy means that the main

contribution to the cross section of the process gives unprofitable configurations of nuclei which can be reached as a result of vibrational excitation of the molecule. Within the framework of the one-dimensional model, the behaviour of the electron terms in this case corresponds to Fig. 1c.

Note that the cross section of electron attachment to the CH_3Br molecule at 300 K has a maximum at an electron energy of 0.38 eV [175]. Increasing the temperature leads to a shift of this maximum to small electron energies, and above 400 K the cross section of electron attachment increases monotonically with decreasing electron energy. Such behaviour of the cross section can be explained only by a two-dimensional dependence for the parameters of the electron terms. Then the optimal configurations of nuclei are different depending on their availability and the parameters of the electron terms. Hence, at a given electron energy but different vibrational excitation the process may be determined by different regions of the autodetachment term.

Thus, in the case of diatomic and complex molecules the temperature dependence of the rate constant for the electron attachment process has a different nature. For diatomic molecules the temperature dependence of the process rate constant is connected with the survival probability $\exp(-\zeta)$ which increases with increasing vibrational excitation of the molecule (see Section 3.4). In the considered cases of complex molecules (SF_6, CF_3Cl, CH_3Br, $CHCl_3$) the main contribution to the rate constants of the process is given by more compact nuclear configurations compared to the probable ones, and these compact configurations of nuclei are present in vibrationally excited states to a higher degree than in the ground state. In order to demonstrate this, let us compare the contributions to the rate constants from the first excited and ground vibrational states, considering molecular vibrations within the framework of one-dimensional harmonic oscillations. Then for the ratio of these contributions if the electron term of the autodetachment state directs almost vertical, and the turning point is located left from the bottom of the potential well, we have

$$\frac{|\varphi_0(R)|^2}{|\varphi_1(R)|^2}\exp\left(-\frac{\hbar\omega}{T}\right) = 2\left(\frac{R-R_0}{\Delta R}\right)^2 \exp\left(-\frac{\hbar\omega}{T}\right). \tag{4.17}$$

Here $\varphi_0(R)$, $\varphi_1(R)$ are the wave functions for the ground and first excited states of the oscillator [see formula (3.8)], $\hbar\omega$ is the vibrational energy, and T is the vibrational temperature. In particular, if the intersection of terms proceeds at the turning point for the first excited state, for the ratio of the above contributions we have $6\exp(-\hbar\omega/T)$. Hence, if $\hbar\omega \sim T$, excited vibrational states may determine the rate constant of the electron attachment process for a given position of electron terms.

4.5 Products of the electron attachment process

The decay of an autodetachment state resulting from electron capture by a complex molecule can proceed by different ways depending on the energetics and positions of the electron terms for different channels of the process. Let us consider the case of electron attachment to the SF_6 molecule which has been investigated in detail. At small electron energies the negative ion SF_6^- is formed. At higher energies, when this process is accompanied by dissociation of the SF_6 molecule, it proceeds by the channels

$$e + SF_6 \rightarrow (SF_6^-)^{**} \rightarrow SF_5^- + F, \tag{4.18}$$

$$e + SF_6 \rightarrow (SF_6^-)^{**} \rightarrow SF_5 + F^-. \tag{4.19}$$

The lowest autodetachment state of $(SF_6^-)^{**}$ partakes in these channels of the process. For higher electron energies, with the participation of other electron terms of $(SF_6^-)^{**}$, other negative ions, such as F_2^-, SF_4^-, SF_3^-, SF_2^-, can result from the electron attachment process to SF_6 [198, 199]. At zero electron energy channels (4.18), (4.19) are closed because of energetics of these processes, and the positions of the threshold of these processes are of importance.

The energy of processes (4.18), (4.19) can be obtained from analysis of the temperature dependence of the cross section or the rate constant for this channel of the process. Figure 15 gives such a dependence which allows one to determine the activation energy of this channel. Values of the activation energy of process (4.18) are collected in Table 17. Note the physical peculiarities of this process which can influence the measured activation energy. The formed autodetachment state $(SF_6^-)^{**}$ has a long lifetime, and its subsequent fate depends on the surrounding gas. If the density of surrounding gas is low, so that collisions with its atoms and molecules are absent in the course of the occurrence of $(SF_6^-)^{**}$, the temperature dependence of the probability of this channel is determined by the temperature of $(SF_6^-)^{**}$. Note that the temperature of $(SF_6^-)^{**}$ during its decay may differ from its initial temperature during the electron capture if the lifetime of the autodetachment state exceeds the typical time of radiative transitions between vibrational states of the negative ion $(SF_6^-)^{**}$. In the case of a high-density buffer gas, collisions with atoms or molecules of the gas establish the internal temperature of $(SF_6^-)^{**}$. The

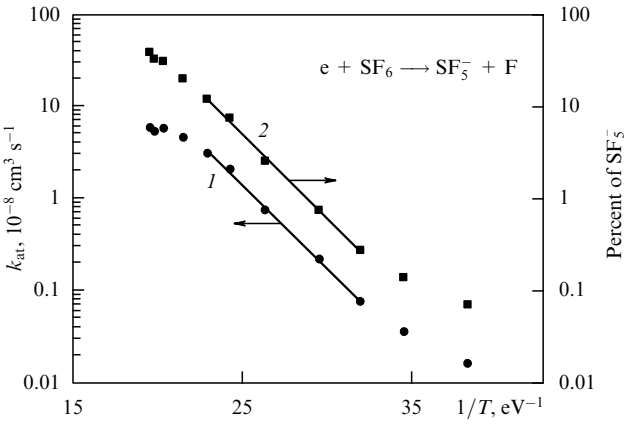

Figure 15. Temperature dependence of the rate constant of electron attachment to the molecule SF_6 with the formation of ions SF_5^- and the contribution of this channel to the total rate constant of the process [194].

Table 17. Activation energy E_a for the process (4.18).

E_a, eV	0.1 ± 0.1	0.2 ± 0.1	0.15	0.43	0.42 ± 0.02	0.39 ± 0.04	0.2 ± 0.1
References	[12]	[21]	[196]	[184]	[194]	[200]	[201]

boundary number density of atoms for these limiting cases is of the order of $10^{15}-10^{16}$ cm^{-3}. Hence, in swarm and afterglow techniques the gas temperature determines the

equilibrium of the autodetachment state, while in those with rare beams the effective molecular temperature may be lower than the gas temperature.

The value of the activation energy for process (4.18) allows one to determine the energetic parameters of negative ions partaking in the process. In particular, these parameters according to [21] are $EA(SF_5) = 3.8 \pm 0.15$ eV, $EA(SF_6) = 1.15 \pm 0.15$ eV, and the binding energy $D(SF_5^- - F) = 1.35 \pm 0.15$ eV. From this it follows that the activation energy of process (4.19) is about 0.6 eV. In addition note that the binding energy for the bond $SF_5 - F$ equals 3.4 eV according to [202], 3.9 ± 0.15 eV according to [203], 4.1 ± 0.13 eV according to [204], and 4.35 eV according to [205]. The diversity of these data shows that measurements of the threshold of the electron attachment processes are useful for obtaining reliable energetic parameters of complex molecules and their negative ions.

In conclusion of this section we note that the data for the cross sections and rate constants of electron attachment to complex molecules obtained on the basis of different experimental methods are in accordance if we take into account their limited accuracy.

5. Electron attachment to bulk systems

5.1 Electron attachment in the formation of negatively charged particles in a glow discharge plasma

The wide spread case of electron attachment to bulk atomic systems relates to particles located in an ionized gas. Then electrons or negative ions and positive ions move to the particle surface and attach to it. As a result, the particle obtains a charge whose sign depends on the relation between the mobilities of positively and negatively charged atomic particles carrying the charge. We consider below the case of gas discharges of low electron number densities and small gas temperatures, as in a glow discharge, when clusters are negatively charged because the electron mobility is higher than the ion one. A high negative charge for particles in a dusty plasma can lead to specific phenomena. Charged particles can be captured by various electric traps in a gas discharge plasma, and then particles of the negative charge can form crystal structures in such a trap [206–213]. The negative charge of dielectric particles of such structures can reach $10^3 - 10^5 e$ [212, 213]. This large charge can make this plasma, consisting of charged particles of plasma crystal and electrons, a non-ideal plasma in spite of the large distances between particles.

The character of charging of dielectric particles differs from that of metallic ones. In the case of a metallic particle, valent electrons are located over all the particle surface whereas in the case of dielectric particles there are active centres on their surface which capture electrons. Actually, these centres are electronegative molecules which partially conserve their individuality on the surface of dielectric particles. Hence, electron attachment in this case is like that of free gaseous molecules, but the parameters of these processes are different.

The transition of electrons from negative active centres of the particle surface to positive ones leads to mutual neutralization of surface charges. Below we consider the process of charging of small dielectric particles in the regime when it is limited by fluxes of negative and positive ions to its surface. Note the principal difference in charging of dielectric and metallic particles due to the character of the process. In the case of metallic particles, an electron can move over all the particle, so that the recombination process is a three-body one. It is valid for clusters and particles of submicron sizes. In the case of dielectric particles, captured electrons are located in the boundaries of corresponding active centres, and the ionization equilibrium results from pair processes

$$e + A_n^{-Z} \rightarrow \left(A_n^{-(Z+1)}\right)^{**}, \tag{5.1a}$$

$$\left(A_n^{-(Z+1)}\right)^{**} + M \rightarrow A_n^{-(Z+1)} + M, \tag{5.1b}$$

$$B^+ + A_n^{-(Z+1)} \rightarrow B + A_n^{-Z}, \tag{5.1c}$$

so that an autodetachment state $\left(A_n^{-(Z+1)}\right)^{**}$ is quenched by collisions with surrounding atoms M. Because the rate constant of pair attachment of an electron to a dielectric particle significantly exceeds the ionization rate constant of the particle by electron impact, these particles are charged negatively.

The electron binding energies with active centres do not depend on the particle size because the action of each centre is concentrated in a small space region. Evidently, the number of such centres is proportional to the area of the particle surface, and for particles of micron sizes this value is large compared to that occupied by charges. Hence, above and below we consider the regime of charging of a small dielectric particle far from saturation of active centres. Then positive and negative charges can exist simultaneously on the particle surface. They travel over the surface and can recombine there. Usually the binding energy of electrons in negative active centres ranges around $EA = 2-4$ eV; the ionization potential for positive active centres is about $I \approx 10$ eV. Hence, recombination of positive and negative charges on the particle surface is an energetically profitable process which is determined by the transport of electrons over the particle surface.

In the case of gas discharges of a low electron number density and low gas temperature, as in a glow discharge, dielectric particles are negatively charged because the electron mobility is higher than the ion one. The charging of a dielectric particle in a plasma of glow discharge results from the attachment of electrons and positive ions to active centres — molecules located on the surface of the particle. Because the number of occupied active centres is small compared to their total number, the rate of the charging process is determined by the motion of charged atomic particles in the plasma near the particle, and one can evaluate fluxes of positive ions and electrons to the particle surface separately. Let us take into account that the motion of ions or electrons is determined by their diffusion in a gas and drift under the action of the electric field of a charged particle. Then the number density of ions equals zero on the particle surface and tends to the equilibrium value at large distances from the particle. Taking a particle charge to be Ze, we get for the current of positive ions to the particle at a distance R from it:

$$J = 4\pi R^2 \left(- D_+ \frac{dN}{dR} + K_+ EN \right) e. \tag{5.2}$$

The first term relates to diffusion motion, the second term describes drift motion, N is the number density of ions, D_+, K_+ are the diffusion coefficient and the mobility of positive ions, e is an ion charge which usually is equal to the electron charge, and $E = Ze^2/R^2$ is the electric field strength which is created by the particle. Using the Einstein relationship

between the diffusion coefficient and mobility of ions $D_+ = eK_+/T$, where T is the ion temperature, we obtain for the positive ion current over the particle surface:

$$J = -4\pi R^2 D_+ e\left(\frac{\mathrm{d}N}{\mathrm{d}R} - N\frac{Ze^2}{TR^2}\right). \tag{5.3}$$

Taking into account that ions do not recombine in a space, we have that the ion current does not depend on R. Then one can consider the above relation for the ion current as the equation for the ion number density. Solving this equation with the boundary condition $N(r) = 0$, where r is the particle radius, we obtain

$$N(R) = \frac{J}{4\pi D_+ e}\int_r^R \frac{\mathrm{d}R'}{(R')^2}\exp\left(\frac{Ze^2}{TR'} - \frac{Ze^2}{TR}\right)$$
$$= \frac{JT}{4\pi D_+ Ze^2}\left[\exp\left(\frac{Ze^2}{Tr} - \frac{Ze^2}{TR}\right) - 1\right].$$

Let us use that at large R the ion number density tends to the equilibrium value N_+ in a plasma far from the particle. This leads to the following expression for the ion current

$$J_+ = \frac{4\pi D_+ N_+ Ze^3}{T\{\exp[Ze^2/(Tr)] - 1\}}. \tag{5.4}$$

This formula is named the Fuks formula. Though it describes the current of positive ions, by the same manner one can find the current of negative ions or electrons which has the form

$$J_- = \frac{4\pi D_- N_- Ze^3}{T\{1 - \exp[-Ze^2/(Tr)]\}}, \tag{5.5}$$

this formula follows from (5.4) as a result of changing $Z \to -Z$ and the parameters of positive ions for the parameters of negative ions or electrons.

Assuming a Maxwell distribution of electrons and positive ions by energy with identical temperatures T, we obtain the equilibrium particle charge Z from the equality of currents of positive and negative ions (5.4), (5.5) onto the particle surface:

$$Z = \frac{rT}{e^2}\ln\frac{D_+}{D_-}. \tag{5.6}$$

In an ionized gas where the negative charge is connected with electrons, the particle has a negative charge because $D_+ < D_-$, i.e. positive ions have a lower mobility than electrons. These formulae are valid under the conditions

$$r \gg \lambda, \qquad r \gg \frac{e^2}{T}, \tag{5.7}$$

where λ is the mean free path of electrons or ions.

Let us consider the case of a glow gas discharge plasma where the negative plasma charge relates to electrons, but the electron distribution function over velocities differs from Maxwellian. Then the Fuks formula without using the Einstein relation between the mobility and diffusion coefficient of attaching electrons has the following form for the current of electrons onto a small particle:

$$J_e = \frac{4\pi K_e N_e Ze^3}{1 - \exp[-Ze^2/(T_e r)]}, \tag{5.8}$$

where we introduce the effective electron temperature T_e as $T_e = eD_e/K_e$, and K_e, D_e are the mobility and diffusion coefficient of electrons in the gas. We take the charge of a small particle to be $-Z$, and use that a typical electron energy eD_e/K_e significantly exceeds a typical ion energy. The ion current onto the particle surface according to the Langevin formula, which follows from formula (5.5) in the limit $Ze^2/(rT) \gg 1$, is

$$J_+ = 4\pi Ze^2 K_+ N_+,$$

where N_+ is the number density of positive ions far from the particle. Equalizing the fluxes of charged particles and taking into account the plasma quasineutrality $N_e = N_+$, for the charge of a small particle we get

$$Z = r\frac{D_e}{eK_e}\ln\frac{K_e}{K_+}. \tag{5.9}$$

According to this formula we have $Ze^2/(rT_e) \gg 1$, where T_e is the effective electron temperature.

Thus, the process of electron and ion attachment to a dielectric particle results from their interaction with active centres which are electronegative molecules located on the particle surface. The charge of these active centres does not spread over all the particle surface, and the recombination process involving electrons and positive ions corresponds to a pair process of attachment of an electron or ion to a particle. In the regime under consideration, when the total particle charge is small compared to the total number of active centres on the particle surface, the establishment of the particle charge results from moving positive and negative charges towards the particle, and these currents are formed independently.

Due to its charge Z, the particle obeys the electric potential $\varphi = Ze/r$, where r is the particle radius. If $e\varphi < EA$, where EA is the electron affinity of an individual active centre, the electron state is stable, while in the case $e\varphi > EA$ a tunnel transition is possible which leads to the decay of the electron state. The system particle – plasma exists under this condition, if new electrons attach to the particle. An isolated charged particle emits electrons until it reaches the limiting charge

$$Z_* = r\frac{EA}{e^2}. \tag{5.10}$$

In particular, for a dielectric particle of radius $r = 1\,\mu\mathrm{m}$ and $EA = 3\,\mathrm{eV}$ this charge is $Z_* = 2 \times 10^3$ and the particle electric potential is 3 V.

Evidently, this regime, when the charging of a small dielectric particle is determined by the fluxes of electrons and positive ions onto the particle surface, arises if electrons or ions contacted with the particle surface are found in the field of action of active centres. Then they attach to the surface or recombine with centres of opposite charge. Because the number of active centres must be large compared to the particle charge, the particle size is fairly large. It is valid for micron particles. In particular, the above numerical example corresponds to distances between neighboring charged centres of about 0.3 μm, which is larger by one-two orders of magnitude than a typical distance between neighboring active centres.

One more condition is required in the case when the particle negative charge exceeds the value of Z_*. Then the bound states of captured electrons become autodetachment

ones and can decay as a result of a tunnelling electron transition. To support this regime it is necessary that the decay of autodetachment states be compensated by formation of new bound states of electrons as a result of electron capture by active centres.

Let us estimate the dependence on the parameters of the problem for the lifetime of a negatively charged centre on the surface of a dielectric particle in the case when the particle charge exceeds the critical one. Its decay has a tunnelling character, and the probability per unit time for escape of an electron through the potential barrier has the following exponential dependence [11]

$$\frac{1}{\tau} \sim \exp(-2S), \quad S = \int_r^{R_c} \mathrm{d}R \sqrt{\frac{2m_e}{\hbar^2}\left[EA - V(r) + V(R)\right]}. \tag{5.11}$$

Here EA is the electron binding energy, $V(R) = Ze^2/R$ is the potential of an electron interaction with the Coulomb field of the particle, if its distance from the particle centre is R, and R_c is the turning point, i.e.

$$R_c = \frac{r}{1 - EA/\varepsilon_0},$$

and $\varepsilon_o = Ze^2/r$. Thus we have

$$S = \frac{\pi}{2} r \sqrt{\frac{2m_e}{\hbar^2} \frac{\varepsilon_0}{1 - EA/\varepsilon_0}}. \tag{5.12}$$

Assuming ε_o to be of the order of a typical atomic value, we obtain $S \sim r/a_0$, where a_0 is the Bohr radius. Being guided by small particles of micron sizes, we obtain very high lifetime of surface negative ions in autodetachment states with respect to tunnelling transitions of electrons. Hence, these autodetachment states have very long lifetimes, and the particle charge can exceed the critical charge Z_* of formula (5.10). Let us consider an example of an argon glow discharge in which a particle is located. A typical reduced electric field strength of the positive column of this discharge $E/N = 1$ Td corresponds to an effective electron temperature $eD_e/K_e = 4$ eV that relates to the reduced electron mobility $1.1 \times 10^3\,\mathrm{cm^2\,(V\ s)^{-1}}$. Assuming the positive ions to be atomic Ar^+, we have for their reduced mobility at room temperature $K_+ = 1.6\ \mathrm{cm^2\ (V\ s)^{-1}}$. In this case we have according to formula (5.9) $Z/r = 1.8 \times 10^4\,\mu\mathrm{m}^{-1}$, i.e. a particle of radius 1 μm has a charge 1.8×10^4 that exceeds by several times the critical particle charge (5.10). The electric potential of the particle Ze/r does not depend on its radius and is 26 V in this example. Note that these results are valid under assumption (5.7), so that the number density of argon atoms must be fairly high. For particles of 1 μm radius this criterion gives $N \gg 3 \times 10^{18}\,\mathrm{cm^{-3}}$, and in the case of particle radius $r = 10\,\mu\mathrm{m}$ this criterion is $N \gg 3 \times 10^{17}\ \mathrm{cm^{-3}}$. Thus, according to the above analysis, the charge of a dielectric particle located in a gas discharge plasma is determined by the process of electron and ion attachment to the particle surface and this charge can be fairly large.

5.2 Electron attachment to complexes and clusters

Let us analyze the general character of the electron attachment process involving complexes or clusters of electronegative molecules. Molecules constituting such a complex or cluster conserve their individuality in the bound state. Hence the electron attachment to these systems of bound molecules has the same mechanism as in the case of free molecules, i.e. the process proceeds through electron capture in an autodetachment state of the negative ion. Below we analyze the peculiarities of this process on the basis of results of an experimental study of this problem within the framework of general concepts of electron attachment processes. We note the following peculiarities of the electron attachment process involving complexes or clusters in comparison with that involving free molecules. First, the number of autodetachment terms increases in a cluster proportionally to the number of cluster molecules. Hence, new resonances can arise in the energy dependence of the cross section of electron attachment to complexes or clusters compared to that of free molecules. Second, assuming the electron properties of molecules are identical when they are free or in the bound state in complexes or clusters, one can conclude that resonances in the cross section of electron attachment as a function of the electron energy for free molecules are conserved in the case of complexes or clusters. But, because of the interaction of molecules in complexes or clusters, the positions of these resonances are shifted and their intensities may vary. Third, the electron attachment process involving complexes or clusters admits new channels which lead to the formation of new products.

One can analyze these general conclusions from the standpoint of experimental results. Electron attachment to oxygen complexes or clusters $(O_2)_n$ [9, 214–217] is convenient for the analysis of general peculiarities of the process involving complexes and clusters because of the weak interaction between oxygen molecules. For this reason it is

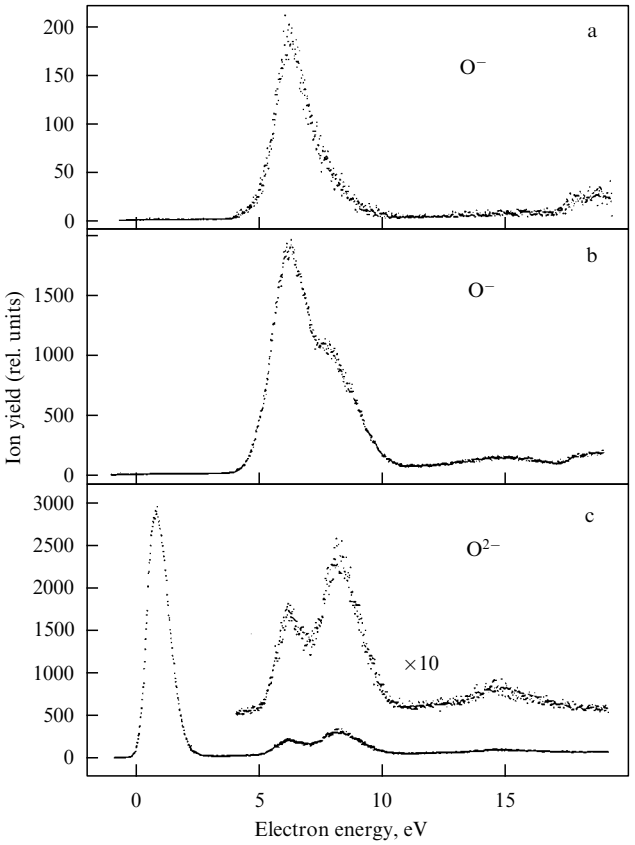

Figure 16. Spectra of electrons attaching to oxygen complexes [9, 218] which are formed in an expanding oxygen beam passing through a jet. The oxygen stagnation pressure and products of the process are indicated.

possible to separate autodetachment states for different vibrations inside oxygen molecules constituting clusters [217]. Figure 16 gives the relative intensities for electron attachment to O_2 and $(O_2)_2$. Complex molecules $(O_2)_2$ are formed as a result of free jet expansion of oxygen. Passing through a jet, the gas expands and is cooled. At the end of the process, a beam of cold oxygen molecules is formed, consisting of an admixture of complexes $(O_2)_2$. The more the stagnation (initial) pressure before the jet, the higher the concentration of these clusters.

The presence of complexes $(O_2)_2$ in the oxygen beam leads to new resonances in the electron attachment process. In addition, new channels occur in the cross section of electron attachment as a function of the electron energy. In particular, at small electron energies the following process is possible:

$$e + (O_2)_2 \rightarrow O_2^- + O_2 . \tag{5.13}$$

In the case of oxygen clusters the attachment of slow electrons takes place due to the formation of the ground state of negative molecular oxygen ion $O_2^-(^2\Pi_g)$. In the case of a free oxygen molecule this channel is closed because of the attractive character of this electron term. This channel is of importance for three-body attachment of electrons to the oxygen molecule to form the negative ion O_2^-, when the autodetachment state of this ion is quenched by buffer gas atoms. In clusters, neighboring molecules play the role of the third body, so that the negative molecular ion O_2^- and negative cluster ions $(O_2)_n^-$ are formed at low electron energies.

Alongside the formation of atomic negative ions O^-, electron attachment to the cluster $(O_2)_2$ admits the release of the oxygen atom O. In this case the complex ion $O^- \cdot O_2$ is formed. The basis of both processes is electron attachment to the oxygen molecule:

$$e + O_2 \rightarrow (O_2^-)^{**} \rightarrow O^- + O , \tag{5.14}$$

when the process proceeds through formation of the autodetachment states $^2\Pi_g$ and $^2\Pi_u$. Hence, the positions of resonances in the electron attachment cross section involving complexes $(O_2)_2$, when the products of this process are O^- and $O^- \cdot O_2$, are close to those in the case of the oxygen molecule [9].

The other peculiarity relates to channels which lead to the formation of the negative ion O^- and negative cluster ions $O^- \cdot (O_2)_n$. In the case of the oxygen molecule, an attaching electron does not change the configuration of valent electrons in the molecule, so that this process proceeds according to channels (3.17). In the case of oxygen clusters, an incident electron can lead to the transition of a valent σ-electron in a π-state [9, 215, 216], so that the following channels are possible:

$$\begin{aligned} e + (O_2)_n \cdot O_2(\sigma_g^2\sigma_u^2\pi_g^2\pi_u^2) &\rightarrow \left[(O_2)_n \cdot O_2^-(\sigma_g\sigma_u^2\pi_g^4\pi_u^2)\right]^{**} \\ &\rightarrow O^- \cdot (O_2)_m + O \cdot (O_2)_{n-m} , \end{aligned} \tag{5.15}$$

$$\begin{aligned} e + (O_2)_n \cdot O_2(\sigma_g^2\sigma_u^2\pi_g^2\pi_u^2) &\rightarrow \left[(O_2)_n \cdot O_2^-(\sigma_g^2\sigma_u\pi_g^4\pi_u^2)\right]^{**} \\ &\rightarrow O^- \cdot (O_2)_m + O \cdot (O_2)_{n-m} . \end{aligned} \tag{5.16}$$

Process (5.15) proceeds via the autodetachment state of symmetry $^2\Sigma_g$, and process (5.16) goes through formation of the autodetachment state $^2\Sigma_u$. These resonances are connected with the observed structureless and broad resonance in the range of electron energies 5–11 eV and the resonance at an electron energy of about 15 eV [9, 215, 216]. These resonances are also observed in spectra of O^-, $O^- \cdot (O_2)_4$, etc. Thus, the interaction of molecules of complexes and clusters with surrounding bound molecules partially violates the laws of conservation of some quantum numbers which are valid for free molecules in electron-molecule collision processes. Electron collisions with bound molecules can proceed by new channels (5.15), (5.16) in contrast to collisions of free molecules. This effect is stronger for condensed oxygen [9, 219, 220].

In the case of the complex $(CF_3Cl)_2$, the electron attachment process proceeds according to the schemes

$$e + (CF_3Cl)_2 \rightarrow CF_3Cl^- + CF_3Cl , \tag{5.17}$$

$$e + (CF_3Cl)_2 \rightarrow Cl^- \cdot CF_3Cl + CF_3 , \tag{5.18}$$

if the molecular beam includes CF_3Cl molecules and an admixture of these complexes. The main resonance in the cross section of electron attachment to the molecule CF_3Cl is located at an electron energy of 1.5 eV and is typical for the complex $(CF_3Cl)_2$ if the electron attachment process proceeds according to schemes (5.17), (5.18). Note the resonance at zero electron energy in the attachment cross section. This resonance is absent for a free CF_3Cl molecule at room temperature, but occurs at high temperatures (Fig. 13) and in the case of the complex $(CF_3Cl)_2$. This effect marks a general peculiarity of the electron attachment process involving bound molecules. Because of the stronger interaction of an electron with a molecule in negative ions of complexes and clusters, the excitation energy of an autodetachment state decreases with increasing number of molecules in the system. Hence, the electron attachment process involving bound molecules is like this process with the participation of free molecules in vibrationally excited states.

The formation of complexes consisting of two molecules doubles the number of autodetachment states. If different molecules form the complex, it has shifted electron terms of initial molecules as autodetachment electron terms. This is demonstrated by the analysis of $SF_6 \cdot N_2$ and $O_2 \cdot N_2$ complexes [9, 221, 222] which are formed as a result of free jet expansion of the corresponding gases with a nitrogen admixture and used for the electron attachment process. The nitrogen molecule does not have a stable negative ion, but the autodetachment state of its negative ion $N_2^-(^2\Pi_g)$ with an excitation energy of about 2 eV is responsible for vibrational excitation of the nitrogen molecule by electron impact. Hence, the parameters of this autodetachment state are determined from the analysis of elastic and inelastic $e-N_2$ collisions [3, 4, 223, 224]. This autodetachment state gives a broad resonance in the cross section of electron attachment to the above complexes, and in the case of the complex $SF_6 \cdot N_2$ this autodetachment state partially crushes the resonance of SF_6 at zero electron energy. Figure 17 contains spectra of attaching electrons to complexes and clusters in pure oxygen and in an oxygen — nitrogen mixture. Complexes and clusters containing the nitrogen molecule obtain an additional autodetachment state due to $N_2^-(^2\Pi_g)$ which forms a bond with oxygen molecules.

Thus, the properties of individual electronegative molecules constituting a complex or cluster are conserved in the cluster, i.e. the properties of bound and free molecules are identical. Hence, the cross section of electron attachment to complexes and clusters contains resonances corresponding to free molecules. The peculiarities of electron attachment to

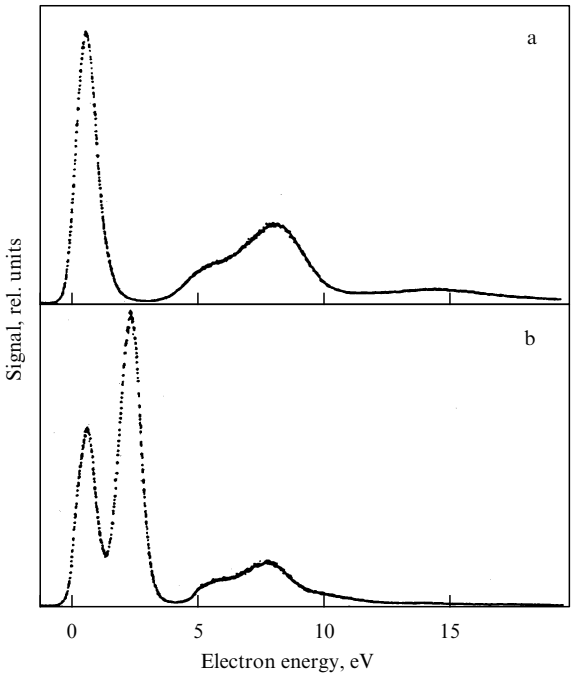

Figure 17. Spectra of attaching electrons to complexes formed in a pure oxygen (a) and in an oxygen — nitrogen mixture (10:1) (b) as a result of free jet expansion [9, 221]. The stagnation pressure is 4 atm; products of the electron attachment process are complex negative ions $(O_2)_2^-$.

clusters are as follows. First, new channels may be opened in clusters due to the cluster structure and the large number of autodetachment states. Second, forbidden and weak channels of the process are opened or become more intensive due to the interaction of molecules in the cluster. Third, different sorts of simple and cluster negative ions may be formed as a result of the process, and the basis of resonances for different negative ions are the resonances of free molecules.

5.3 Peculiarities of electron attachment to surfaces

Actually, electron attachment to surfaces containing electronegative molecules was considered in Section 5.1. We called electronegative surface molecules 'active surface centres' capable of capturing electrons. Under the conditions of charging a dielectric particle, the number of such centres is large in comparison with those occupied, so that the charging process is determined by the transport of electrons and ions to the surface through a non-uniform plasma. Now we consider the character of the surface process on the basis of experimental study.

Let us ascertain firstly which parameters can characterize the elementary processes of electron collisions with condensed molecules. In the case of gaseous molecules, such parameters are the cross section and the rate constant of the process. The cross section of electron attachment remains the parameter of the elementary act of its collision with the molecule for a low density of electronegative molecules on the surface. If the whole surface is covered by electronegative molecules, i.e. the layer thickness exceeds 1 ML (ML means monolayer), the parameter of this process is the probability of electron attachment as a result of scattering by the surface. Usually this probability is small in comparison to unity. Then the electron attachment cross section per surface molecule can remain the parameter of the elementary act of electron attachment to the surface because this cross section is smaller than the surface area per molecule.

The peculiarities of experimental studies of the electron attachment to surfaces are as follows. Usually, the base of the target for electrons is a metallic plate (for example, a silver, gold or platinum foil substrate) which is cleaned by multiple heating and annealing at high temperatures. A target is covered by several layers of a rare gas (Ar, Kr, Xe). This number of layers is measured and is a parameter of the process. After this, a calibrated sublayer of molecules is leaked onto the surface. Thus, electronegative molecules are found in the condensed phase and are separated from the metallic surface by several layers of condensed inert gas.

An important peculiarity of the condensed layer of electronegative molecules consists in their interaction with the metallic surface which is determined by the interaction of a surface negative ion with the charge induced on the metallic surface. As a result of this interaction, the electron term of the autodetachment state, which is formed due to electron capture, is shifted to lower excitation energies. If the distance l between a surface electronegative molecule and the metallic surface significantly exceeds typical atomic sizes (i.e. there are several intermediate layers of rare gas between them), one can use the classical formula for the shift of the electron energy $\Delta\varepsilon$ which is equal to the classical potential of a charge interaction with an induced charge on the metallic surface:

$$\Delta\varepsilon = \frac{e^2}{2l}\,, \tag{5.19}$$

where e is the electron charge. One can see that the interaction of the negative ion in the autodetachment state with the metallic surface may transit the negative ion into the stable state. Moreover, under the action of this attractive force a negative ion formed in an autodetachment state may transfer into a stable state as a result of a shift towards the metallic surface.

Thus, one can vary the resonant electron energy with respect to the surface electronegative molecule by variation of the thickness of the inert gas layer. This is demonstrated in Fig. 18. Note that as a result of capture of electrons by surface molecules and partial stabilization of the forming negative ions, the surface becomes charged. The rate of charging is determined by the rate of formation of stable negative ions on the surface.

The other peculiarity of the electron attachment to condensed molecules is connected with new channels of the process in comparison with free molecules because of the interaction of condensed molecules. For example, in the case of electron attachment to oxygen molecules such channels as (5.15), (5.16) were first observed in condensed oxygen [218, 220]. These processes are characterized by the excitation of σ-electrons in π-states, and this process is enforced by the interaction with surrounding oxygen molecules. Because of the increased interaction in the condensed phase in comparison with the gaseous one, the electron attachment cross section in the condensed phase is usually larger than in the gaseous one. For example, in the case of electron attachment to the free molecule CH_3Cl [225] the maximum cross section is 2×10^{-21} cm^2 at an electron energy of 0.8 eV. When these molecules are attached to a krypton film, the maximum cross section of electron attachment per molecule is 1.3×10^{-17} cm^2 and is reached at an electron energy 0.5 eV [225].

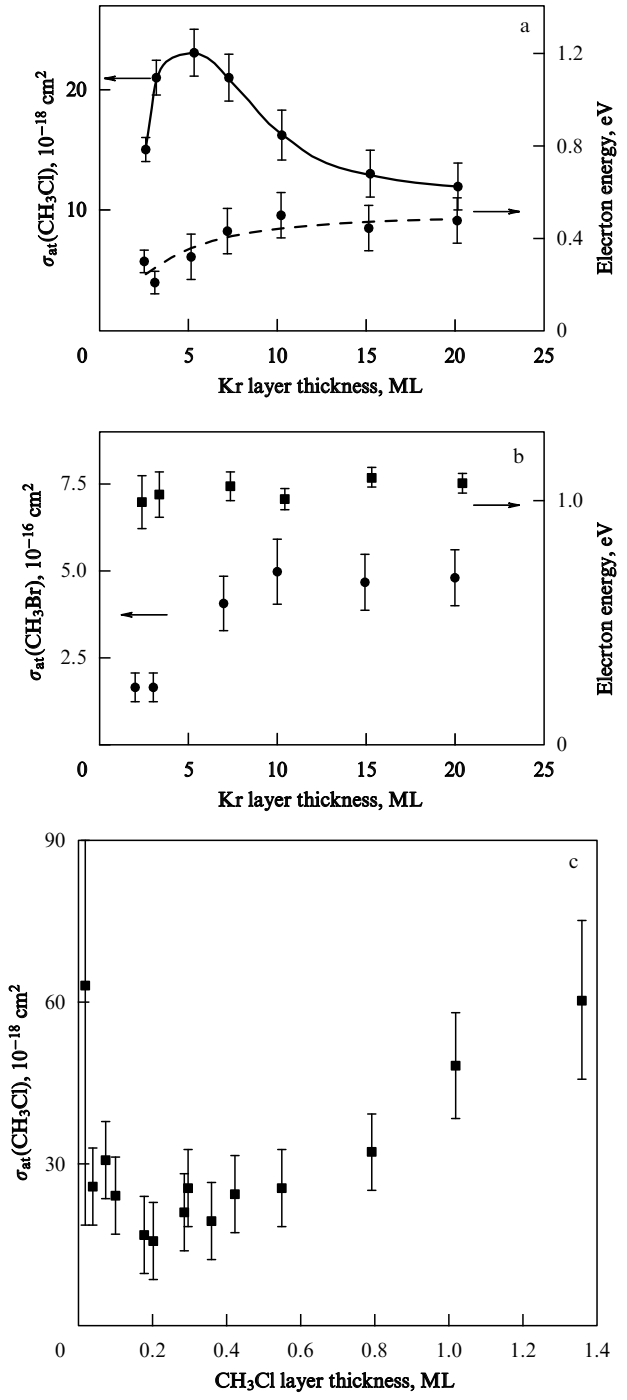

Figure 18. Low-energy electron attachment to condensed CH_3Cl and CH_3Br located on solid krypton separating these molecules from a platinum surface [225]. (a) The maximum cross section and position of the low-energy maximum for electron attachment to CH_3Cl depending on the thickness of the Kr spacer for 0.1 ML (monolayers) of CH_3Cl. (b) The maximum cross section and position of the low-energy maximum for electron attachment to CH_3Br depending on the thickness of the Kr spacer for 0.1 ML of CH_3Br. (c) The maximum cross section of electron attachment to CH_3Cl depending on the thickness of CH_3Cl at a thickness of 5 ML for the Kr spacer.

One more peculiarity of the interaction of absorbed molecules results in the formation of only simple negative ions in electron attachment collisions. In particular, electron attachment to the fluoromethane molecule CF_4 in the gaseous phase leads to the formation of the negative ions F^- and CF_3^- depending on the electron energy, and two resonances are observed for the electron attachment process, at 6.8 eV and 8 eV [9, 226]. The first resonance leads to the formation of F^- and CF_3^-, the second resonance relates to the formation of F^- [9, 226–224] (see Fig. 19). In the condensed phase only the negative ion F^- is a product of this process [9, 226]. Note that the considered processes of electron-molecule scattering proceed through the formation of an autodetachment state. But the maximum cross section of electron attachment to the molecule CF_4 is 1.6×10^{-18} cm^2 [229, 230], while the maximum cross section of vibrational excitation at resonant energies is about 5×10^{-16} cm^2. Because the excitation

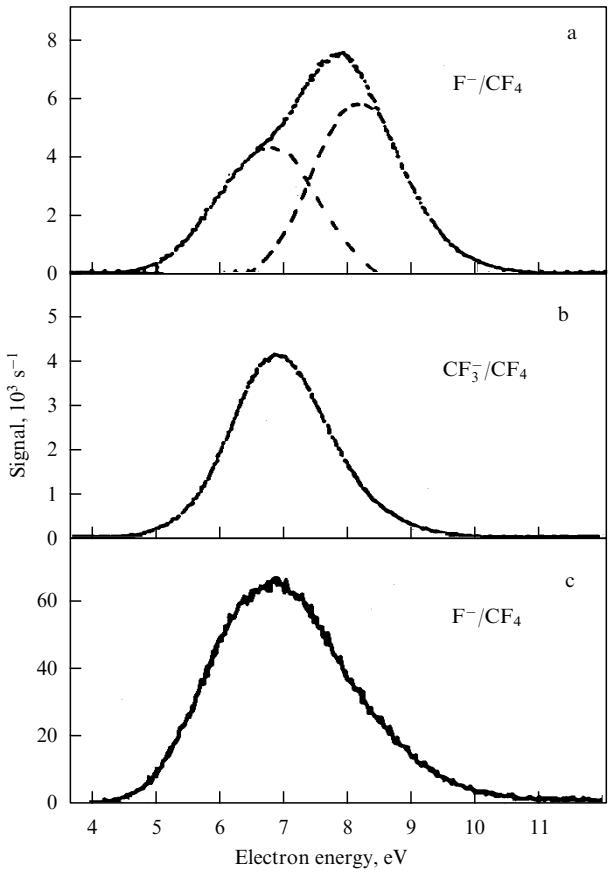

Figure 19. Spectra of electrons attaching to CF_4 in the gaseous (a), (b) and condensed (c) phases [9, 226]. The products of this process are F^- (a), (c) and CF_3^- (b).

process proceeds via the formation of the autodetachment state, the probability of decay of the autodetachment state to form a negative ion is relatively small. Hence, a slight change of parameters of the electron terms may lead to a significant variation of the electron attachment cross sections and the channels of the process.

One can explain the above effect also as follows. The decay of autodetachment states of CF_4^- leads to the formation of atomic particles F^- or F. In the case of condensed CF_4, the release of CF_3 and CF_3^- radicals requires additional energy for breaking the bonds involving fluorine atoms. Therefore, only an atomic negative ion F^- is formed as a result of the electron attachment to condensed CF_4, and the negative ion

CF_3^- is not observed in this case [9, 226]. In this case the negative ion CF_3^- remains in the film of electronegative molecules, so that this surface is charged negatively with respect to the metallic surface. This charging process is detected by measurement of the electric potential of the surface film.

One more example of the different character of electron attachment to molecules in gaseous and condensed phases relates to the case of CF_3I [9] (see Fig. 14 for the electron terms). Two resonances are observed in the spectrum of the electron attachment to this molecule — at zero energy and at an energy of about 4 eV [9]. The first resonance leads to the formation of I^-, and the second relates to the formation of CF_3^- and F^-. In the gaseous phase the intensity of the I^- resonance at zero energy exceeds that of F^- by two orders of magnitude, and CF_3^- by three-four orders of magnitude. On the contrary, in the condensed phase the intensity of the I^- resonance is lower than for the CF_3^- resonance by two orders of magnitude, and this resonance is observed at an electron energy of about 2 eV. The F^- resonance also shifts to higher energies.

Because electronegative molecules form a condensed phase on the surface of solid rare gases (Ar, Kr, Xe) as on a substrate, the structure of the solid rare gases is of importance. Evidently, in the most stable construction of rare gas atoms, they are found in the hollows of surface metallic atoms on the boundary of the metallic surface. Rare gas atoms in the solid state form a face-centred cubic lattice which has three different planes (100, 110 and 111). Correspondingly, the crystal lattice of rare gas borders the metallic surface with such a plane as is most profitable for the energetics of the surface and film covering it. This plane of rare gas atoms is the base for the film of absorbed electronegative molecules. From this consideration it follows that both the type of metallic surface and the sort of rare gas are important for the formation of stable films of condensed electronegative molecules. If the electronegative molecules are located comfortably in the hollows of surface atoms of a rare gas and the electronegative molecules form chemical bonds with each other, the film of condensed electronegative molecules is stable and has a certain structure. Then the data on desorption of negative ions as a result of electron attachment to condensed electronegative molecules should be repeatable.

Note that electronegative molecules include halogen atoms which can take a negative charge in molecular compounds. If an electronegative molecule contains different halogen atoms, it will have a dipole moment because of the different electronegativities of atoms. For example, the dipole moment of a molecule CH_3X, where X is the halogen atom, is directed along the C–X bond as follows from the symmetry of the electron system. Evidently, for a stronger interaction, the dipole moments of neighboring molecules must be directed oppositely. Hence, if the layer thickness of condensed electronegative molecules of such a type exceeds 1 ML (monolayers), surfaces 100 and 110 of the rare gas crystal are more profitable for the film of condensed electronegative molecules. Investigations [231, 232] of such structures show the complexity of this problem. Thus, the above analysis marks the importance of the structure of the substrate for properties of condensed electronegative molecules.

5.4 Electron attachment in surface gas discharge processes

The electron attachment process can be responsible for the recombination of electrons and ions on walls of a gas discharge tube in a glow discharge and other gas discharges. Indeed, in this case electrons and ions drift to the walls of the discharge tube, and since the electron mobility significantly exceeds that of the positive ions, the walls have a negative charge. This charge can be created as a result of attachment of slow negative ions to walls which, in turn, are formed under the action of electron attachment to electronegative molecules absorbed by the walls. Thus, the surface recombination of charges results from the collisions of positive ions with negative ions which are absorbed by the walls. As is seen, the recombination of electrons and ions in glow and other discharges proceeds through the electron attachment to molecules which are absorbed by the walls. But the scheme of the recombination process depends on the gas discharge conditions and the types of atoms and molecules in the discharge.

Electron attachment to condensed electronegative molecules also takes place during the etching process in the course of fabrication of microelectronic elements [233, 234]. Then, a wafer structure of layers of different materials is created, and the last layer contains a photoresist — an organic material which does not react with chemically active radicals, but evaporates under the action of UV-radiation. The first step of fabrication of a given microcircuit is the replication (lithography) process which consists in the creation of a replicative pattern on the sample. Then UV-radiation is directed onto the sample through a replicator. The incident radiation evaporates the photoresist and thus transmits the pattern to the sample. The following stage is the etching process which consists in the removal of the next film at the points where the photoresist is absent. This may be done by different methods as by means of electron or ion beams, X-rays, chemical or plasma methods. On the one hand, the etching process must be anisotropic, i.e. a material must be removed in the vertical direction only. On the other hand, this process must be selective, i.e. acts only on the removal material. These requirements seem to be contradictory. For example, the ion beam method is anisotropic because ions are directed perpendicular to the surface. But it is not selective because ions destroy the etching layer and the photoresist to an almost equal degree. Discharge methods which use chemically active particles (O, F, Cl) are selective, as are chemical methods, but are not anisotropic. Chemically active particles do not act on the photoresist, but they react over all the surface of the removal layer, and the structure formed does not have vertical walls. The best result for the etching process uses a combination of plasma methods which joins selective and anisotropic etching processes.

Let us consider this combination for the example of etching of Al-film [233]. This film may be removed as a result of reaction with chlorine atoms which are formed in a gas discharge, and also with chlorine molecules. The product of these reactions is gaseous $AlCl_3$ which is removed from the system. Because Cl and Cl_2 does not act on the photoresist, such a process is selective, but not anisotropic. Addition of the chloromethanes CCl_4 or $CHCl_3$ to chlorine as a discharge gas leads to the formation of a polymer which covers the sample with a thin film. The film hampers the penetration of Cl and Cl_2 to the Al and brakes the chemical process. But as a result of ion bombardment, the chlorocarbon-protected film is destroyed, and the chemical reactions between Cl, Cl_2 and Al proceed at these points, until a chlorocarbon-film grows there. This provides an anisotropy to the etching process due to the vertical direction of the ions. Thus this process

combines selectivity and anisotropy.

Note that the process of formation of a polymer film is based on the electron attachment to chloromethane molecules on the surface. Indeed, the CCl_4 molecule is a relatively passive molecule and its polymerization is possible if it is dissociated. The bounds in the polymer are formed between CCl_3 radicals. Dissociation of this molecule results from the electron attachment process, so that this process is of importance for etching technology in microelectronics.

6. Conclusions

The concept of electron attachment to molecules via the formation of autodetachment states has existed several decades and is the basis of our understanding of these processes. But experimental research has given a more detailed picture of electron attachment processes and considered, along with gaseous molecules, other atomic systems partaking in these processes, such as complexes, clusters, and films. Therefore, knowing of the electron attachment processes can be useful for the analysis of various processes on a plasma — surface boundary or on the surface of a particle in a plasma. An example is the desorption of molecules from a surface resulting from the attachment of electrons to the surface. Hence, understanding electron attachment processes and the experimental methods created for their investigation can be used for the analysis of some processes in dusty plasmas or for the analysis of processes and phenomena on walls bounding a plasma.

This work was supported within a joint grant between the Russian Foundation of Basic Research (RFFI) and the German Science Foundation (DFG, RUS 113/433).

References

1. Massey H S W *Negative Ions* (Cambridge, New York: Cambridge Univ. Press, 1976)
2. Smirnov B M *Negative Ions* (New York, London: McGraw-Hill, 1982)
3. Illenberger E, Momigny J *Gaseous Molecular Ions: An Introduction to Elementary Processes Induced by Ionization* (Darmstadt: Steinkopf Verlag, 1992)
4. Schulz G J *Rev. Mod. Phys.* **45** 423 (1973)
5. Caledonia G E *Chem. Rev.* **75** 333 (1975)
6. Eletskiĭ A V, Smirnov B M *Usp. Fiz. Nauk* **147** 459 (1985) [*Sov. Phys. Usp.* **28** 956 (1985)]
7. Oster T, Kühn A, Illenberger E *Int. J. Mass Spectrom. Ion Proc.* **89** 1 (1989)
8. Illenberger E *Chem. Rev.* **92** 1589 (1992)
9. Ingolfsson O, Weik F, Illenberger E *Int. J. Mass Spectrom. Ion Proc.* **155** 1 (1996)
10. Chutjian A, Garscadden A, Wadehra J M *Phys. Rep.* **264** 393 (1996)
11. Landau L D, Lifshitz E M *Kvantovaya Mekhanika* (Quantum Mechanics) (Moscow: Nauka, 1974) [Translated into English (Oxford: Pergamon Press, 1977)]
12. Kay J, Page F M *Trans. Faraday Soc.* **60** 1042 (1964)
13. Hughes B M, Lifshitz C, Tiernan T O *J. Chem. Phys.* **59** 3162 (1973)
14. Compton R N, Cooper C D *J. Chem. Phys.* **59** 4140 (1973)
15. Hubers M M, Los J *Chem. Phys.* **10** 235 (1975)
16. Refaey K M A, Franklin J L *Int. J. Mass Spectrom. Ion Proc.* **26** 125 (1978)
17. Streit G E *J. Chem. Phys.* **77** 826 (1982)
18. Heneghan S P, Benson S W *Int. J. Chem. Kinet.* **15** 109 (1983)
19. Grimsrud E P, Chowdhury S, Kebarle P *J. Chem. Phys.* **83** 1059 (1985)
20. Klobukowski M et al. *J. Chem. Phys.* **86** 1637 (1987)
21. Chen E C M et al. *J. Chem. Phys.* **88** 4711 (1988)
22. Leffert C B et al. *J. Chem. Phys.* **61** 4929 (1974)
23. Harland P W, Thynne J C *J. Inorg. Nucl. Chem. Lett.* **7** 29 (1971)
24. Harland P W, Thynne J C *J. Phys. Chem.* **75** 3517 (1971)
25. Compton R N et al. *J. Chem. Phys.* **45** 4634 (1966)
26. Edelson D, Griffiths J E, McAffe K B *J. Chem. Phys.* **37** 917 (1962)
27. Naff W T, Cooper C D, Compton R N *J. Chem. Phys.* **49** 2784 (1968)
28. Harland P W, Thynne J C Preprint of Edinburgh University (Scotland, 1972)
29. Harland P W, Thynne J C *J. Chem. Soc. Comm.* 478 (1972)
30. Harland P W, Thynne J C *Int. J. Mass Spectrom. Ion Phys.* **10** 11 (1972)
31. Naff W T, Compton R N, Cooper C D *J. Chem. Phys.* **54** 212 (1971)
32. Compton R N, Huebner R H *J. Chem. Phys.* **51** 3132 (1969)
33. Chaney E L et al. *J. Chem. Phys.* **52** 4413 (1970)
34. Collins P M et al. *Chem. Phys. Lett.* **4** 646 (1970)
35. Robinson P J, Holbrook K A *Unimolecular Reactions* (London, New York: Wiley-Interscience, 1972)
36. Kompaneets A S *Teoreticheskaya Fizika* (Theoretical Physics) (Moscow: Fizmatgiz, 1958) [Translated into English (New York: Dover, 1962)]
37. Lifshitz C, Tiernan T O, Hughes B M *J. Chem. Phys.* **59** 3182 (1973)
38. Finch C D et al. *J. Chem. Phys.* **106** 9594 (1997)
39. Kalamarides A et al. *J. Chem. Phys.* **93** 4043 (1990)
40. Popple R A, Finch C D, Dunning F B *Int. J. Mass Spectrom. Ion Proc.* **149/150** 37 (1995)
41. Foltz G W et al. *J. Chem. Phys.* **67** 1352 (1977)
42. Zollars B G et al. *Phys. Rev. A* **32** 3330 (1985)
43. Zollars B G et al. *J. Chem. Phys.* **84** 5589 (1986)
44. Beterov I M et al. *Z. Phys. D* **6** 55 (1987)
45. Dunning F B *J. Phys. Chem.* **91** 2244 (1987)
46. Harth K, Ruf M -W, Hotop H *J. Phys. D* **14** 149 (1989)
47. Ling X et al. *Phys. Rev. A* **45** 242 (1992)
48. Smirnov B M, Firsov O B *Zh. Eksp. Teor. Fiz.* **73** 454 (1977) [*JETF* **46** 238 (1977)]
49. Chen J C Y *J. Chem. Phys.* **40** 3513 (1964)
50. Bardsley J N, Biondi M A *Adv. Atom. Mol. Phys.* **6** 3 (1970)
51. Demkov Yu N *Phys. Lett.* **15** 235 (1965)
52. Schulz G J, Asundi R K *Phys. Rev. Lett.* **15** 946 (1965)
53. Schulz G J, Asundi R K *Phys. Rev.* **158** 25 (1967)
54. Christophorou L G, Compton R N, Dickson H W *J. Chem. Phys.* **48** 1949 (1968)
55. Rapp D, Sharp T E, Briglia D D *Phys. Rev. Lett.* **14** 533 (1965)
56. Ehrhardt H et al. *Phys. Rev.* **173** 222 (1968)
57. Boness M J W, Hasted J B, Larkin I W *Proc. R. Soc. London Ser. A* **305** 493 (1968)
58. Hasted J B, Awan A M *J. Phys. B* **2** 367 (1969)
59. Alajajian S H, Chutjian A *Phys. Rev. A* **37** 3680 (1988)
60. Hagstrum H D *Rev. Mod. Phys.* **23** 185 (1951)
61. Schulz G J *Phys. Rev.* **128** 178 (1962)
62. Chantry P J, Schulz G J *Phys. Rev.* **156** 134 (1967)
63. Kraus K *Z. Naturforsch.* **16a** 1378 (1961)
64. Craggs J D, Tozer B A *Proc. R. Soc. London Ser. A* **254** 229 (1960)
65. Van Brunt R J, Kieffer L J *Phys. Rev. A* **2** 1899 (1970)
66. Christophorou L G, McCorkle D L, Carter J G *J. Chem. Phys.* **54** 253 (1971)
67. Christophorou L G et al. *J. Chem. Phys.* **43** 4273 (1965)
68. O'Malley T F, Taylor H S *Phys. Rev.* **176** 207 (1968)
69. O'Malley T F *Phys. Rev.* **155** 59 (1967)
70. Henderson W R, Fite W L, Brackmann R T *Phys. Rev.* **183** 157 (1969)
71. Spence D, Schulz G J *Phys. Rev.* **188** 280 (1969)
72. Compton R N, Christophorou L G *Phys. Rev.* **154** 110 (1967)
73. Chantry P J *J. Chem. Phys.* **57** 3180 (1972)
74. Schulz G J, Spence D *Phys. Rev. Lett.* **22** 47 (1969)
75. Spence D, Schulz G J *J. Chem. Phys.* **54** 5424 (1971)
76. Burrow P D *J. Chem. Phys.* **59** 4922 (1973)
77. Belic D S, Hall R I *J. Phys. B* **14** 365 (1981)
78. Jaffke T et al. *Chem. Phys. Lett.* **193** 62 (1992)
79. Azria R et al. *Rev. Phys. Appl.* **9** 469 (1974)
80. Allan M, Wong S F *J. Chem. Phys.* **74** 1687 (1981)
81. Fox R E *J. Chem. Phys.* **26** 1281 (1957)
82. Gallagher J W et al. *J. Phys. Chem. Ref. Data* **12** 109 (1983)

83. Frost D C, McDowell C A *J. Chem. Phys.* **29** 503 (1958)
84. Chantry P J *J. Chem. Phys.* **57** 3180 (1972)
85. Ziesel J P, Nenner I, Schulz G J *J. Chem. Phys.* **63** 1943 (1975)
86. Abouaf R, Teillet-Billy D *J. Phys. B* **10** 2261 (1977)
87. Azria R et al. *J. Phys. B* **13** 1909 (1980)
88. Bardsley J B, Wahedra J M *J. Chem. Phys.* **78** 7227 (1983)
89. Rohr K, Linder F *J. Phys. B* **8** L200 (1975); **9** 2521 (1976)
90. Taylor H S, Goldstein E, Segal G A *J. Phys. B* **10** 2253 (1977)
91. Sides G D, Tiernan T O, Hanrahan R J *J. Chem. Phys.* **65** 1966 (1976)
92. Kurepa M V, Belic D S *Chem. Phys. Lett.* **49** 608 (1977)
93. Tam W-C, Wong S F *J. Chem. Phys.* **68** 5626 (1978)
94. Kurepa M V, Belic D S *J. Phys. B* **11** 3719 (1978)
95. Christodoulides A A, Schumacher R, Schlinder R N *J. Chem. Phys.* **79** 1904 (1975)
96. Rokni M, Jacob J H, Mangano J A *Appl. Phys. Lett.* **34** 187 (1979)
97. Ayala J A, Wenworth W E, Chen E C M *J. Phys. Chem.* **85** 3989 (1981)
98. Smith D, Adams N G, Alge E *J. Phys. B* **17** 461 (1984)
99. Schultes E, Christodoulides A A, Schlinder R N *Chem. Phys.* **8** 354 (1975)
100. Truby F K *Phys. Rev. A* **4** 613 (1971)
101. Biondi M A *Phys. Rev.* **109** 2005 (1958)
102. Truby F K *Phys. Rev.* **172** 241 (1968); **188** 508 (1969)
103. Chantry P J, in *Applied Atomic Collision Physics* (Pure and Applied Physics, Vol. 43, Eds H S W Massey, E W McDaniel, B Bederson) (New York: Academic Press, 1982) p. 35
104. Chen H-L et al. *J. Appl. Phys.* **48** 2297 (1977)
105. Nygaard K J et al. *Appl. Phys. Lett.* **32** 351 (1978)
106. Schneider B I, Brau C A *Appl. Phys. Lett.* **33** 569 (1978)
107. Trainor D W, Jacob J H *Appl. Phys. Lett.* **35** 920 (1979)
108. Chutjian A, Alajajian S H *Phys. Rev. A* **35** 4512 (1987)
109. Bethe H A *Phys. Rev.* **47** 747 (1935)
110. Wigner E P *Phys. Rev.* **73** 1002 (1948)
111. Shimamori H, Hatano Y *Chem. Phys.* **21** 187 (1977)
112. Chanin L M, Phelps A V, Biondi M A *Phys. Rev.* **128** 219 (1962)
113. Van Lint V A, Wickner E G, Trueblood D L *Bull. Am. Phys. Soc.* **5** 122 (1960)
114. Shimamori H, Hatano Y *Chem. Phys. Lett.* **38** 242 (1976)
115. Hirsch M H, Eisner P N, Slevin J A *Phys. Rev.* **178** 175 (1969)
116. Spence D, Schulz G J *Phys. Rev. A* **5** 724 (1972)
117. Goans R E, Christophorou L G *J. Chem. Phys.* **60** 1036 (1974)
118. Hackam R, Lennon J J *Proc. R. Soc. London Ser. A* **86** 123 (1965)
119. Mentzoni M H, Donohue J *Bull. Am. Phys. Soc.* **11** 199 (1968)
120. Parkes D A, Sugden T M *J. Chem. Soc. Far. Trans.* Part 2 **68** 600 (1972)
121. Pack J L, Phelps A V *J. Chem. Phys.* **45** 4316 (1966)
122. Stockdale J A, Christophorou L G, Hurst G S *J. Chem. Phys.* **47** 3267 (1967)
123. Buby L, Adgal H, in *Proc. 5 Int. Conf. Phys. Electr. Atom. Collis.* (Leningrad, 1967) p. 584
124. Hurst G S, Bortner T E *Phys. Rev.* **114** 116 (1959)
125. Bloch F, Bradbury N E *Phys. Rev.* **48** 689 (1935)
126. Palkina L A, Smirnov B M, Firsov O B *Zh. Eksp. Teor. Fiz.* **61** 2319 (1971) [*Sov. Phys. JETP* **34** 1242 (1972)]
127. Pack J L, Phelps A V *J. Chem. Phys.* **44** 1870 (1966)
128. Gunton R C, Shaw T M *Phys. Rev.* **140** A748 (1965)
129. Weller C S, Biondi M A *Phys. Rev.* **172** 198 (1968)
130. Linder F, Schmidt H *Z. Naturforsch.* **26a** 1617 (1971)
131. Land J E, Raith W *Phys. Rev. Lett.* **30** 193 (1973)
132. Koike F, Watanabe T *J. Phys. Soc. Jpn.* **34** 1022 (1973)
133. Schulz G J, in *Electron-Molecule Scattering* (Ed. S C Brown) (New York: Wiley, 1979) p. 43
134. Roszak S *Chem. Phys. Lett.* **215** 427 (1993)
135. Roszak S *J. Chem. Phys.* **101** 2978 (1994)
136. Kaufman J J et al. *Chem. Phys.* **204** 233 (1996)
137. Roszak S et al. *J. Chem. Phys.* **106** 7709 (1997)
138. Illenberger E *Chem. Phys. Lett.* **80** 153 (1981)
139. Klar D, Ruf M W, Hotop H *Austr. J. Phys.* **45** 263 (1992)
140. Klar D, Ruf M W, Hotop H *Chem. Phys. Lett.* **189** 448 (1992)
141. Chutjian A, Alajajian S H *Phys. Rev. A* **31** 2885 (1985)
142. Chutjian A, Alajajian S H *Phys. Rev. A* **35** 4512 (1987)
143. Orient O J, Chutjian A *Phys. Rev. A* **34** 1841 (1986)
144. Christodoulides A A, Christophorou L G *J. Chem. Phys.* **54** 4691 (1971)
145. Christophorou L G, McCorkle D L, Anderson V E *J. Phys. B* **4** 1163 (1971)
146. Alajajian S H, Bernius M T, Chutjian A *J. Phys. B* **21** 4021 (1988)
147. Alajajian S H, Chutjian A *J. Phys. B* **20** 2117 (1987)
148. Mothes K G, Schlinder R N *Ber. Bunsenges. Phys. Chem.* **75** 936 (1971)
149. Warman J M, Sauer M C *Int. J. Rad. Phys. Chem.* **3** 273 (1971)
150. Mothes K G, Schlutes E, Schlinder R N *Chem. Phys. Chem.* **76** 3758 (1972)
151. Davis F J, Compton R N, Nelson D R *J. Chem. Phys.* **59** 2324 (1973)
152. Wenworth W E, Becker R S, Tung R *J. Phys. Chem.* **71** 1652 (1967)
153. Blaunstein R P, Christophorou L G *J. Chem. Phys.* **49** 1526 (1968)
154. Bouby L, Fiquet-Fayard F, Abgrall H *Sci. Acad. Paris* **261** 4059 (1965)
155. Lee T G *J. Phys. Chem.* **67** 360 (1963)
156. Shimamori H et al. *J. Chem. Phys.* **97** 6335 (1992)
157. Warman J M, Sauer M C *J. Chem. Phys.* **52** 6428 (1970)
158. Shimamori H, Nakatani Y *Chem. Phys. Lett.* **150** 109 (1988)
159. Orient O J et al. *Phys. Rev. A* **39** 4494 (1989)
160. Christopher J M, Cheng-ping T, David L M *J. Chem. Phys.* **91** 2194 (1989)
161. Fessenden R W, Bansal K M *J. Chem. Phys.* **53** 3468 (1970)
162. Christodoulides A A, Schumacher R, Schindler R N *Z. Naturforsch.* **30a** 811 (1975)
163. Bansal K M, Fessenden R W *Chem. Phys. Lett.* **15** 21 (1972)
164. Wentworth W E, George R, Keith H *J. Chem. Phys.* **51** 1791 (1969)
165. Christophorou L G, Stockdale J A D *J. Chem. Phys.* **48** 1956 (1968)
166. Schumacher R et al. *J. Phys. Chem.* **82** 2248 (1978)
167. Crompton R W et al. *J. Phys. B* **15** L483 (1982)
168. Crompton R W, Haddad G N *Austr. J. Phys.* **36** 15 (1983)
169. Christophorou L G, McCorkle D L, Pittman D *J. Chem. Phys.* **60** 1183 (1974)
170. Buchel'nikova N S *Zh. Eksp. Theor. Fiz.* **35** 1119 (1958) [*Sov. Phys. JETP* **8** 783 (1958)]
171. Chen C L, Chantry P J *Bul. Am. Phys. Soc.* **17** 1133 (1972)
172. Bansal K M, Fessenden R W *J. Chem. Phys.* **59** 1760 (1973)
173. Christophorou L G, Blaunstein R P *Radiat. Res.* **37** 229 (1969)
174. Szamrej I et al. *Radiat. Phys. Chem.* **38** 541 (1991)
175. Datskos P G, Christophorou L G, Carter J G *J. Chem. Phys.* **97** 9031 (1992)
176. Petrovic Z Lj, Crompton R W *J. Phys. B* **20** 5557 (1987)
177. Alge E, Adams N G, Smith D *J. Phys. B* **17** 3827 (1984)
178. Shimamori H, Tatsumi Y, Sunagawa T *Chem. Phys. Lett.* **194** 223 (1992)
179. Adams N G, Smith D, Herd C R *Int. J. Mass Spectrom. Ion Proc.* **84** 243 (1988)
180. Spence D, Schulz G J *J. Chem. Phys.* **58** 1800 (1973)
181. Sherwell J et al. *Austr. J. Chem.* **41** 1491 (1988)
182. Davis E J, Nelson D R *Chem. Phys. Lett.* **6** 277 (1969)
183. Davis E J, Nelson D R *Chem. Phys. Lett.* **7** 461 (1970)
184. Fehsenfeld F C *J. Chem. Phys.* **53** 2000 (1970)
185. Shimamori H, Fessenden R W *J. Chem. Phys.* **71** 3009 (1979)
186. Petrovic Z Lj, Crompton R W *J. Phys. B* **18** 2777 (1985)
187. Hunter S R, Carter J G, Christophorou L G *J. Chem. Phys.* **90** 4879 (1989)
188. Chen E, George R D, Wentworth W E *J. Chem. Phys.* **49** 1973 (1968)
189. Christophorou L G et al. *J. Phys. D* **14** 1889 (1981)
190. Mothes K G, Schlinder R N *Phys. Chem.* **75** 936 (1971)
191. Le Garrec J L et al. *J. Chem. Phys.* **107** 54 (1997)
192. Klots C E *Chem. Phys. Lett.* **38** 61 (1976)
193. Canosa A et al. *Chem. Phys. Lett.* **228** 26 (1994)
194. Miller T M et al. *J. Chem. Phys.* **100** 8841 (1994)
195. Mahan B H, Young C E *J. Chem. Phys.* **44** 2192 (1966)
196. Spanel P, Matejcik S, Smith D *J. Phys. B* **28** 2941 (1995)
197. Matejcik S et al. *J. Chem. Phys.* **107** 8955 (1997)
198. Fenzlaff M, Gerhard R, Illenberger E *J. Chem. Phys.* **88** 149 (1987)
199. Lehmann B *Z. Naturforsch.* **25a** 1755 (1970)
200. Lifshitz C, Weiss M *Chem. Phys. Lett.* **15** 266 (1972)
201. Chen C L, Chantry P J *J. Chem. Phys.* **71** 3897 (1979)
202. Hildenbrandt D L *J. Phys. Chem.* **77** 897 (1973)
203. Kiang T, Estler R C, Zare R N *J. Chem. Phys.* **70** 5925 (1979)

204. Babcock L M, Streit G E *J. Chem. Phys.* **74** 5700 (1981)
205. Tsang W, Herron J *J. Chem. Phys.* **96** 4272 (1992)
206. Chu J H, Lin I *Phys. Rev. Lett.* **72** 4009 (1994)
207. Thomas H et al. *Phys. Rev. Lett.* **73** 652 (1994)
208. Hayashi Y, Tachibana K *Jpn. J. Appl. Phys.* **33** L804 (1994)
209. Melzer A, Trottenberg T, Piel A *Phys. Lett. A* **191** 301 (1994)
210. Trottenberg T, Melzer A, Piel A *Plasma Sour. Sci. Technol.* **4** 450 (1995)
211. Morfill G E , Thomas H *J. Vac. Sci. Technol. A* **14** 490 (1996)
212. Fortov V E et al. *Pis'ma Zh. Eksp. Teor. Fiz.* **63** 176 (1996) [*JETP Lett.* **63** 187 (1996)]
213. Fortov V E et al. *Pis'ma Zh. Eksp. Teor. Fiz.* **64** 86 (1996) [*JETP Lett.* **64** 92 (1996)]
214. Märk T D et al. *Phys. Rev. Lett.* **55** 2559 (1985)
215. Walder G et al. *Z. Phys. D* **20** 201 (1991)
216. Hashemi R, Illenberger E *Chem. Phys. Lett.* **187** 623 (1991)
217. Matejcik S et al. *Phys. Rev. Lett.* **77** 3771 (1996)
218. Jaffke T et al. *Z. Phys. D* **25** 77 (1992)
219. Sanche L *Phys. Rev. Lett.* **53** 1638 (1984)
220. Huels M A et al. *Phys. Rev. A* **51** 337 (1995)
221. Hashemi R et al. *J. Phys. Chem.* **96** 10605 (1992)
222. Ingolfsson O, Illenberger E *Chem. Phys. Lett.* **241** 180 (1995)
223. Birtwistle D T, Herzenberg A *J. Phys. B* **4** 53 (1971)
224. Allan M *J. Electron. Spectrosc.* **48** 219 (1989)
225. Ayotte P et al. *J. Chem. Phys.* **106** 749 (1997)
226. Weik F, Illenberger E *J. Chem. Phys.* **103** 1406 (1995)
227. Illenberger E *Chem. Phys. Lett.* **80** 153 (1980)
228. Le Coat Y, Ziesel J-P, Guillotin J-P *J. Phys. B* **27** 965 (1994)
229. Mann A, Linder F *J. Phys. B* **25** 545 (1992)
230. Cristophorou L G, Olthoff J K, Rao M V S S *J. Chem. Phys. Ref. Data* **25** 1341 (1996)
231. Marsh E P et al. *J. Chem. Phys.* **92** 2004 (1990)
232. Rowntree P A, Scoles G, Ruiz-Suarez J C *J. Phys. Chem.* **94** 8511 (1990)
233. Lieberman M A, Lichtenberg A J *Principles of Plasma Discharges and Materials Processing* (New York: Wiley, 1994)
234. *Plasma Science: from Fundamental Research to Technological Applications* (Washington, D.C.: National Academy Press, 1995)